PARTICLE SIZE AND MOISTURE EFFECTS ON THE LOW-TEMPERATURE OXIDATION OF COAL

Cavan Raymond Hill

A dissertation submitted to the Faculty of Engineering, University of the Witwatersrand, Johannesburg, in fulfilment of the requirements for the degree of Master of Science in Engineering.

Johannesburg, 1986.

I declare that this dissertation is my own, unaided work. It is being submitted for the Degree of Master of Science in Engineering in the University of the Witwatersrand, Johannesburg. It has not been submitted before for any degree or examination in any other University.

G.R. Hill

10th day of JANUARY 1986.

ABSTRACT

The effects of particle size and coal moisture content on the kinetics of the low-temperature oxidation of coal were investigated by measuring the temperature-time and concentration-time curves in a semi-adiabatic batch reactor. In addition, carbon dioxide desorption isotherms were measured to give an insight into the porous structure of coal. The initial rate of reaction was found to follow a non-linear chemisorption-type kinetic model. The drop in rate due to the ageing of the coal was studied by non-linear regression of various kinetic models on the experimental data. A pore-diffusion controlling mechanism approximated the ageing effect, but gave too steep a drop in the rate for the later stages of the reaction. A maximum in the rate, expressed as a function of the coal moisture content, was found.

ACKNOWLEDGEMENTS

Financial support was received from the Cooperative Scientific Program (CSI) of the Council for Scientific and Industrial Research (CSIR), the University of the Witwatersrand (in the form of a Senior Bursary), and from Sasol Limited. This is gratefully acknowledged.

I wish to thank the supervisors of this project, Mr D.F. Williams and Professors D. Glasser and A.W. Bryson, for their help and encouragement during the course of this work.

I am also very grateful to Donald Williams for writing the word-processing and graph-plotting computer programs which greatly simplified the production of this dissertation.

Finally, I wish to thank Diana Huggett for her assistance with the typing and compilation of this dissertation.

CONTENTS Page

LIST OF FIGURES

LIST OF TABLES

LIST OF SYMBOLS

c	Constant in BET equation
C	Gas-phase oxygen concentration ($mol.m^{-3}$)
C_o	Initial oxygen concentration
C'_o	Fictitious initial oxygen concentration for pre-ageing model
C_s	Surface oxygen concentration
C_p	Heat capacity ($J.K^{-1}$)
D	Diffusion coefficient ($m^{-1}.min^{-1}$)
D	Product of D and ρ_m ($mol.m^{-2}.min^{-1}$)
e_r	Extent of reaction r (mol)
H	Enthalpy (J)
$\bar{H}_s$	Partial molar enthalpy of component s ($J.mol^{-1}$)
ΔH_r	Heat of reaction for reaction r ($J.mol^{-1}$)
k,K	Kinetic constants
N	Number [illegible] points used for sum of squared errors
n	Amount [illegible]bed on surface in BET equation (mol)
n_m	Amou[illegible]sorbed in monolayer on surface (mol)
N_s	Number of moles of component s (mol)
P	Number of parameters
p	Pressure (kPa)
p_o	Saturation pressure (kPa)
r	Rate of reaction ($mol.m^{-3}.min^{-1}$)
S	Total surface area (m^2)
	Sum of squared errors
	Time (min)
T	Temperature (^oC)
T_{ad}	Adiabatic temperature
T_o	Oven temperature
T_s	Steady-state temper[illegible]ture
T_h	Reactor temperature when heater on
U	Heat transfer coef[illegible]ficient ($W.K^{-1}$)
U/C_p	Heat transfer time constant (min^{-1})
V	Reactor volume (m^3)
X	Sensitivity matrix
Δx	Thickness of oxy[illegible]layer (m)
α_{sr}	Stochiometric coefficient of component s in reaction r (-)
α	S/V (m^{-1})
β	Term in equation [illegible]
ρ_m	Molar density of reactive groups in coal ($mol.m^{-3}$)
Ω	Diagonal matrix of weighting factors

CHAPTER 1: INTRODUCTION

1.1 General Overview

The low-temperature oxidation of coal has been studied by many researchers, as the reaction with oxygen at ambient conditions can lead to self-heating which in certain cases may result in the spontaneous combustion of coal stockpiles. The oxidation also has an adverse effect on many coal properties which are needed when the coal is processed to obtain economic products. If the extent of this oxidation can be reduced, it will be advantageous from both the economic and safety standpoints.

Investigations into the spontaneous combustion of coal can be placed into two categories: studies related to the kinetics of the reaction and the associated heat effects; and studies of the behaviour of dumps/bunkers/silos/ships' holds packed with coal or any other material (eg fishmeal, hay, soap chips, pyrite ore) where the possibility of exothermic reaction exists. This study falls into the former category.

All coals, ranging from low rank subbituminous to high rank anthracitic, react with oxygen at atmospheric conditions, but to different degrees (Schmidt, 1945). It has been established that low rank coals are most prone to self-heating, and that the rate of oxygen adsorption (and thus of heating) falls off with the amount of reaction (Schmidt, 1945). The reaction rate is a strong function of temperature (doubling of the rate for a temperature increase of 10°C has been reported by Sondreal & Ellman (1974)), and also depends on the particle size, with smaller sizes reacting and ageing quicker. The adsorption (exothermic) and desorption (endothermic) of water vapour can also play a part in the self-heating of coal (Schmidt, 1945).

1.2 Coal Structure

Studies of the reactivity are difficult due to the complex, and not yet fully understood, physical and chemical structure of coal. The main building blocks of coal are aromatic and hydro-aromatic groups connected by crosslinks such as methylene, oxygen and sulphur. Mineral matter in various forms is also found (Meyers, 1982).

The main feature of the physical structure of coal is the extensive porosity ranging from cracks of micron dimensions down to pores with openings of less than one nanometre (Meyers, 1982). Pores with dimensions ranging from 0.8 to 2 nm are classified as micropores (IUPAC, 1972). Most of the porosity of coal is located in these micropores and even as submicropores (openings of less than 0.8 nm).

1.3 Moisture in Coal

A review of this topic is given by Allardice & Evans (1978), and only a few features will be discussed here. An exact definition of moisture in coal is difficult as it can be present as surface water or be adsorbed in the pores. It may also result from the thermal decomposition of oxygen-containing functional groups, or from water of hydration of minerals present in the coal.

One of the methods used to study water in coal is the measurement of the water sorption isotherm. This measures the moisture content of the coal as a function of the humidity of the atmosphere with which it is in equilibrium. An important feature of these isotherms is the hysteresis between the desorption and readsorption curves, which has been attributed to shrinkage and swelling of the coal on removal and addition of water. Excessive drying of coals has been found to result in collapse of the pore structure, which is not recovered on subsequent wetting (Gorbaty, 1978).

Standard methods (Allardice & Evans,1978) of determining the moisture content in coal are based on drying the coal at 110°C (in an inert atmosphere or under vacuum) and measuring the amount of water removed. These conditions are chosen as a compromise between removing the physically adsorbed water and decomposing the coal.

1.4 Measurement of the Surface Area of Coal

A thorough review of the methods used to study coal porosity, and the surface area in particular, is given by Mahajan & Walker (1978). A more recent review, with reference to the structure of coal, has been published by Mahajan (1982). A brief overview of this field is provided here.

One of the first methods used for the determination of coal surface area relied on the measurement of the heat of immersion of the coal in

a liquid g...erally methanol. This was criticized on the basis that it involves specific interactions between methanol and groups on the coal surface, and is thus no longer used.

The standard technique for the measurement of the surface areas of porous and non-porous coals involves the determination of the adsorption isotherm of nitrogen at liquid nitrogen temperatures (-196°C). From this isotherm the amount of gas required to cover the surface with a layer one molecule thick can be calculated using the equation developed by Brunauer, Emmet & Teller (1938).

The BET equation is:

$$\frac{n}{n_m} = \frac{c\ p/p_o}{[1-p/p_o][1+(c-1)p/p_o]}$$

where n is the amount adsorbed at a relative pressure of p/p_o, n_m the amount on a monolayer, p_o the saturation pressure and c is a fitting constant. The constants n_m and c are calculated from the straight line form of this equation, viz.:

$$\frac{p}{n(p_o-p)} = \frac{1}{n_m} + \frac{c-1}{n_m c}\frac{p}{p_o}$$

When nitrogen isotherms on coal were analysed using the BET method, very low areas, in disagreement with those from the heat of wetting method, were found (Mahajan, 1982). It was then postulated that these low areas were due to the small diffusion coefficient of N_2 at liquid N_2 temperatures, and the large diffusional resistance of the micropores. This was proved by adsorption of other gases at higher temperatures.

Carbon dioxide isotherms measured at -78°C have been used extensively for the measurement of coal surface areas, as the minimum dimension of the CO_2 molecule is less that of N_2, and because the higher temperature reduces the diffusional problems. Walker & Kini (1965) compared the surface areas obtained from CO_2 at 25°C with those obtained using CO_2 at -78°C, N_2 at -196°C, Kr at -78°C and Xe at 0°C, and concluded that the adsorption of CO_2 at -78°C should usually measure essentially the total surface area of coals. The low temperature system is more convenient as a high-pressure apparatus is not required.

Application of the BET equation to microporous adsorbents has been

criticized on the basis that layer-by-layer filling as envisaged by Brunauer *et al* (1938) probably does not occur. The Polyani-Dubinin equation, an alternative description of the adsorption process for microporous adsorbents based on the volume filling of pores, was shown by Marsh & Siemienewska (1965) to give essentially the same areas as the BET equation.

Objections to the use of carbon dioxide isotherms have been made on the grounds that the quadropole moment of the CO_2 molecule could interact with the oxygen functional groups, but this is not borne out by the agreement obtained between the values obtained from Xe and CO_2 isotherms.

A very important part of the measurement of the surface areas of coals is the preparation of the sample, specifically drying. If any water is present, it could freeze when the temperature is lowered, leading to crack formation and the generation of new surface. On the other hand, excessive drying could lead to a collapse of the pore structure and loss of surface. Outgassing (drying) at 110°C overnight in the absence of O_2 is thus recommended by Mahajan (1982) as the most practical approach.

1.5 Possible Mechanisms for the Low-Temperature Oxidation of Coal

Work in this area has been scarce due to the complex structure of coal and the lack of suitable techniques to determine specific changes on the coal surface. Most studies of the self-heating of coal have ignored the details of the mechanisms, and have only measured reaction rates.

The first step in the low-temperature oxidation of coal appears to be the formation of an unstable coal-oxygen complex which later breaks down to form mainly carbonic gases and water (Schmidt, 1945). The amount of oxygen released in the carbonic gases is much less than the amount adsorbed, resulting in an accumulation of this complex.

Chamberlain, Barass & Thirlaway (1976) proposed a mechanism whereby peroxides are formed. These then decompose, releasing carbonic gases, water and other low-molecular-weight hydrocarbons. Free-radical mechanisms were also postulated. Marinov (1977) studied changes of the coal functional groups, spin concentration and infrared spectra during oxidation. Mechanisms based on the coal as a solid acid were th n

proposed, thus making charge transfer an important step. An electrochemical mechanism was proposed by Aleksandrov, Gavrilov & Kamneva (1984), based on the formation of redox systems of bi- and trivalent iron which would catalyse the decomposition of organic peroxides. The successful electrochemical protection of a coal dump from spontaneous ignition, as compared to a control dump, was described.

1.6 Detecting the Extent of Oxidation of Coal

Most kinetic studies have have not measured the changes to the coal. Marinov (1977) has discussed some of the changes, but this cannot yet be applied on a practical scale. Most of the work has concentrated on the effects of oxidation on the physical and chemical properties of the coal. A comprehensive review of this area has been given by Andersen & Hamza (1982).

Some of the physical properties which are affected by oxidation are the free swelling index (a measure of the caking propensity of coal when gasified), the plastic properties (oxidation restricts the plastic temperature range), the coke strength (oxidation results in inferior quality coke) and the hydrophobicity of the coal surface (resulting in decreased floatability and increased problems in solid-liquid separation). Oxidation can also lead to a decrease in the calorific value. One instance where oxidation has an advantageous effect is in the gasification of bituminous coals, where caking, leading to solid masses which can block reactors, can be reduced by pre-oxidation (Kam, Hixson & Perlmutter, 1976).

1.7 Kinetic Studies

1.7.1 Experimental techniques

The most common techniques which have been used for kinetic studies are the crossing point temperature method, the adiabatic method and the static isothermal method. These are discussed below.

In the crossing point technique, a sample of coal packed in a quartz tube is aerated continuously whilst situated in an oven heated at a constant rate. The temperature of the coal and oven are monitored, and the point at which a sharp increase of the coal temperature above that of the oven is found is called the crossing point temperature. Hedden & Wilhelm (1980) analysed this technique and found that the

crossing point temperature depended on the operating variables such as heating rate and gas flowrate, as well as the coal properties. Standardization of the experimental conditions would at best provide a relative measure of the reactivities of a group of coals.

The adiabatic method involves placing a sample of coal into a calorimeter and immersing this in a bath whose temperature follows that of the coal. When the coal is aerated, a temperature rise occurs which is related to the reactivity.

The static isothermal method consists of monitoring the change in gas concentration, either in a batch or flow system, as oxidation of the coal proceeds.

A recently described method (Nordon, Bainbridge, Szemes & Myers, 1985) uses an isothermal flow calorimeter of the Calvet type, where the rate is measured as the temperature diff[illegible] across a small air gap. The authors report high sensitivity [illegible] by using a thermopile to measure the temperature differen[illegible] tability over several weeks of operation.

A combination of the adiabatic and static isothermal methods was used by Itay (1983). The reaction took place in a sealed Dewar flask situated in a constant-temperature oven. The rate of heat loss was measured independently which then allowed the adiabatic curve to be constructed from the experimental temperature-time plot. In addition, gas concentration measurements were carried out.

1.7.2 Effect of initial oxygen concentration

The order of the reaction with respect to the oxygen concentration has been reported by various authors as ranging from first order down to fractional orders. A distinction must be made between the effect of oxygen concentration and the effect of the extent of oxidation. Studies of the order of reaction must thus be carried out on coal which has not been oxidized at all, *i.e.* initial rates must be used.

Van Krevelen (1981) proposed that the reaction was first order, which was supported by the work of Banerjee, Banerjee & Chakravorty (1970), who determined first-order rate constants and activation energies by measuring the drop in concentration of the oxygen in air flowing over a packed bed of coal. A reaction order of unity was also found by

Sondreal & Ellman (1974). Both studies are confused by the ageing effect, and the influence of this on the reaction order is unknown.

Carpenter & Giddings (1964) studied the reaction of fresh coal at different oxygen concentrations, and found orders of about one-half for six coals. A similar result was obtained by Winmill (1915).

Many authors have found that at the early stages of reaction, where oxygen adsorption is fast, bear no relation to the later stages (Wood, 1958), or have found a discontinuity in the effect of temperature on the reaction (Schmidt, 1945; Jones & Townend, 1946). This suggests that a change in the controlling mechanism of reaction could occur. Wood (1958) and Sevenster (1961) found that the early stages of reaction were fitted by the Elovich equation (which describes chemisorption kinetics), but not the later stages.

Itay (1983) found that the addition of carbon monoxide to the reactant gas inhibited the reaction, but did not appear to affect the rate of formation of the carbonic gases. A similar effect, but to a lesser degree, was found for carbon dioxide.

1.7.3 Ageing of the coal

One of the first successful descriptions of the ageing phenomenon in coal was given by Schmidt (1945), who found that, for the data of Winmill (1913, 1914, 1915), the amount of oxygen consumed as a function of time could be described satisfactorily by the power-law model $X=Ct^b$, where X is the amount of oxygen consumed, t the time and C and b are fitting constants. The constant b was found to be the same for all coals of the same particle size, and to range from 0.37 for minus 200-mesh samples to 0.8 for 0 to 1/4 inch coal.

Kam *et al* (1976) proposed a two-path mechanism based on chemisorption, and found that under certain conditions the rate exhibited an exponential decay with time, which corresponds to the empirical rate expression of Georgiadis & Gaillard (1953).

Sondreal & Ellman (1974) also proposed an exponential decay of the rate with time, but found in some instances that this was not sufficient to accomodate the large drop in rates unless the number of exponential terms was increased to three. This six-constant equation was then fitted to data obtained on a wide variety of coals.

Several authors (Huntjens, unpublished (quoted, with photographs, in Van Krevelen, 1981) ; Mason & Schora, 1967; Gray, Rhoades & King, 1976) have examined oxidized coal particles with a microscope under special lighting/staining conditions, and have found that the reaction is confined to near the surface, leading to the formation of "oxidation rims" of the reacted coal. The reacted coal forming the rim is a coal-oxygen complex known as oxycoal (Van Krevelen, 1981). This provides a physical reason for the drop in reactivity with time, as the rate is limited by diffusion across the oxidized layer.

Mathematical analysis of this system leads to the classical "shrinking core" type of model. In the case of diffusion through the product layer limiting the rate, and no change in particle size on reaction, Carberry (1976) has shown that the conversion is proportional to the square root of the reaction time. This result is very similar to the empirical expression of Schmidt (1945), who found the conversion proportional to some power of time ranging from 0.37 to 0.8. The power-law models show that the rate is proportional to a negative power of time, and negative powers may be expanded as infinite series very similar to those for negative exponentials.

1.7.4 Particle size effects

It is known that smaller coal oxidizes faster, but this effect is not yet completely understood. Schmidt (1945) correlated the reactivity after one day of oxidation with the external surface area of the coal particles calculated from the formula of Needham & Hill (1935). The reactivity was found to be proportional to the cube root of the external area.

Sondreal & Ellman (1974) found that this relationship did not fit well for fine coals, and thus proposed an alternative model based on oxidation occurring both on the exterior surface, and in the particle up to a certain depth, with the oxidation in the particle falling off exponentially. In this model the rate drops to zero as the particle size tend to zero, rather than becoming infinite as the cube-root law predicts.

If a "shrinking core" model is used, the variation in reactivity with particle size is implicit. The use of this model raises the problem of how to divide the very porous structure of coal into internal and

external surface. The pore size distribution of the coal is obviously of importance here.

1.7.5 Effect of water

The role of water vapour in the self-heating of coal is not very well understood at present. There are two effects associated with water vapour: the adsorption (exothermic) and desorption (endothermic) from the coal surface, and the possible effect of water on the oxidation reaction itself. Problems also arise due to the difficulty of defining the moisture content of coal (discussed in 1.3).

The rates of heat generation in coals under oxidizing and non-oxidizing conditions where both adsorption and desorption of water vapour were occurring, have been investigated by Bhattacharyya (1970, 1971), Bhattacharyya, Hodges & Hinsley (1969), and Gunay (1971). It was found that at low temperatures the heat release was primarily due to the adsorption of water vapour; that desorption of water reduced the rate of heat release; and that the rate of adsorption/ desorption was proportional to the difference in the equilibrium humidities of the coal and the atmosphere surrounding it.

The rates of oxidation under conditions where adsorption or desorption of water did not take place were measured by Sondreal & Ellman (1974), who found a maximum in the rate at a coal moisture content of approximately 20% (corresponding to nearly 100% atmospheric relative humidity). Moxon and Richardson (1985) found that the rate of oxidation in the absence of moisture is very slow, and that the water acts as a contact catalyst in the reaction between coal and oxygen. A similar result was reported by Itay (1983), where dry coal did not exhibit any reaction until some water was added.

Several of the mechanisms mentioned in 1.4 involve water, and it is also possible that water can aid in charge transfer for the electrochemical mechanisms.

An important fact is that the heat capacity of coal is a strong function of, and increases with, the coal moisture content. Moist coal might thus react faster than dry coal, but the observed temperature rise could be less.

1.8 Heat Effects of Oxidation

The temperature rise which occurs in a sample of coal when it undergoes a certain amount of oxidation is obviously a very important parameter in modelling the storage of coal. The heat of reaction (and also the heat of wetting) are the parameters of interest here.

The heat of wetting (the binding energy for moisture on coal over and above the heat of condensation) has been measured by Porter & Ralston (1916, reported in Sondreal & Ellman, 1976). It was found to be approximately 25 cal/g for dry coal and to drop as the coal moisture content increased.

The heat of reaction for oxidation has been measured by Sondreal & Ellman (1974), and found to vary from 75 kcal/mol at 20°C to 90 kcal/mol at 90°C. Itay (1983) reported a value of approximately 120 kcal/mol, but this was based on very few measurements and on one coal only. To place these values in perspective, the standard heat of formation of carbon dioxide is 94 kcal/mol, and steps in the progressive oxidation of benzene to pyrogallol each release about 90 kcal/mol.

CHAPTER 2. EXPERIMENTAL APPARATUS AND PROCEDURE

2.1 Coal Preparation

Coal is known to lose reactivity on exposure to oxygen, so precautions must be taken to prevent this from happening prior to studying the reaction. The coal used in this study was obtained directly from the washing plant with a particle size of approximately 10 mm. This coal was stored under water until required. The reaction rate of particles of this size is too low to be measured by the techniques used here, so size reduction of the particles was performed. The procedure used involved rinsing a sample of the large coal particles in fresh water to remove the fines which might have been oxidised already. This coal was left to dry in a glovebox in an inert nitrogen atmosphere. Leaks of oxygen from the air into the glovebox were prevented by keeping a slight positive pressure at all times.

The coal was prevented from drying out completely (which could lead to cracking and collapse of the pore structure) by bubbling the nitrogen supply through water. Once the coal had partially dried, partial crushing was carried out using a steel pestle and mortar. These particles could then be fed to a rod mill. Size fractions were obtained by screening using a Macsalab sieve shaker and standard test sieves of the following dimensions: 45μm, 63μm, 90μm, 125μm, 180μm, 250μm, 355μm, 500μm, 710μm and 1mm. All the size reduction operations were carried out in the glove box in a humid nitrogen atmosphere. The coal samples were then stored in screw-top bottles in the glove box until required.

2.2 Choice of Experimental Method

The distinguishing features of this reaction are that the rates under conditions which are found in practice are relatively slow, and thus difficult to monitor. For this reason this kinetic study was carried out at a higher temperature and with smaller particles than would be encountered under practical conditions.

A problem in kinetic studies is that rates cannot usually be measured directly, thus some effect of the rate has to be monitored. The classical method involves comparison of the integrated form of the rate expression to measured concentrations, usually at a fixed temperature.

Experiments carried out at different temperatures can then be used to find the temperature dependence of the kinetics. This approach was used by Sondreal & Ellman (1974) to study the kinetics of spontaneous heating of North Dakota lignite. The main problem with this method is that concentrations cannot be measured accurately, thus discrimination between the integrated forms of various rate expressions is difficult.

Another approach which can be used is the measurement of other properties which can be measured more accurately, and which are related to the rate. The most suitable "property" to use here is the temperature, as it can be measured relatively easily and accurately with modern equipment. Some researchers have attempted to measure adiabatic temperature-time curves, but this is experimentally difficult as heat transfer to and from the surroundings must be minimised. A better approach is to allow heat transfer to take place under controlled conditions, and then correct for it mathematically. This method was pioneered by Glasser & Williams (1971) who used temperature-time curves measured in a reactor of known thermal characteristics to determine liquid-phase kinetics. Scott (1971) extended this technique to solid-liquid reactions by studying a leach reaction. In these experiments the kinetic parameters were obtained using a non-linear regression technique on the integrated mass and energy balances.

The reactions studied by Glasser & Williams (1971) and Scott (1971) had half lives of the order of ten minutes, and the temperature changes were small. No special precautions to limit the heat loss were thus required, as any correction would be small. In the low-temperature oxidation of coal the rates are much lower, which necessitates a well-insulated reactor in order to reduce the heat loss to the surroundings so that the temperature changes caused by reaction can be measured. The insulation of the reactor must not result in the energy loss not being well defined (eg if there was distributed heat capacity which could act as a heat sink/source depending on whether the temperature was increasing or decreasing), as this complicates the analysis and reduces the accuracy of the results.

It is also possible to follow the concentration changes in addition to the temperature changes, and thus get more information. A technique of this type was used by Itay (1983) for the study of the low-temperature oxidation of coal. An improved apparatus, based on Itay's design was used in this study, and is described in detail below.

2.3 Description of Experimental Apparatus

2.3.1 Oven

As mentioned above, the correction for the heat loss must be kept simple in order not to complicate the analysis of the results unnecessarily. The major simplification is to keep the reactor in a constant-temperature environment, in this case a modified commercial laboratory oven. Short term fluctuations of the reactor temperature due to the element switching on and off (i.e. those with a duration of minutes) are not important as they are damped out by the low heat transfer coefficient to the reactor. Long term drift must be avoided if the oven temperature is to be considered constant.

The oven used here was of approximately 160 litre capacity, with the element not directly exposed to the bulk of the reactor to reduce radiation effects, and was fitted with a fan to ensure an even temperature distribution. The discrete proportional-integral controller was adjusted to have the smallest bandwidth possible, and the power supply to the oven was fed through constant-voltage transformers in order to prevent mains voltage fluctuations from affecting the oven temperature. In addition to this, the power supply to the element was fed through a variable voltage transformer in order to reduce the amount by which the element heated up, and thus minimise the overshoot when the element was switched off. The setpoint on the oven as supplied was controlled by a variable resistor acting as a voltage divider; in order to ensure reproducibility of the temperature and to guard against accidental setpoint changes, this was replaced by two resistance boxes in series.

In addition to the above, the experiments were carried out in a constant-temperature room to prevent fluctuations in oven temperature caused by the daily temperature changes. This arrangement was found to be satisfactory, with long term stability (24 hours) assured. The standard deviation of the oven temperature over this period was found to be about 0.35°C.

2.3.2 Reactor

The requirements for the reactor are that it must have a low heat capacity and a low rate of heat loss to the surroundings, while at the same time remaining gas-tight. The reactor used here was constructed

from a thin-walled glass Dewar flask, whose neck was sealed by a silicone rubber washer backed by an aluminium plate which could be bolted in place. A sketch of the reactor and lid is given in figure 2.1 below. The heat transfer from the reactor contents to the lid was minimised by the use of expanded polyurethane foam. The aluminium plate was fitted with nipples through which passed the thermocouple and hypodermic tubing used for gas sampling. The sample lines extending into the bulk of the reactor consisted of Teflon tubing, rather than the metal hypodermic tubing, in order to reduce the heat loss by conduction. Two sample lines, of different lengths in order to reduce bypassing, were used to allow the reactor to be purged with oxygen-free nitrogen.

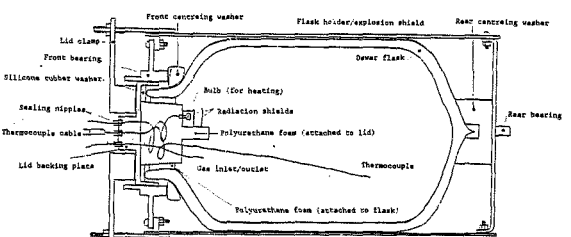

Figure 2.1 Cross-section of reactor and lid

The cylinder gas supply was fed through a two stage regulator, then through two Dreschel bottles in series (which could be filled with a saturated salt solution or pure water) in order to humidify the gas, and then through a valve into the reactor. The outlet line from the reactor was fitted with a valve and a low-dead-volume septum which allowed gas samples to be withdrawn using a syringe. The inlet and outlet lines to the reactor were 1mm ID Teflon tubing so as to reduce the dead volume of the reactor.

The reactor was enclosed in a steel explosion shield (Itay (1983) reported two explosions), and was rocked from side to side through an angle of 30° at a speed of 10 revolutions per minute. This ensured

homogeneity of the contents, and reduced any external mass transfer effects.

One of the gases present during the reaction is known to be water vapour, and it is possible that it could condense in the sample lines if the concentration is high enough. This was prevented by blowing hot air onto the sample lines and sample valve using a hairdryer. The syringe was kept heated when not in use in another oven, and could not cool down substantially during sampling because of its thick-walled construction.

The rate of heat transfer is very important in the analysis of the temperature-time curves, and it must thus be known under the exact conditions of the reaction. For this reason the reactor was fitted with a small torch bulb which acted as a heater. This has the advantage of a low heat capacity, but the bulb must reach a high temperature in order to dissipate a sufficient quantity of energy. These high temperatures could lead to a non-uniform temperature distribution due to radiation effects, thus the bulb was shielded by a piece of thin copper sheeting. The bulb was also physically removed from the thermocouple, and separated from it by polyurethane foam, to prevent heating the thermocouple and thus obtaining a spurious temperature reading. The leads to the bulb were of thin gauge wire and were coiled in the foam plug to reduce heat loss by conduction.

2.3.3 Temperature measurement

The temperature measurement device was a chromel-alumel (type K) thermocouple encased in a 1mm OD stainless steel sheath. This was coiled slightly in the foam plug in order to reduce heat losses by conduction. The thermocouple shield was earthed and kept away from the power leads to prevent interference from the mains. The thermocouple was connected to a Hewlett-Packard 3421A Data Acquisition/Control Unit, which allows software compensation of the thermocouple voltage. This instrument has a resolution of 1μV, which converts to 0.025°C for a type K thermocouple with a Seebeck coefficient of 40μV/°C.

The data acquisition and timing was performed using a 41CV handheld calculator connected to the 3421A, an 82162A Digital Cassete Drive and 82163A Thermal Printer connected by an HP-IL interface (all manufactured by Hewlett-Packard). This system allowed the times and temperatures to be stored in digital form and also to be printed out during

the experiment. On completion of a run the data were transferred to a HP9816 microcomputer (using an HP-IL/HP-IB interface) for data analysis and plotting. The programs used are reproduced in appendix A.

2.3.4 Concentration measurement

The gas samples were analysed for CO_2, H_2O, O_2, N_2 and CO using a Hewlett-Packard 5840A gas chromatograph fitted with a thermal conductivity detector. Separation of these gases with one column is not possible, so two columns and an automated valve were used. Porapak Q (5m, 1/8" ID column) was used to resolve CO_2, H_2O and a composite N_2 / O_2 / CO peak, and this peak separated using molecular sieve 5A (6m, 1/8" ID). These long column lengths were required as the analysis was run isothermally at 140°C to reduce the tailing of the water peak. The injector block and the valve were also kept at this temperature to prevent any condensation of the water vapour. The carrier gas was helium at a pressure of 600 kPa and a flowrate of 20 ml/min at atmospheric pressure.

Gas sampling from the reactor was performed using a Precision Sampling 0.5 ml Pressure-Lok syringe fitted with a reproducibility adapter set at a sample size of 0.1 ml. The sampling method was to insert the needle through the septum connected to the reactor and to withdraw a syringe full of gas, and then discard it to the atmosphere. A representative sample could then be obtained by re-insertion of the syringe through the septum.

The mole percentages of the gases present were calculated from the peak areas by normalising, using response factors obtained from calibration using a commercial standard gas mixture and air saturated water vapour. The concentrations were then calculated using the ideal gas law and the measured reactor pressure.

The settings and the time program for the gas chromatograph are given in appendix A.

2.4 Experimental Procedure

A sample of coal (usually 100 grams) was weighed out in the glove-box, and was then quickly transferred to the reactor, whose lid could then be bolted tight. A thin film of silicone grease was used on the neck of the flask and on the rubber washer to aid in sealing. The reactor

was then connected to the rocking mechanism and the motor was started.

The reactor was purged with oxygen-free nitrogen to prevent oxidation from taking place. The nitrogen could be bubbled through pure water or a saturated $ZnCl_2$ solution to dry the coal to different levels. This purging/drying was usually run overnight, except in some cases where very wet or dry coal was required and a shorter or longer period respectively was used.

A run was commenced by starting the data acquisition program and purging the reactor with pure oxygen, which was also passed through the Dreschel bottles. The oxygen purge usually ran for five minutes, resulting in about 90% concentration, but this time could be reduced if a lower initial concentration was required. Gas samples were then taken and analysed at regular intervals on the gas chromatograph. This was continued for eight to twelve hours, when the nitrogen purge was switched on again to stop the oxidation and the associated heat effects which would affect the rest of the experiment.

The heater was then switched on, and the temperature, voltage and current monitored until the temperature stabilised. The heater was then switched off and the reactor temperature recorded until it stabilised once more. This allowed the heat transfer to be recorded under the exact conditions of the experiment. The heating/cooling procedure could be carried out automatically overnight using the timing and switching facilities of the HP3421A Data Acquisition / Control Unit.

2.5 Surface Area Measurement

The adsorption isotherms of carbon dioxide onto the coal at dry ice temperatures were determined using a Quantasorb sorption apparatus manufactured by Quantachrome Corporation. An instrument of this type was first described by Nelsen and Eggertsen (1958). In this apparatus a mixture of carrier gas and adsorbate flows over the sample. On changing the sample temperature, adsorption or desorption occurs, resulting in a change in adsorbate concentration in the gas stream. The concentration change is measured by a pair of thermal conductivity cells. The sorbed volume is obtained by integrating the output from these cells, and comparing this to the signal obtained on injection of a known volume of the adsorbate.

The carrier gas used here was helium, which does not adsorb at dry ice

temperatures because of its very low critical temperature. Carbon dioxide was used as the adsorbate for reasons discussed in 1.4. The coal samples used for the measurement of surface areas were prepared (or "outgassed") by heating them overnight at 110°C in a stream of CO_2. A check was carried out on the effect of longer times, but no significant differences between the surface areas were found.

The refrigerant baths were made from a slush of powdered dry ice and acetone; the temperature was measured using a thermocouple connected to the 3421A system. The standard software voltage-to-temperature conversion was not used as there was some doubt whether it applied at dry ice temperatures (approximately -80°C). A calibration table specifically for low temperatures was used. The gas mixture was purified by passing it through a cold trap placed in a dry ice/acetone bath. This removed any traces of water which could condense on the coal.

As suggested by Mahajan & Walker (1978), the desorption, rather than the adsorption, isotherms were used for the calculation of the surface areas. It was found, due to the microporosity present in the coal, that adsorption of the CO_2 onto the coal required about 30 minutes to reach equilibrium. For this reason a time of at least 45 minutes was allowed for adsorption so that reproducible results could be obtained.

The procedure used for the measurement of the desorption isotherms was to flow a mixture of carbon dioxide and helium over the coal sample (of mass about 0.5g) for at least 45 minutes while immersed in the dry ice/acetone bath. The CO_2 concentration, and thus the relative pressure, was determined from the flowrates of the pure gases as measured by the rotameters on the Quantasorb. The detector electronics were then zeroed and the bath replaced by a beaker of water at room temperature. This produced a signal which was integrated, from which the volume desorbed was calculated by injection of a known amount of pure CO_2. Calibration was necessary at every point because of the non-linear concentration response of the thermal conductivity cells, and also because the cells were not kept at a constant temperature. In this way the desorption isotherm could be constructed over the range of relative pressures from 0.01 to 0.1, which covered the range over which a monolayer on the surface is formed.

The surface areas were then calculated using the straight line form of the BET equation as discussed in 1.4.

CHAPTER 3: MATHEMATICAL ANALYSIS OF SYSTEM

3.1 Energy Balance - Reaction Runs

The energy balance describing the system can be written as

$$\frac{dT}{dt} = -\frac{1}{C_p}\sum_{r=1}^{R}\Delta H_r\frac{de_r}{dt} - \frac{U}{C_p}(T-T_s) \qquad \ldots 3.1$$

where C_p is the heat capacity of the reactor and contents, ΔH_r the heat of reaction for reaction r, U the heat transfer coefficient, t the time, T the reactor temperature and T_s the temperature when reaction reaches steady state. The derivation of this expression and the simplifying assumptions are detailed in appendix D.1.

The above expression is simplified by assuming that the only significant heat-producing reaction is the oxidation of coal, thus removing the summation sign. The extent of reaction can be replaced by the oxygen concentration using the definition in appendix D.1, thus

$$\frac{de}{dt} = -V\frac{dC}{dt} \qquad \ldots 3.2$$

with V the reactor volume and C the oxygen concentration. The minus sign arises as the oxygen is a reactant whose stoichometric coefficient is assigned the value unity.

Thus 3.1 above becomes

$$\frac{dT}{dt} = \frac{VAH}{C_p}\frac{dC}{dt} - \frac{U}{C_p}(T-T_s) \qquad \ldots 3.3$$

3.2 Energy Balance - Heat Transfer Runs

The heat transfer characteristics of the reactor were determined as described in 2.4. An analysis of the energy balance under these conditions is presented below.

3.2.1 Heating

In this portion of the experiment the heater is switched on and the

temperature, voltage and current measured until steady state is reached. The reactor is filled with nitrogen to prevent heat effects due to oxidation.

The energy balance at steady state with the heater on is

$$U\,(T_h - T_s) = IV \qquad \ldots 3.4$$

where T_h is the steady state temperature when the heater is on, and I and V are the current and voltage passing through the heater. This allows the heat transfer coefficient U to be determined.

3.2.2 Cooling

Once stabilisation of the temperature with the heater on was reached, the current was switched off and the decay back to the steady state temperature T_s was measured.

Equation 3.3 in this case simplifies to

$$\frac{dT}{dt} = -\frac{U}{C_p}(T - T_s) \qquad \ldots 3.5$$

This linear first order differential equation can be solved to give

$$T = T_s + (T_i - T_s)\exp\left[-\frac{U}{C_p}(t - t_i)\right] \qquad \ldots 3.6$$

where T_i is the temperature at some initial time t_i. The time constant for the reactor was determined from a log plot of $T - T_s$ versus t, which from the above equation should be a straight line with a slope of $-U/C_p$.

3.3 Calculation of the Heat of Reaction

If the reactor was adiabatic, the energy balance would be

$$\frac{dT_{ad}}{dt} = \frac{V\Delta H}{C_p}\frac{dC}{dt} \qquad \ldots 3.7$$

If the rise in temperature during the course of the reaction is small, the rate of reaction and hence the oxygen concentration will not be significantly affected by the temperature change. The concentration derivatives in 3.3 and 3.7 will thus be the same, therefore on substitution

$$\frac{d(T_{ad}-T)}{dt} = \frac{U}{C_p}(T-T_s) \qquad \ldots 3.8$$

Integrating:

$$T_{ad} = T + \frac{U}{C_p}\int_{t_o}^{t}(T-T_s)\,dt' \qquad \ldots 3.9$$

where t_o is the time of starting the reaction and t' is a dummy variable. The program used for the calculation of the corrected curves is in appendix B.1.

The adiabatic energy balance 3.7 above may also be integrated from time t_o when the temperature and concentration are T_o and C_o. This results in

$$T_{ad}-T_o = \frac{V\Delta H}{C_p}(C-C_o) \qquad \ldots 3.10$$

Thus a plot of the adiabatic temperature rise versus the concentration drop should be a straight line passing through the origin with a slope of $V\Delta H/C_p$. The computer program used for this is reproduced in appendix B.2.

3.4 Calculation of Rates of Reaction

If an expression for the rate of reaction is known, the kinetic parameters can be determined by non-linear regression on the integrated form of 3.3. This technique was used by Glasser and Williams (1971) for measurement of the rate constant and activation energy of acetic anhydride hydrolysis. When the kinetics are unknown, rate expressions must be postulated, and then non-linear regression on the integrated mass and energy balances must be carried out. A comparison of the best-fit temperature-time and concentration-time curves will then show whether the kinetic expression is satisfactory.

The drawback of this method is that the integrated expressions have very similar shapes, and thus the best-fit plots will look much the same. An alternative approach is to compare the measured rates to the postulated kinetics expressions directly, which allows better discrimination between the different kinetic models. The problem here is that the integrated form of the rate is measured, meaning that differentiation of the experimental data is required, which could lead to magnification of errors. This approach is suitable here as the tem-

perature-time curves are not subject to much noise and consist of many points (typically 400 per curve).

The rate of reaction is defined as

$$r = -\frac{dC}{dt} \qquad \ldots 3.11$$

Substituting in 3.3 and rearranging:

$$r = -\frac{\frac{dT}{dt} + \frac{U}{Cp}(T-T_s)}{\frac{V\Delta H}{C_p}} \qquad \ldots 3.12$$

The rate as a function of time for an experimental run can thus be calculated from the above expression. This can be converted to a function of concentration by interpolation with the concentration-time curve.

The numerical differentiation was performed by fitting a polynomial to a group of adjacent points, and then differentating the fitted polynomial at the midpoint of this group of points. This technique smooths the points, while at the same time preventing later portions of the curve from interfering with the earlier ones and *vice versa*. The amount of smoothing can be adjusted by changing the degree of the polynomial or the number of points in each group. Quadratics fitted over twenty points were found to be satisfactory.

The program used for this is reproduced in appendix B.3.

3.5 Non-linear Regression

The kinetic parameters may be estimated from the differential equations in concentration and temperature using a modification of the Gauss-Newton method described by King (1967). In this technique a set of additional differential equations is solved to obtain the derivatives of the dependent variables (in this case temperature and concentration) with respect to the parameters. The values of these derivatives at the experimental data points are known as the sensitivity coefficients (or the sensitivity matrix if put into matrix form). The use of the sensitivity matrix to obtain the variance-covariance matrix and other statistical information about the parameters is discussed by Beck & Arnold (1977).

The algorithm of King (1967) was implemented in a computer program discussed in appendix B.4. This program was written in a general format so that only the kinetic expressions and the appropriate derivatives would have to be changed when comparing different rate models. Statistical information (the variance-covariance matrix, standard errors and the correlation matrix) at the best-fit parameter values are also calculated.

At the first concentration data point the temperature curve was affected by the flushing of the reactor with oxygen, thus the initial condition used in the solution of the differential equations was at some later time, where this effect had died away. The concentration at this point was obtained by linear interpolation.

CHAPTER 4: EXPERIMENTAL RESULTS: CONCENTRATION, AGEING AND PARTICLE SIZE EFFECTS

4.1 Surface Area Results

The specific surface areas of the various size fractions of the coal were determined as described in 2.5, and summarized in table 4.1 and figure 4.1 below. An indication of the error present in these results is given by the replicate runs performed on the -180+125μm coal. The isotherms and typical straight-line plots are given in appendix 3. The monolayer volumes were converted to surface areas by taking the area of a CO_2 molecule as 0.17 nm^2 (the value suggested by Gregg & Sing, 1967). The exact numerical value is not too important here as all that is required is a relative ranking of the areas.

Table 4.1 Specific surface areas

Particle size range /μm	Geometric mean particle size/μm	Specific surface area/m^2g^{-1}
-45	30*	96.2
-63+ 45	53	89.2
-90+ 63	75	79.2
-125+ 90	106	62.8
-180+125	150	47.8,49.9,50.8 average 49.5
-355+250	298	45.7
-500+355	421	35.8
-710+500	596	32.5

*mean particle size assumed.

The specific surface area of a non-porous sphere with density ρ and radius r is $3/\rho r$. Taking ρ=900 kg/m^3 and r=30 nm gives an area of only 0.1 m^2/g, as compared to the measured area of almost 100 m^2/g. This indicates the large porosity present in the coal. Most of the pores must have very small openings to obtain this large area (this is backed up by the fact that a large amount of adsorption occurs even at relative pressures as low as 0.01).

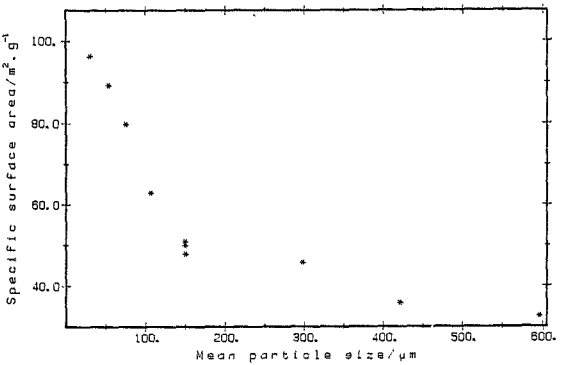

Figure 4.1 Variation of specific surface area with particle size

If the coal was very porous, it would be expected that the surface area would be independent of the particle size, which is not indicated by these results. The shape of figure 4.1 shows that many pores are blind, and can only be exposed if the particle size is reduced. Thus the variation of the area is steep for small particles, and flattens out for the larger sizes - as shown by figure 4.1.

4.2 Kinetic Study Results

4.2.1 Reaction conditions

A series of runs for the different particle sizes at various initial oxygen concentrations was carried out. All runs were conducted at the same moisture content and initial temperature of approximately 20°C. The humidity level was kept constant by bubbling the gases through a saturated zinc chloride solution before entering the reactor. The mass of coal in each case was 100 grams (weighed in the glovebox under saturated humidity conditions). The conditions are summarized in table 4.2 below.

Table 4.2 Experimental conditions for runs 1-1 to 1-7

Run number	Particle size range/μm	Initial O_2 concentration/mol m^{-3}	Steady state temperature T_s/°C
1-1	-180+125	27.0	80.39
1-2	-180+125	52.3	80.65
1-3	-180+125	11.3	79.72
1-4	-63+45	48.9	80.09
1-5	-500+355	50.7	79.94
1-6	-710+500	53.3	80.39
1-7	-125 90	35.3	79.44

The steady state temperature T_s was determined as the average of a group of temperatures measured when the reactor had been flushed with nitrogen and allowed to stabilize. The average oven temperatures during reaction, and during the period when T_s was being measured, were also calculated. These temperatures were usually not exactly equal due to controller drift, but were in all cases less than 0.1°C. The difference of these temperatures was added to T_s to obtain the steady-state temperature during reaction.

4.2.2 Heat transfer from reactor

The heat transfer coefficient U and heat transfer time constant U/C_p were determined using the techniques mentioned in 3.2, for a blank run and for the runs (except 1-3) of table 4.2 above. As the reaction conditions should not affect the heat transfer, the values were averaged for use in later calculations. From table 4.3 below, it can be seen that the heat transfer characteristics are well determined as there is not much variation over the series of runs.

From the data of the blank run the heat capacity of the reactor is:

$$0.187 \;/\; 0.0503 \times 60 = 223 \text{ J K}^{-1}$$

The average heat capacity of the coal is thus:

$$[0.189 \;/ 0.02261 \times 60 - 223] \;/\; 100 = 2.79 \text{ J K}^{-1}\text{g}^{-1}$$

Table 4.3 Heat transfer characteristics of reactor

Run number	Heat transfer coefficient U /WK^{-1}	Heat transfer time constant U/C$_p$ /min^{-1}
Blank run	0.187	0.0503
1-1	0.189	0.02194
1-2	0.184	0.02194
1-4	0.188	0.02353
1-5	0.188	0.02258
1-6	0.191	0.02337
1-7	0.191	0.02273
Average (reaction runs)	0.189	0.02261

4.2.3 Correction to adiabatic curves

The temperature-time curves that would have been measured, had there been no heat loss from the reactor, but with the reaction still taking place at the experimental conditions (the "adiabatic" curves), were calculated for the runs mentioned above. The procedure used is given in 3.3, and as the maximum experimental temperature rise was only 2.5°C, the true adiabatic curves and these curves will be very similar. The curves will only differ when the temperature change is large enough to affect the rate constant.

The corrections required to obtain the adiabatic curve were found to be very large, as the rate of heat loss is larger than the rate of heat generation, except in the initial stages of the reaction. The "adiabatic" temperature plots were calculated for a typical run of table 4.2, for the experimental value of T_s, as well as deviations from this temperature by 0.1°C. This small error was found to affect the corrections to a large extent. As explained above, this is due to the poor heat transfer characteristics of the reactor. A plot of these curves, together with the experimental data, is given as figure 4.2 below.

4.2.4 Calculation of the heat of reaction

The heat of reaction of the oxygen with the coal can be calculated using the technique discussed in 3.3, and the computer program in ap-

pendix B.2. To check the sensitivity of this procedure to variations in T_s, the ΔT_{ad} versus ΔC plots for the curves of figure 4.2 above were constructed (see figure 4.3 below). A change in T_s of only 0.1°C changes the slope of the plot by about 12%. At the same time the fit obtained does not appear to be affected much. The heats of reaction obtained by this method will thus not be accurate because of the slight variation in the oven temperature.

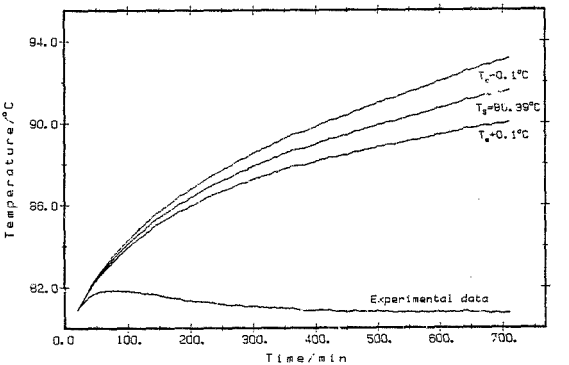

Figure 4.2 Corrected curves for various T_s (data of run 1-1)

The values obtained for VAH/C_p are summarized in table 4.4 below. With the exception of run 1-1, the deviation from the average is not too large. The reactor volume is 1.87 litres, and the combined heat capacity of the coal and reactor from 4.2.2 is

$$0.189 \ / \ 0.02251 \times 60 = 502 \ J/K.$$

The heat of reaction is thus:

$$1.25 \times 502 \ / \ 1.87 = 335 \ kJ \ / \ mol = 80 \ kcal/mol.$$

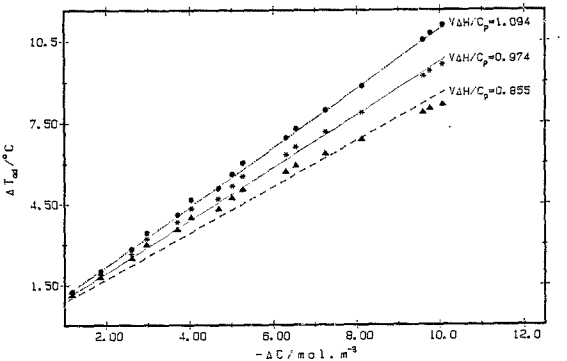

Figure 4.3 Sensitivity of method used for $V\Delta H/C_p$ to changes in T_s

Table 4.4 Values of heat of reaction term for runs 1-1 to 1-7

Run number	1-1	1-2	1-3	1-4	1-5	1-6	1-7	Average
$V\Delta H/C_p$ $m^3.K.mol^{-1}$	0.974	1.36	1.47	1.15	1.24	1.27	1.28	1.25

Sondreal & Ellman (1974) found the heat of reaction to vary from 75 kcal/mol at 25°C to 90 kcal/mol at 90°C, which brackets these results. Itay's (1983) value was 120 kcal/mol, which is considerably different, even though the coal in his work and this work are from the same mine.

4.3 Effect of Oxygen Concentration on the Initial Rate

The initial rates of reaction for runs 1-1, 1-2 and 1-3 were calculated using the method described in 3.4. The experimental conditions, except for the initial oxygen concentration, were the same. The rates were all calculated at the second concentration data point, as the

temperature curve at the first data point was affected by the flushing through of the reactor with oxygen. All three samples of coal had thus undergone about 25 minutes of oxidation at the reaction temperature.

The rates, together with the concentrations at which they were measured, are reproduced in table 4.5 below. In addition the temperature-time derivative and the corresponding rate of heat loss are shown.

Table 4.5 Initial rates for runs 1-1, 1-2 and 1-3

Run number	1-1	1-2	1-3
Concentration/mol m^{-3}	25.5	52.3	10.7
dT/dt /K min^{-1}	0.02661	0.03553	0.01298
UAT /K min^{-1}	0.02479	0.02659	0.01289
Rate /mol m^{-3} min^{-1}	0.0412	0.0498	0.0206

A plot of the initial rate against the concentration (figure 4.4 below) would be a straight line if the reaction rate was first order. The plot in this case shows distinct deviations from linearity. These deviations are more than any experimental error in determining T_s, as can be seen from the relative magnitudes of the temperature-time derivative and heat loss terms. A change in T_s of $0.1^{o}C$, which affects the heat of reaction greatly as shown earlier, only changes the initial rate slightly in this case as the temperature-time derivative is not affected.

It must thus be concluded that the reaction kinetics are non-linear. Previous studies in this area (see 1.7.2) have suggested that chemisorption is important in the initial stages of the reaction. This was supported by Itay (1983), who found that carbon monoxide, and to a lesser degree carbon dioxide, inhibited the reaction. This result can be explained on the basis of chemisorption, where the oxygen and carbon monoxide (and also carbon dioxide, but to a lesser extent due to its lower activity) compete for the same reaction sites.

An analysis of this situation leads to a single-site, first-order Langmuir-Hinshelwood type mechanism, which can be described mathematically as: (Carberry, 1976)

$$r = \frac{kC}{1 + KC}$$

At low concentrations this behaves like a first order reaction, but as the concentration increases the rate flattens off and asymptotes to $1/K$ as $C \to \infty$. Over a limited concentration range, this model may be approximated by:

$$r = kC^n \quad \text{where } n < 1$$

which does not asymptote as the concentration increases.

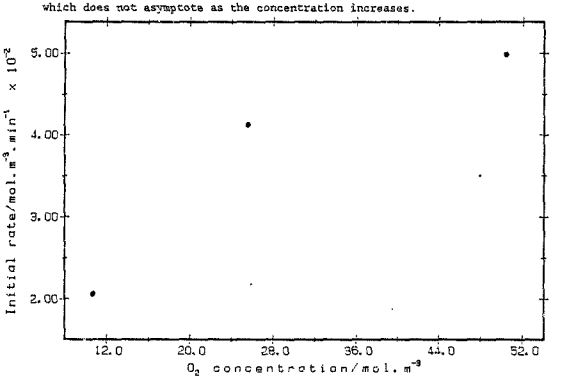

Figure 4.4 Initial rates as a function of concentration for runs 1-1, 1-2 and 1-3

The initial rates were fitted to the Langmuir-Hinshelwood model (by plotting $1/r$ versus $1/C$, from which the slope is $1/k$ and the intercept K/k), and to the power-law model (by plotting log r against log C, with slope n and intercept log k). The results are:

Langmuir-Hinshelwood: $k = 2.5 \times 10^{-3}$ min^{-1} $K = 2.66 \times 10^{-3}$ m^{3}mol^{-1}
Power-law: $n = 0.58$ $k = 5.51 \times 10^{-3}$min^{-1}

The agreement of these two models with the experimental data is shown in figure 4.5. Both models appear to be equally adequate, but no real conclusions can be drawn as only three data points are available.

4.4 Modelling of the Ageing Effect

4.4.1 Model formulation

As discussed in 1.7.3, several researchers have found that the reaction is limited to near the surface, and that "oxidation rims" of the reacted coal are formed. Itay (1983) accounted for the ageing effect by considering the rate of diffusion of oxygen through the oxycoal to be equal to the rate of reaction (assumed to be first order). A similar analysis for Langmuir-Hinshelwood kinetics will be carried out here. Only the oxygen reaction will be considered as it is the major heat-producing reaction.

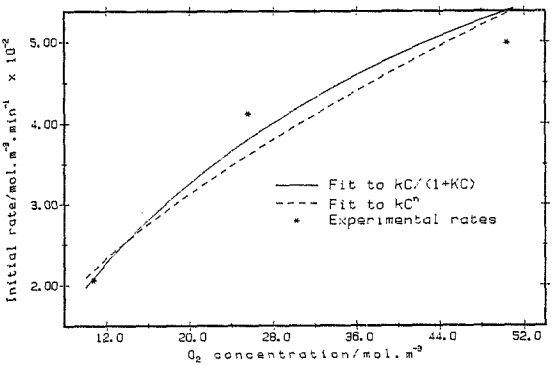

Figure 4.5 Fit of kinetic models to initial rates

To simplify the analysis, the reduction in area due to the shrinking of the reacted core will be ignored. This assumption (known as the "flat-plate" assumption) has been shown to have negligible error for conversions of less than 30% (Carberry, 1976). The amount of reaction with the coal is small, thus this simplification may be used.

The rate of diffusion of oxygen through a thickness Δx of the reacted coal is:

$$r = \frac{SD}{\Delta x} (C - C_s) \qquad \ldots 4\text{-}1$$

where S is the external surface area
D is the effective diffusion coefficient
C_s is the oxygen concentration at the surface
C is the bulk oxygen concentration

At the interface between the reacted and unreacted coal, the rate of reaction is:

$$r = \frac{SkC_s}{1+KC_s} \qquad \ldots 4\text{-}2$$

where k,K are the Langmuir-Hinshelwood constants.

The amount of oxycoal formed is directly proportional to the drop in oxygen concentration, thus:

$$V (C_o - C) = S \rho_m \Delta x \qquad \ldots 4\text{-}3$$

where V is the reactor volume
C_o is the initial oxygen concentration
ρ_m is the molar density of the reactive groups

The capacity of the reacted layer for oxygen is much smaller than that of the reactive layer, thus the oxygen concentration through the reacted layer may be considered to be at steady state. This is known as the "pseudo steady-state" assumption.

From equations *4-1*, *4-2* and *4-3*, together with the pseudo steady-state assumption, it can be shown that:

$$\frac{dC}{dt} = \frac{-\alpha SD}{C_o - C}\left[C - \frac{-\beta + \sqrt{\beta^2 + 4KCa^2D^2}}{2KaD} \right] \qquad \ldots 4.4$$

where $\alpha = S/V$

$D = D\,\rho_m$

$\beta = \alpha D\,(1-KC) + k(C_o - C)$

The detailed derivation of equation 4-4 above is given in appendix D.2.

4.4.2 Fitting combined kinetic/ageing model to experimental data

In order to test whether the equation above is valid, non-linear regression on the experimental concentration-time curves is required. A brief description of this method is given in 3.5, and the computer program together with the statistical assumptions required is listed in appendix B.4.

The method simultaneously fits both the temperature-time curve (described by the energy balance, equation 3.3), and the rate expression 4-4 above, by minimizing the weighted sum of squared errors. The weighting factors used were the inverses of the squares of the errors in the temperature and concentration data. The error in the temperature points was taken as the standard deviation of the data which was used to calculate the steady-state temperature; this was found to be about approximately 0.015°C, which is the limit of the resolution of the digital voltmeter/thermocouple combination. The concentration error was set equal to the standard deviation of the nitrogen concentration values measured during a typical run. The standard deviation of the concentration data was approximately eleven times larger than that of the temperature, indicating the greater accuracy of the temperature measurements.

Attempts were made to fit the rate expression 4-4 above to the experimental data of table 4.2, but satisfactory convergence could not be achieved. This was due to the optimization routine taking very large steps in the directions of k and K, which shows that the sum of squares surface is not very sensitive to these parameters. In physical terms this means that these concentration-time and temperature-time curves are not affected much by changes in the kinetic con-

stants, but only by changes in the diffusion term D, i.e. the reaction is diffusion limited.

This analysis is supported by the plot of the rate (as a function of concentration) as the reaction proceeds (figure 4.6 below). This plot, for runs 1-1, 1-2 and 1-3, shows that the reaction rate drops off sharply as the reaction proceeds, and that it does not follow the form suggested by the fit of the initial rates at all.

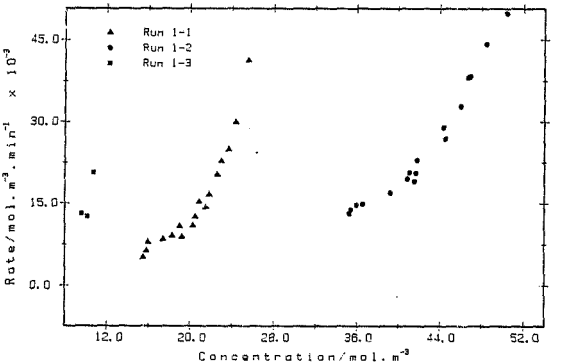

Figure 4.6 Drop in rate as reaction proceeds (runs 1-1, 1-2 and 1-3)

4.4.3 Diffusion-limiting model

As shown in the previous section, the rate of reaction appears to be controlled by the rate of diffusion of the oxygen to the reacting front. The rate expression for this model will now be formulated and fitted to the experimental data. The rate equation in this case is obtained from equations 4-2 (with the surface concentration set to zero) and 4-3. In appendix D.3, this is shown to result in :

$$\frac{dC}{dt} = - \frac{\alpha SDC}{C_o - C} \qquad \ldots 4\text{-}5$$

with the symbols defined as before.

The parameter αSD in equation 4-5 above was then estimated using the non-linear regression technique as described previously. The best-fit parameters for runs 1-1 to 1-7 are given in table 4.6 above. The fits obtained for run 1-1 are shown in figures 4.7 and 4.8, and are typical of the results for the whole series of runs. All the fits and the statistical details are shown in appendix E.

The standard error in the table below is the standard deviation of the fitted parameter expressed as a percentage of the value of that parameter. As all the standard errors are small, the best-fit parameters are well defined. This means that a small change in the data will not change the parameters much.

The fitted temperature curve for run 1-1 initially rises quicker than the experimental curve, then peaks before the experimental data and then drops below the experimental curve. The concentration curve, which was fitted simultaneously with the temperature, mirrors this behaviour: initially it drops as quickly as the experimental data, and then flattens out while the experimental curve carries on dropping. The fits for the other runs also display this type of behaviour.

Table 4.6 Best-fit parameters for diffusion-limiting model

Run number	Mean particle size d/μ_m	αSD / $mol.m^{-3}.min^{-1}$	Standard error / %
1-1	150	2.67×10^{-3}	0.08
1-2	150	3.27×10^{-3}	0.15
1-3	150	1.19×10^{-3}	0.67
1-4	53	6.74×10^{-3}	0.22
1-5	421	6.12×10^{-3}	0.28
1-6	596	2.92×10^{-3}	0.13
1-7	106	1.86×10^{-3}	0.68

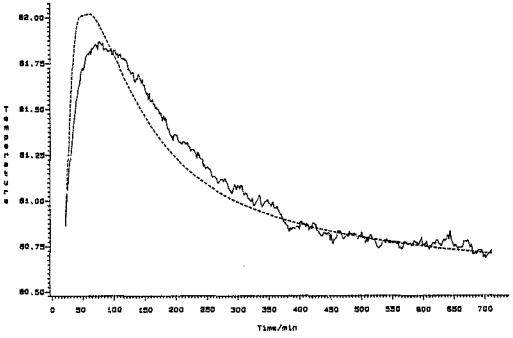

Figure 4.7 Fit of diffusion-limiting model to temperature data of run 1-1

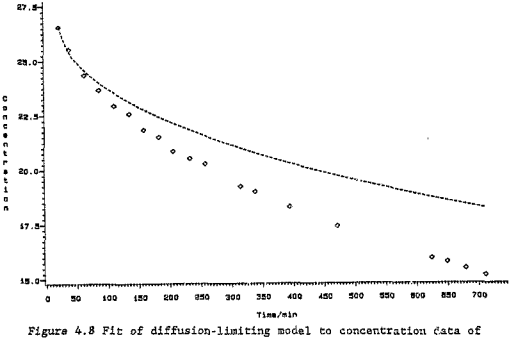

Figure 4.8 Fit of diffusion-limiting model to concentration data of run 1-1

The reason for this poor agreement is that the diffusion-limiting model predicts the rate as dropping off sharply as reaction proceeds, while the experimental rate, although it does fall off, does not quite do so in the same manner as the model. In order to minimize the sum of squared errors, the fitted temperature curve first has to rise above, and then drop below, the experimental data. For this reason the best-fit parameters will be found to vary with the reaction time. No agreement between the diffusion coefficients for the runs of table 4.6 can thus be expected.

The parameter used in the minimisation was αSD, which should be proportional to the square of the external surface area. The external surface area is inversely proportional to the particle size (any variation of the particle shape with degree of crushing should be minimal), thus the term αSD should vary with the inverse of the square of the mean particle size. It can be seen that this does not hold, as the αSD is approximately constant, while the particle size changes by a factor of ten. This is due to the model not fitting the data properly, so that the parameter depends on the extent of reaction.

In formulating the model, the "flat-plate" assumption was used. If the decrease in reactive surface area due to reaction was taken into account, an even larger decrease in rate would be found, which is the opposite of the effect observed here. Conversely, the fit could be improved if a model involving some form of increase in the area as reaction proceeds was used. The physical validity of this type of model is doubtful.

One assumption used in the formulation of the diffusion-limiting model was that the coal had not undergone any reaction prior to the experiment. The experimental procedure was designed to prevent this, but it is possible that the precautions taken were not sufficient. If preaging had taken place, this could account for the poor agreement between the model and experiment.

4.4.4 Diffusion-limiting model with pre-ageing

In appendix D.4 it is shown that, when the coal has undergone some previous oxidation, but to an unknown extent, the rate expression becomes:

$$\frac{dC}{dt} = -\frac{\alpha SDC}{C_o' \cdot C} \qquad \ldots 4\text{-}6$$

where C_o' is a fictitious initial concentration, greater than C_o, and the other symbols have the same definitions. The difference between these two concentrations is a measure of the extent of pre-oxidation.

The parameters αSD and C_o' were estimated using the non-linear regression method. The statistical output from the program and the plots of the fits obtained are given in appendix E. The fitted temperature-time and concentration-time curves for run 1-1 are shown in figures 4.9 and 4.10, and are typical of the other runs. The best-fit parameters are given in table 4.7 below, together with the true initial concentration C_o.

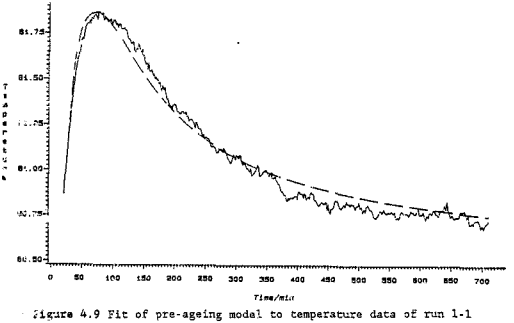

Figure 4.9 Fit of pre-ageing modal to temperature data of run 1-1

The correlation, which can range from zero to one, is a dimensionless representation of the covariance between the parameters. A large correlation implies that a small change in the data will affect the values of the best-fit parameters significantly, without affecting the fit obtained.

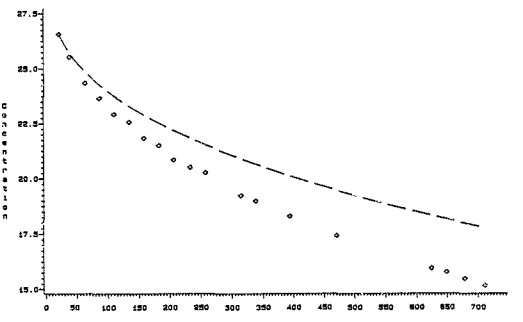

Figure 4.10 Fit of pre-ageing model to concentration data of run 1-1

Table 4.7 Best-fit parameters for pre-ageing model

Run number	αSD / $mol.m^{-3}.min^{-1}$	C'_o / $mol.m^{-3}$	C_o / $mol.m^{-3}$	Correlation
1-1	3.58×10^{-3}	28.0	27.0	0.19
1-2	8.75×10^{-3}	59.4	52.3	0.33
1-3	2.88×10^{-3}	12.3	11.3	0.86
1-4	18.1×10^{-3}	56.8	48.9	0.46
1-5	26.7×10^{-3}	68.9	50.7	0.66
1-6	7.06×10^{-3}	59.7	53.3	0.33
1-7	3.31×10^{-3}	36.9	35.3	0.79

From the data of table 4.7, it can be seen that this model is not a valid description of the coal oxidation as either a large increase in the initial concentration is found, or else there is a large correlation between the parameters. The agreement with the experimental data is in most cases no better than that for the previous model.

The pre-ageing model is thus no improvement over the previous model.

4.5 Discussion

The analyses of the experimental data carried out in 4.3 and 4.4 show that the kinetics of the reaction can be approximated as diffusion-controlled. Allowing for pre-oxidation of the coal does not improve the model. It is possible that the rate of reaction is determined by some process other than pore diffusion control, and that this process looks very similar to the models investigated here. A model-free analysis of the experimental data showed that the rate dropped off very sharply as the amount of oxidation increased. This also revealed that the rate, expressed as a function of concentration as the reaction proceeded, in no way mirrored the trend of the initial rates plotted as a function of concentration.

In the derivation of the kinetic expression, it was assumed that no change in reactive area, or in the diffusion coefficient, would be found as the amount of reaction increased. Relaxing the first assumption, the "flat-plate" assumption, to allow a decrease in the reactive area as the amount of oxidation increases will make the fits worse due to the larger decrease in the rate as the amount of oxidation increases.

Allowing the area to increase with the amount of oxidation would give the same rate trend as for the experimental data. This type of behaviour is found when a highly porous solid is completely converted to gas, and is thus not applicable here as a solid product is formed.

If the diffusion coefficient increased during the run, a better fit to the experimental data would be obtained. An apparent increase could be caused by the formation of cracks. Allowing for the effects of a pore size distribution would give an apparent decrease in the diffusion coefficient since the largest pores react first, then the smaller ones with the larger diffusion resistance. This is the opposite of the measured effect.

A more complicated model than simple diffusion-controlled kinetics is thus required in order to account for the ageing and particle size effects on the rate of oxidation. Pore diffusion is likely to be a major effect in any model as the coal has a lot of very small pores (leading to a large surface area), and these pores will have a high diffusional resistance.

CHAPTER 5: EFFECT OF COAL MOISTURE CONTENT ON THE RATE OF REACTION

5.1 Experimental Results

The experiments carried out for this section are detailed in table 5.1 below. The mass of coal used in each case was 150 grams (weighed under saturated humidity at 20°C in the glove box). The different humidity levels were obtained either by bubbling the oxygen and nitrogen supplies to the reactor through pure water or saturated zinc chloride solutions, or by bypassing the bubblers. Extremely dry conditions were obtained by purging the reactor with dry, oxygen-free nitrogen for long periods (up to several days), and wet conditions by purging the reactor for only an hour, and then sealing it, the water being supplied by desorption as the coal heated up.

The heat-transfer time constant U/C_p and heat transfer coefficient U were determined as described previously. From these results, together with the blank run results of appendix C, the specific heat capacity of the coal was calculated. These results are summarized in table 5.2 below, together with the values of the term VAH/C_p calculated for a heat of reaction of 335 kJ/mol as measured previously.

Table 5.1 Experimental conditions for runs 2-1 to 2-6

Run number	T_s/ °C	Coal particle size/μm	Drying conditions	Moisture level in reactor gas
2-1	60.73	-45	dry N_2 purge overnight	1 %
2-2	60.78	-45	purge saturated with water vapour at 20°C	2.5 %
2-3	66.95	-90+63	purge saturated with water vapour at 20°C	2.5 %
2-4	67.45	-90+63	purged for 2 hours, then sealed	10 %
2-5	67.46	-90+63	dry purge at 80°C for 2 days, then 60°C overnight	0.5 %
2-6	67.42	-90+63	coal left for 6 weeks in N_2 atmosphere, dried by concentrated sulphuric acid, then dry N_2 purge at 60°C overnight	0 % (initially)

Table 5.2 Heat transfer data for runs 2-1 to 2-5

Run number	U/C_p / min^{-1}	U / WK^{-1}	C_p / $J.K^{-1}.g^{-1}$	$V\Delta H/C_p$ / $m^3.K.mol^{-1}$
2-1	0.01404	0.0975	4.17	1.50
2-2	0.01315	0.1070	4.88	1.28
2-3	0.01757	0.1347	4.60	1.36
2-4	0.01295	0.1372	6.36	0.95
2-5	0.02005	0.1282	3.84	1.63

As shown by the table above, the specific heat capacity is a direct function of the moisture content of the coal. The effect of the moisture level on the specific heat capacity is due to the high heat capacity of water. The heat transfer time constant for run 2-6 was not measured, as during the course of this experiment, water was injected into the reactor, which changed the heat capacity and the associated variables. The coal of run 2-6 was drier than that of run 2-5, thus the heat capacity was assumed to be approximately 3.5 $J.K^{-1}.g^{-1}$ for use in later calculations. The heat transfer coefficient U, which is independent of the moisture level, was taken as the average of the values for runs 2-3, 2-4 and 2-5, thus, for run 2-6

$$U/C_p = 0.0229 \text{ min}^{-1} \text{ and } V\Delta H/C_p = 1.79 \text{ m}^3 \text{ K mol}^{-1}$$

5.2 Effect of Moisture on Rate

The rate of reaction was determined as discussed in 3.4 for runs 2-1 and 2-2. The rate-concentration curves are plotted in figure 5.1 below. The major difference between these two runs is the moisture content: the overnight nitrogen purge for run 2-2 was bubbled through pure water, while the overnight purge for run 2-1 bypassed the bubbler. In addition, the oxygen supply to the reactor was passed through the bubblers for run 2-2, and bypassed them for run 2-1. The same humidity level was thus found in the oxygen as in the nitrogen during the purging/equilibration period, which prevented any adsorption or desorption of water from occurring during the run. A minor difference between these two runs is that the initial oxygen concentration was not exactly the same due to experimental limitations (C=30.6 $mol.m^{-3}$ for 2-1 versus C=34.1 $mol.m^{-3}$ for 2-2), but this slight difference is

not important in isolating the trend of the results.

From figure 5.1 it can be seen that the rate of reaction for the drier coal (run 2-1) is higher than that for the wetter coal (run 2-2), even though the initial oxygen concentration for run 2-2 was slightly larger. The difference in the initial rates ($r=0.023$ mol.m^{-3}.min^{-1} @ $C=31.5$ mol.m^{-3} for run 2-1; and $r=0.018$ mol.m^{-3}.min^{-1} @ $C=34.6$ mol.m^{-3} for run 2-2), is more than can be caused by errors in T_s or $V\Delta H/C_p$. It must thus be concluded that in this case the additional moisture in the coal results in a lower rate than is found for the dry coal.

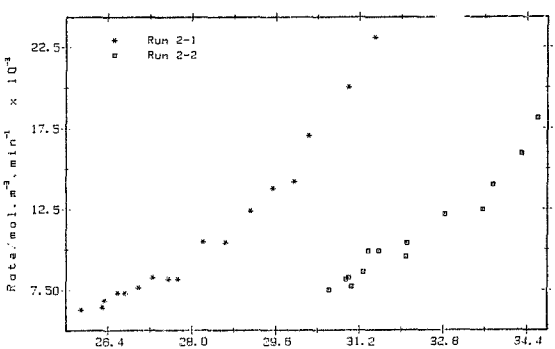

Figure 5.1 Rate-concentration plot for runs 2-1 and 2-2

Additional experiments (runs 2-2 to 2-6 in tables 5.1 and 5.2 above), at a higher temperature, and at four different moisture levels, were carried out in order to confirm this result. An attempt was made to keep th oxygen concentration constant over these runs, but the initial oxygen concentration for run 2-5 was considerably higher than the rest, while the others were much the same. The rate-concentration curves are shown in figure 5.2.

The most reactive coal was that of run 2-3, which was equilibrated with nitrogen saturated with water vapour at 20°C. The lowest rates were found for run 2-6, where the coal was exposed to concentrated sulphuric acid in an oxygen-free nitrogen atmosphere for six weeks. On the addition of a small amount of water (0.1 ml), an increase in the rate (as determined by the technique discussed in 3.4), was found.

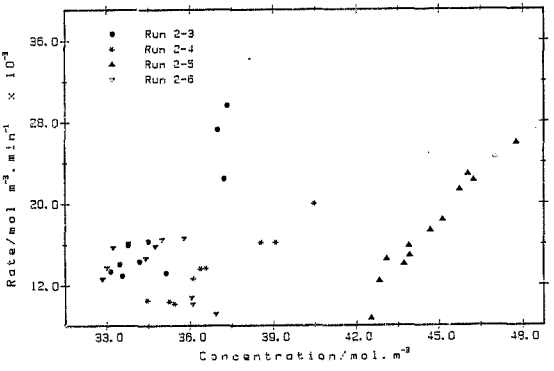

Figure 5.2 Rate-concentration plot for runs 2-3 to 2-6

The injection of the water led to an increase in the temperature, which could have been due to the heat of wetting and/or an increase in the rate of oxidation. The oxygen concentration curve would show the effect of an increase in the rate, but not any heat of wetting effects. The experimentally measured oxygen concentration curve, with the concentrations expressed on a water-free basis, does not show any significant change at the point where the water was added, thus the apparent increase in rate is due only to the temperature increase caused by the heat of wetting. The concentration data are noisy, thus this result is not conclusive.

The rates of reaction for the very wet coal (run 2-6) and for the dry

coal (run 2-5) are both lower than the rate for run 2-3 (where the coal moisture was intermediate), even though the initial concentrations are larger. The differences in rates between these runs are larger than experimental error, thus there is a maximum in the rate at different moisture contents.

5.3 Discussion

At very low and very high moisture contents the coal oxidises slowly, with the maximum rate being found at some intermediate point. In addition to this there is a large heat of wetting for water on coal, which can lead to a temperature rise even when oxidation is not occurring.

The reasons for the rate, as a function of the moisture content, exhibiting a maximum are not known. It is possible that water acts as a catalyst in the oxidation, but a sharp increase in the rate was not found when water was injected into the reactor. Also, this reason does not agree with the work of the previous chapter, where it was found that the oxidation was probably diffusion-controlled, and thus independent of the kinetics. The shrinkage and swelling of coal on the desorption and adsorption of water vapour is well documented (Allardice & Evans, 1978), and this could account for the increase in the rate from low to intermediate moisture levels, as the diffusional resistance would be reduced. At very high moisture levels blocking of the pores could occur, leading to a drop in the rate, which would account for the maximum.

CHAPTER 6: CONCLUSIONS

The main limitation of the experimental method used here is the large heat transfer coefficient of the reactor, which meant that the oxidation had to be carried out on relatively fine coal particles at relatively high temperatures, as compared to those found in practical situations. The experimental apparatus could be improved by reducing the rate of heat loss from the reactor. The only way to achieve this appears to be in the use of an improved Dewar flask, which is difficult to construct due to the constraint on the heat capacity.

The investigation of the effect of the oxygen concentration on the initial rate of reaction showed that the reaction kinetics were non-linear, and could be fitted by a Langmuir-Hinshelwood type expression. The concentrations found in practice are much lower than those used in this study, thus it is possible that the initial rates could be approximated as a linear function of the concentration, but this depends on the characteristics of the particular coal. This nonlinear kinetic expression suggests that chemisorption controls the initial rate of reaction.

Modelling of the ageing effect on the low temperature oxidation of coal was attempted, but a satisfactory kinetic expression could not be found. Good approximations to the drop in rate were found using a diffusion-controlled mechanism, but this exhibited too steep a drop in rate as compared to the experimental data. More sophisticated structural models, possibly allowing for cracking of the particle caused by reaction, are required to account for the ageing effect. It is not known whether the amount of ageing measured in this study bears any relation to that encountered in practice as changes to the coal could not be measured. A very different extent of ageing might require another type of model.

The effect of the coal moisture content on the rate of reaction appears to be two-fold: at low moisture levels increasing the moisture level raises the rate of reaction; while at higher coal moisture contents, an increase in the moisture leads to a drop in the rate. The rate of reaction thus exhibits a maximum at some intermediate moisture level. The reasons for this are not known. If the kinetics were pore diffusion controlled, the increase in the rate could be explained by the swelling of coal due to the increased moisture content. This

hypothesis is not easy to test, as the standard methods of determining pore volume involve extremes of pressure or temperature, where the water induced swelling of coal would probably be swamped by other effects.

The drop in reaction rate at high moisture levels is probably due to condensation of water in the pores, which reduces the area available for reaction. The study of the effect of the moisture content on the oxidation rate is complicated by the difficulty experienced in measuring gas-phase water concentrations accurately, and by the problem of defining and measuring coal moisture contents.

The coal used in this study was from the same mine as that used by Itay (1983). Much lower rates of reaction were found here, which could be due either to the natural variation in the coal seam (the studies were two years apart), or else to the lengthy period this coal spent under water (eighteen months) to prevent oxidation by the air while the experimental apparatus was being set up. The underwater storage could possibly have affected the coal properties adversely. All the work in this study concerned this coal, and is thus not representative of all coals.

Before more complex ageing models can be tested, an improved apparatus, or a more accurate method, is required as the accuracy of the present data does not warrant a more sophisticated analysis. If better data becomes available, especially at lower temperatures, the structural effects can be properly investigated, as the implications of the breakdown of the oxycoal complex will be reduced. Analysis of the moisture in the gas will be simpler due to the lower absolute humidity levels. Methods of investigating the structural changes in coal on oxidation or sorption of water must also be investigated.

REFERENCES

Abbott, M.M. & Van Ness, H.C., 1976. *Thermodynamics (Schaum series)*, McGraw-Hill, New York.

Aleksandrov, I.V., Gavrilov, Yu V., & Kamneva, A.I., 1984. *Khimiya Tv. Topliva* [Solid Fuel Chemistry], 18(5), 23-29.

Andersen, N.E. & Hamza, H.A., 1982. In *Coal: Phoenix of the '80s - Proceedings 64th CIC Coal Symposium*, ed. Al Toweel, A.M., pp.117-124.

Allardice, D.J. & Evans, D.G., 1978. In *Analytical Methods for Coal and Coal Products*, Vol I, ed. Karr, C. Jr, pp.247.

Banerjee, S.C., Banerjee, B.D. & Chakravorty, R.N., 1970. *Fuel*, 49, 324.

Beck,J.V. & Arnold, K.J., 1977. *Paremeter Estimation in Engineering and Science*, John Wiley & Sons, New York.

Bhattacharyya, K.K., 1970. *J. Mines Metals Fuels*, 18(1), 5.

Bhattacharyya, K.K., 1972. *Fuel*, 51(7), 214.

Bhattacharyya, K.K., Hodges, D.J. & Hinsley, F.B., 1968. *Min. Eng., Lond.*, 77, 274.

Brunauer, S., Emmet, P.H. & Teller, E., 1938. *J. Am. Chem. Soc.*, 60, 309.

Carberry, J.J., 1976. *Chemical and Catalytic Reaction Engineering*, McGraw-Hill, New York. pp.320.

Carpenter, D.L., & Giddings, D.G., 1964. Fue',43, 375.

Chamberlain, E.A.C., Barass, G. & Thirlaway, J.T., 1976. *Fuel*, 55(7), 217.

Georgiadis, C., & Gaillard, G., 1952. *Chim. et Ind.*, 70, 383.

Glasser, D. & Williams, D.F., 1971. *Ind. Eng. Chem. Fund.*, 10(3), 517.

Gorbaty, M.L., 1978. *Fuel*, 57(12), 796.

Gregg, S.J. & Sing, K.S.W., 1967. *Adsorption, Surface Area and Porosity*, Academic Press, London.

Guney, M., 1971. *CIM Bulletin*, March, 138.

Hedden, K. & Wilhelm, A., 1980. *Ger. Chem. Eng.*, 3, 89.

Itay, M., 1983. Ph.D thesis, University of the Witwatersrand, Johannesburg.

International Union of Pure and Applied Chemistry (IUPAC), 1972. *Manual of Symbols and Terminology for Physico-Chemical Quantities and Units*. Butterworth, London.

Jones, R.E. & Townend, D.T.A., 1946. *Trans. Faraday Soc.*, 42, 297.

Kam, A.Y., Hixson, A.N. & Perlmutter, D.D., 1976. *Chem. Eng. Sci.*, 31(9), 815.

King, R.P., 1967. *S. Afr. J. of Sci.*, March, 91.

Liley, P.E. & Gambill, W.R., 1973. In *Chemical Engineer's Handbook*, 5th edition, ed. Perry, R.H. & Chilton, C.H., McGraw-Hill, Kogakusha.

Mahajan, O.P., 1982. In *Coal Structure*, ed. Meyers, R.A., Academic Press, New York.

Mahajan, O.P. & Walker, P.L. Jr., 1978. *Analytical Methods for Coal and Coal Products*, Vol I., ed. Karr, C. Jr., Academic Press.

Marinov, V.N., 1977. *Fuel*, 56(4), 165.

Marsh, H. & Siemienewska, T., 1965. *Fuel*, 44, 355.

Meyers, R.A., 1982. In *Coal Structure*, ed Meyers, R.A., Academic Press, New York.

Merson, N.T. & Richardson, S.B., 1985. *Coal Preparation*, Vol 2, in press.

Needham, L.W. & Hill, N.W., 1935. *Fuel*, 14, 226.

Nelsen, F.M. & Eggertsen, F.T., 1959. *Analyt. Chem.*, 35, 259.

Nordon, P., Bainbridge, N.W., Szemes, F. & Myers, G., 1985. *J. Phys. E: Sci. Instrum.*, 18, 338.

Porter, H.C. & Ralston, O.C., 1916. *Bu. Mines Tech. Paper 113.*

Schmidt, L.D., 1945. In *Chemistry of Coal Utilization*, Vol I, ed. Lowrey, H.H., Chap 18, John Wiley and Sons, New York.

Scott, E.D., 1971. MSc dissertation, University of the Witwatersrand, Johannesburg.

Sevenstar, P.G., 1959. *Fuel*, 38, 463.

Sondreal, E.A. & Ellman, R.C., 1974. *Report of Investigation 7887*, Bureau of Mines, United States Department of the Interior.

Van Krevelen, D.W., 1981. *Coal*, Elsevier, Amsterdam.

Walker, P.L. Jr. & Kini, K.A., 1965. *Fuel*, 44, 453

Winmill, T.F., 1913. *Trans. Inst. Mining Engrs.*, 46, 563.
1914. *48*, 503, 535.
1915. 51, 493, 510.

Wood, T., 1958. *J. Appl. Chem., London*, 8, 565.

APPENDIX A: EXPERIMENTAL DETAILS

A.1 Gas chromatograph

A printout of the settings and time program used for the Hewlett-Packard 5840A gas chromatograph is given below.

```
TEMP1     175  140   37
TIME1      22.00
INJ TEMP  175  140   25
FID TEMP  400    0   22
TCD TEMP  400  200   28
AUX TEMP  175  140   17

CHT SPD     0.50
ZERO       20.0
ATTN 2↑     2
TCD SGNL    +B
SLP SENS    0.10
AREA REJ          50
FLOW  A    14.6    0.0
FLOW  B    18.6    0.0

 2.90 VLV/EXT       2
 4.50 ZERO         20.0
 6.00 SLP SENS      0.02
12.45 SLP SENS      0.20
12.47 ATTN 2↑       7
12.50 VLV/EXT-      2
14.00 ZERO         20.0
18.90 ATTN 2↑       2
19.00 ZERO         20.0


NORM
  % RTN:   3.00                        CALIB RUNS    1

 CAL  #        RT          AMT              AMT/AREA

 (R) 1      16.37     1.0000 E+ 0      1.0000 E+ 0
     2       3.59     1.0000 E+ 0      5.7220 E- 1
     3       8.70     1.0000 E+ 0      1.7624 E+ 0
     4      15.33     1.0000 E+ 0      1.1358 E+ 0
     5      19.99     1.0000 E+ 0      1.4858 E+ 0

RTL FACTOR: 1.0000 E+ 0
```

A typical chromatogram, with the peaks labelled is:

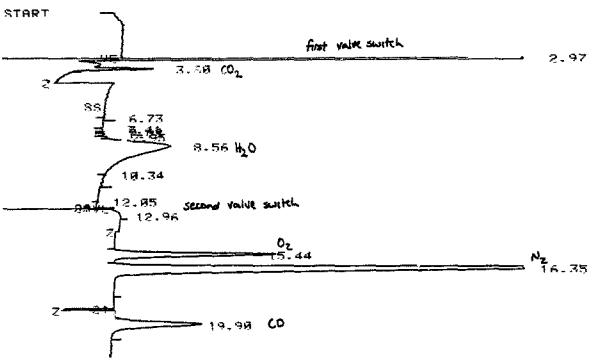

HP RUN # 3
NORM

RT	EXP RT	AREA	CAL #	AMT
3.60	3.58	447	2	0.854
8.56	8.68	4596	3	1.788
15.44	15.31	90120	4	22.415
16.35	16.37	358200	(R) 1	75.183
19.98	19.96	2880	5	0.648

BTL FACTOR: 1.0000 E+ 0

A.2 Data logging programs

The program for the Hewlett-Packard 41CV calculator was written in two sections: an initialisation routine and the actual logging section which took the readings and dumped them on tape. The initialisation routines used for the logging during the reaction and cooling runs were different as the cooling runs were usually started automatically without operator intervention.

A.2.1 Initialisation routine for reaction runs

```
11:21AM 85.11
01*LBL "DXRUN"
02 "FILENAME?"
03 AON
04 PROMPT
05 AOFF
06 ASTO 03
07 ZERO
08 1
09 STO 05
10 "R/S TO START"
11 AVIEW
12 STOP
13 GTO "DXMAIN"
14 END
```

A.2.2 Initialisation routine for cooling runs

```
11 21AM 85.11
01*LBL "COOL"
02 "RUNC"
03 ASTO 03
04 ZERO
05 1
06 STO 05
07 0
08 OFHX
09 GTO "DXMAIN"
10 END
```

A2.3 Main program

```
11:18GN 25.11
01*LBL "OXMAIN"
02 CF 21
03 FIX 3
04 0
05 CLA
06 ARCL 03
07 SEEKP
08 SETSW
09 STO 09
10 RUNSW
11 XEQ A
12*LBL 01
13 "PUSH KEY"
14 AVIEW
15 GETKEY
16 STO 07
17 0
18 X=Y?
19 GTO 02
20 RCL 07
21 14
22 X>Y?
23 GTO 01
24 RCL 07
25 26
26 X<=Y?
27 GTO 01
28 XEQ IND 07
29*LBL 02
30 " "
31 AVIEW
32 RCLSW
33 HR
34 60
35 *
36 RCL 00
37 -
38 RCL 05
39 X>Y?
40 GTO 01
41 XEQ A
42 GTO 01
43 RTN
44*LBL A
45 RCLSW
46 HR
47 60
48 *
49 STO 00
50 9
51 XROM "TEMKX"
52 STO 01
53 8
54 XROM "TEMKX"
55 STO 02
56 8.002
57 CLA
58 ARCL 02
59 WRTKX
60 3
61 ST+ 99
62 RTN
63*LBL 25
64 "NEW STEP?"
65 PROMPT
66 STO 05
67 RTN
68*LBL 21
69 RCLSW
70 HR
71 60
72 *
73 VIEW X
74 PSE
75 PSE
76 RTN
77*LBL 22
78 9
79 XROM "TEMKX"
80 VIEW X
81 PSE
82 PSE
83 RTN
84*LBL 23
85 0
86 XROM "TEMKX"
87 VIEW X
88 PSE
89 PSE
90 RTN
91*LBL 24
92 "LAST?"
93 PROMPT
94 3
95 *
96 STO 04
97 10
98 +
99 SIZE?
100 X>Y?
101 GTO 05
102 "MEM NOT OK"
103 AVIEW
104 BEEP
105 PSE
106 PSE
107 PSE
108 RTN
109*LBL 14
110 "LOW"
111 AVIEW
112 XEQ "LOW"
113 VIEW X
114 PSE
115 PSE
116 RTN
117*LBL 15
118 6
119 XROM "TEMKX"
120 VIEW X
121 PSE
122 PSE
123 RTN
124*LBL 05
125 RCL 99
126 RCL 04
127 -
128 CLA
129 ARCL 03
130 SEEKP
131 RCL 04
132 9
133 +
134 1000
135 /
136 10
137 +
138 HEADPT
139 .000003
140 +
141 STO 03
142 SF 21
143*LBL 06
144 FIX 1
145 RCL IND 00
146 ACX
147 RCL 00
148 1
149 +
150 FIX 2
151 RCL IND X
152 ACX
153 RCL 00
154 2
155 +
156 FIX 2
157 RCL IND X
158 ACX
159 PRBUF
160 ISG 00
161 GTO 06
162 CF 21
163 RCL 99
164 CLA
165 ARCL 03
166 SEEKP
167 FIX 3
168 RTN
169 END
```

APPENDIX B: COMPUTER PROGRAMS

B.1 Calculation of Adiabatic Curve

This program reads the experimental temperature-time data off disk, and then calculates the adiabatic curve using the technique discussed in 3.3. The integral is evaluated using the trapezoidal rule. This integration method is sufficiently accurate as the time interval is small, and the curves are smooth. The computer programs in this, and the following two sections, are written in BASIC for the Hewlett-Packard 9816 microcomputer.

```
10   !THIS CONVERTS MEASURED TEMP-TIME CURVES TO ADIABATIC CURVES
20    OPTION BASE 1
30    DIM Tim(500),Temp(500),Deltat(500),Dummy(1000)
40    ! Read data off disc
50    INPUT "REACTOR TEMP DATA FILENAME?",File$
60    INPUT "FILENAME FOR ADIABATIC TEMPERATURES",File3$
70    Read_data(File$,Tim(*),Temp(*),Lent)
80    !
90    Ts=80.387
100   Uamcp=.022610
110   FOR K=1 TO Lent
120     Deltat(K)=Temp(K)-Ts
130   NEXT K
140   Corr=0
150   !
160   ! Calculate correction using trapezoidal rule, add to temp curve
170   !
180   FOR I=2 TO Lent
190     Addd=Uamcp*(Deltat(I-1)+Deltat(I))*(Tim(I)-Tim(I-1))/2
200     Corr=Corr+Addd
210     Dummy(2*I-3)=Tim(I)
220     Dummy(2*I-2)=Corr+Temp(I)
230     PRINT I,Tim(I),Dummy(2*I-2)
240   NEXT I
250   !
260   ! Dump to disc for plotting and heat of reaction calculation
270   !
280   REDIM Dummy(2*(Lent-1))
290   CREATE BDAT File3$,INT((2*Lent+2)/32)+1
300   ASSIGN @Out TO File3$
310   OUTPUT @Out;1.0,Lent-1,Dummy(*)
320   END
330   !
340   SUB Read_data(File$,Xpts(*),Ypts(*),Npts)
350     OPTION BASE 1
360     ASSIGN @In TO File$
370     ENTER @In;Ng,Npts
380     IF Ng<>1 THEN PRINT "FILE ";File$;" CONTAINS ";Ng;"GRAPHS,PROGRAM WILL O
NLY READ FIRST"
390     ALLOCATE Dummy(2*Npts)
400     ENTER @In;Dummy(*)
410     ASSIGN @In TO *
420     FOR J=1 TO Npts
430       Xpts(J)=Dummy(2*J-1)
440       Ypts(J)=Dummy(2*J)
450     NEXT J
460     DEALLOCATE Dummy(*)
470     REDIM Xpts(Npts),Ypts(Npts)
480   SUBEND
```

B.2 Calculation of the Heat of Reaction

Two computer programs were used for the calculation of the heat of reaction. The first program reads the adiabatic temperature-time data, and the oxygen concentration data, off disk. The adiabatic temperature rise at each concentration data point is then found by linear interpolation, and dumped to disk for plotting purposes.

The second program consists of the adiabatic curve calculation program in B.1, the interpolation routine described above and an additional section that calculates $V\Delta H/C_p$ by fitting $y = ax$ to the interpolated data.

The programs are listed on the following two pages.

```
10    !PROGRAM RHEAT
20    !THIS INTERPOLATES ADIABATIC TEMP AND CONC DATA, DUMPS TO DISC
30    !     FOR PLOT WHOSE SLOPE IS RELATED TO HEAT OF REACTION
40    OPTION BASE 1
50    !
60    ! Read adiabatic temperatures off disc
70    !
80    INPUT "FILENAME FOR ADIABATIC TEMPERATURES",File1$
90    ASSIGN @In1 TO File1$
100   ENTER @In1;Ng,Lent
110   ALLOCATE Tim(Lent),Temp(Lent)
120   ALLOCATE Dummy(2*Lent)
130   ENTER @In1;Dummy(*)
140   ASSIGN @In1 TO *
150   FOR J=1 TO Lent
160     Tim(J)=Dummy(2*J-1)
170     Temp(J)=Dummy(2*J)
180   NEXT J
190   !
200   ! Read oxygen concentration data off disc
210   !
220   INPUT "FILENAME FOR CONCENTRATIONS?",File2$
230   ASSIGN @In2 TO File2$
240   ENTER @In2;Ng,Lenc
250   ALLOCATE Timc(Lenc),Conc(Lenc),Dummyc(2*Lenc),Dconc(Lenc),Dtemp(Lenc)
260   ENTER @In2;Dummyc(*)
270   ASSIGN @In2 TO *
280   FOR J=1 TO Lenc
290     Timc(J)=Dummyc(2*J-1)
300     Conc(J)=Dummyc(2*J)
310   NEXT J
320   !
330   ! Interpolate temperature curve at appropriate conc values
340   !
350   J2=1
360   Counter=0
370   FOR J=1 TO Lenc
380     ! Check if conc value is suitable
390     IF Timc(J)<Tim(1) OR Timc(J)>Tim(Lent) THEN 490
400     REPEAT
410       J2=J2+1
420     UNTIL Tim(J2)>Timc(J)
430     ! Perform linear interpolation on temp data at conc time
440     Adtemp=Temp(J2-1)+(Temp(J2)-Temp(J2-1))/(Tim(J2)-Tim(J2-1))*(Timc(J2)-Tim
c(J))
450     Counter=Counter+1
460     PRINT Timc(J),Conc(J),Adtemp,Counter
470     Dtemp(Counter)=Adtemp
480     Dconc(Counter)=Conc(J)
490   NEXT J
500   REDIM Dummyc(2*(Counter-1)
510   !
520   ! Format as change i              nd dump to disk for PLOT
530   !
540   FOR M=2 TO Counter
550     Dummyc(2*M-3)=Dconc(1)-Dconc(M)
560     Dummyc(2*M-2)=Dtemp(M)-Dtemp(1)
570   NEXT M
580   INPUT "Filename for calculated data ",File3$
590   CREATE BDAT File3$,INT((2*Counter-1)/32)+1
600   ASSIGN @Out TO File3$
610   OUTPUT @Out;1.0,Counter-1,Dummyc(*)
620   END
```

```
10    !THIS CALCULATES HEAT OF REACTION FOR DIFFERENT TS
20    PRINTER IS 701
30    OPTION BASE 1
40    DIM Tim(500),Temp(500),Deltat(500),Timc(30),Conc(30)
50    INPUT "REACTOR TEMP DATA FILENAME?",File1$
60    INPUT "FILENAME FOR CONCENTRATIONS",File2$
70    Read_data(File1$,Tim(*),Temp(*),Lent)
80    Read_data(File2$,Timc(*),Conc(*),Lenc)
90    !
100   ALLOCATE Adtemp(Lent-1),Dtemp(Lenc),Dconc(Lenc)
110   INPUT "TS=",Ts
120   Ucp= 02261
130   PRINT "TS= ";Ts,"RUN NUMBER ";File1$,File2$
140   !
150   ! Calculate adiabatic curve
160   FOR K=1 TO Lent
170     Deltat(K)=Temp(K)-Ts
180   NEXT K
190   Corr=0
200   FOR I=2 TO Lent
210     Addd=Ucp*(Deltat(I-1)+Deltat(I))*(Tim(I)-Tim(I-1))/2
220     Corr=Corr+Addd
230     Adtemp(I-1)=Corr+Temp(I)
240   NEXT I
250   !
260   ! Interpolate adiabatic curve at conc points
270   J2=1
280   Counter=0
290   FOR J=1 TO Lenc
300     IF Timc(J)<Tim(1) OR Timc(J)>Tim(Lent) THEN 400
310     REPEAT
320       J2=J2+1
330     UNTIL Tim(J2)>Timc(J)
340     ! Perform linear interpolation
350     S_temp=Adtemp(J2-1)+(Adtemp(J2)-Adtemp(J2-1))/(Tim(J2)-Tim(J2-1))*(Tim(J
2)-Timc(J))
360     Counter=Counter+1
370     Dtemp(Counter)=S_temp
380     Dconc(Counter)=Conc(J)
390   ! PRINT Timc(J),Conc(J),S_temp,Counter
400   NEXT J
410   REDIM Dconc(Counter),Dtemp(Counter)
420   !
430   ! Calculate VH/C by fitting y=ax to interpolated data
440   Sum_xy=0
450   Sum_x2=0
460   FOR J=1 TO Counter
470     X=Dconc(1)-Dconc(J)
480     Sum_xy=Sum_xy+X*(Dtemp(J)-Dtemp(1))
490     Sum_x2=Sum_x2+X^2
500   NEXT J
510   Rheat=Sum_xy/Sum_x2
520   Sum_err=0
530   FOR J=1 TO Counter
540     Sum_err=Sum_err+(Dtemp(J)-Dtemp(1)-Rheat*(Dconc(1)-Dconc(J)))^2
550   NEXT J
560   PRINT "Ts=";Ts,"RHEAT=";Rheat,"Sum of squares=";Sum_err
570   END
```

B.3 Calculation of the Rate of Reaction

This program fits piecewise polynomials of specified order to a given number of data points. These polynomials are then differentiated in order to obtain the rate as described in 3.4.

```
10    ! PROGRAM TO CALCULATE RATES OF REACTION BY DIFFERENTIATING TEMP CURVE
20    OPTION BASE 1
30    PRINTER IS 701
40    !
50    ! Read data off disc
60    !
70    INPUT "Reactor temp filename",File1$
80    INPUT "Concentration filename ",File2$
90    DIM Temp(500),Ttime(500),Conc(50),Ctime(50),Dummy1(98),Dummy2(98)
100   Read_data(File1$,Ttime(*),Temp(*),Ntemp)
110   Read_data(File2$,Ctime(*),Conc(*),Nconc)
120   !
130   ! Set parameters to be used in calculating rates
140   !
150   Ucp=.02261
160   INPUT "TS ",Ts
170   Rheat=1.250
180   Nspan=20  ! Number of points to be used(must be even)
190   Power=3  ! Order of polynomial (3 for quadratic)
200   ALLOCATE Par(Power),Normal(Power,Power),Xy(Power),Norm_inv(Power,Power)
210   Pstart=0
220   L=1
230   PRINT
240   PRINT "       ",File1$,"      ",File2$
250   PRINT
260   PRINT "   Time      Conc     Temp          dT/dt        U(T-Ts)        Rate"
270   !
280   ! Calculate rate at suitable conc points
290   !
300   FOR M=1 TO Nconc
310     IF Ctime(M)<Ttime(1) OR Ctime(M)>Ttime(Ntemp) THEN 700
320     REPEAT
330       Pstart=Pstart+1
340     UNTIL Ttime(Pstart)>Ctime(M)
350     MAT Normal= (0)
360     MAT Xy= (0)
370     Pbeg=Pstart-Nspan/2
380     Pend=MIN(Pstart+Nspan/2,Ntemp)  !Bound counter to prevent going too far
390     ! Calculate coefficients of normal equations
400     FOR P=Pbeg TO Pend
410       FOR J0=1 TO Power
420         FOR J1=1 TO Power
430           Normal(J0,J1)=Normal(J0,J1)+Ttime(P)^(J0+J1-2)
440         NEXT J1
450         Xy(J0)=Xy(J0)+Ttime(P)^(J0-1)*Temp(P)
460       NEXT J0
470     NEXT P
480     ! Solve normal equations to get polynomial coefficients
490     MAT Norm_inv= INV(Normal)
500     MAT Par= Norm_inv*Xy
510     ! Calculate temp and temp derivative at midpoint of group of points
520     S_temp=0
530     S_slope=0
540     Atime=Ctime(M)
550     FOR J2=1 TO Power
560       S_temp=S_temp+Par(J2)*Atime^(J2-1)
570       S_slope=S_slope+(J2-1)*Par(J2)*Atime^(J2-2)
580     NEXT J2
590     ! Calculate rate and dump to disc
600     Rate=(S_slope+Ucp*(S_temp-Ts))/Rheat
610     C_over_C=Conc(M)/Rate
620     Dummy1(L)=Conc(M)
630     Dummy1(L+1)=Rate
640     Dummy2(L)=Conc(M)
```

```
650     Dummy2(L+1)=C_over_r
660     L=L+2
670     Corr=Ucp*(S_temp-Ts)
680     PRINT USING "4D.DD,4X,4D.7D,4X,4D.7D,4X,4D.7D";Atime,Conc(M),Rate,C_over
_r
690     PRINT USING "2X,3D.D,4X,2D.2D,4X,2D.2D,4X,2D.2D,4X,2D.6D,4X,2D.6D,4X,2D.6D";Atime
,Conc(M),S_temp,S_slope,Corr,Rate
700   NEXT M
710   REDIM Dummy1(L-1)
720   REDIM Dummy2(L-1)
730   !
740   INPUT "Filename for rates?",File3$
750   CREATE BDAT File3$,INT(L/16+2)
760   ASSIGN @F TO File3$
770   OUTPUT @F,1.0,(L-1)/2,Dummy1(*)
780   ASSIGN @F TO *
790   !
800   INPUT "Filename for conc/rate?",File4$
810   CREATE BDAT File4$,INT(L/16+2)
820   ASSIGN @F TO File4$
830   OUTPUT @F;1.0,(L-1)/2,Dummy2(*)
840   ASSIGN @F TO *
850   END
860   !
870   SUB Read_data(File$,Xpts(*),Ypts(*),Npts)
880     OPTION BASE 1
890     ASSIGN @In TO File$
900     ENTER @In;Ng,Npts
910     IF Ng<>1 THEN PRINT "FILE ";File$;" CONTAINS ";Ng;"GRAPHS,PROGRAM WILL O
NLY READ FIRST"
920     ALLOCATE Dummy(2*Npts)
930     ENTER @In;Dummy(*)
940     ASSIGN @In TO *
950     FOR J=1 TO Npts
960       Xpts(J)=Dummy(2*J-1)
970       Ypts(J)=Dummy(2*J)
980     NEXT J
990     DEALLOCATE Dummy(*)
1000    REDIM Xpts(Npts),Ypts(Npts)
1010  SUBEND
```

B.4 Parameter Estimation Program

The sum of squared errors was minimized using a modification of the Gauss-Newton technique described by King (1967). A set of additional differential equations is solved to obtain the derivatives of the temperature and concentration with respect to the parameters. These derivatives, known as the sensitivity coefficients, are used to calculate the step required to reduce the sum of squares, and may also be used to obtain statistical information about the best-fit parameters.

The statistical assumptions used are that all the measurement errors are additive, have zero mean, constant variance and are uncorrelated (i.e. independent in time). In addition the errors will be assumed to have a normal distribution, and the independent variable (time) will be assumed to be errorless. These assumptions hold in this case as any errors in the temperature measurements are caused by random noise, and the independent variable can be measured accurately. Using these assumptions, it can be shown that the approximate variance-covariance matrix of the parameters is: (Beck & Arnold, 1977)

$$\left(X^T \Omega^{-1} X \right)^{-1} \quad \frac{s}{N-P}$$

where X is the sensitivity matrix, Ω a diagonal matrix of the weighting factors, s is the weighted sum of squares, N the number of data points and P the number of parameters.

The correlation matrix is obtained as follows: let the elements of the variance-covariance matrix be P_{ij}, then the ij'th element of the correlation matrix r is

$$r_{ij} = P_{ij} / \left(P_{ii} P_{jj} \right)^{\frac{1}{2}}$$

This has diagonal elements of unity, and off-diagonal elements in the range [-1,1].

This program is written in VS FORTRAN, and was run on an IBM 3083 model J24 mainframe.

```
C PROGRAM TO FIND PARAMETERS USING GAUSS-NEWTON METHOD
C ====================================================
C
      IMPLICIT REAL*8 (A-H),REAL*8 (O-Z)
      EXTERNAL QMIN
      DIMENSION PARSOL(5),GRAD(5,1),HESIAN(5,5)
      DIMENSION WKAREA(5),COVAR(5,5),CORR(5,5),NN(4),SERROR(5)
      DIMENSION PSI(2500,1),SENS(2500,5),PSIX(2500,5),XTPSIX(5,5)
      CHARACTER*25 RUNID
      COMMON /INITL/ TS(5),VOL,CO20(5),RHEAT(5),UCP(5),WCOAL(5),AREA(5)
      COMMON /EXDATA/ LENT(5),LENX(5),ETTIME(500,5),ETEMP(500,5)
      COMMON /EXDATA/ EXTIME(50,5),EXTENT(50,5),TWAIT,GWAIT,NEXP
      COMMON /STPCOM/ STEP(5,1),PARS(5),NPAR
C
C Set constants used in COMMON block INITL
      VOL=1.87D-3
      TWAIT=2.D0/2.0D-4
      GWAIT=2.D0/0.025D0
      NITER=0
      NPAR=2
C
C     Read experimental data off disk
      READ(2,*) NEXP
      WRITE(7,3)NEXP
3     FORMAT (  'NUMBER OF EXPERIMENTS:',I2)
      DO 18 N=1,NEXP
         READ(2,4) RUNID
4        FORMAT ( A25)
         READ (2,*) TS(N),RHEAT(N),UCP(N),WCOAL(N),AREA(N),CO20(N)
         TS(N)=TS(N)+273.15
         WRITE(7,7) TS(N),RHEAT(N),UCP(N),WCOAL(N),AREA(N),CO20(N)
7        FORMAT (6(1X,F10.5))
         READ(2,*) LENX(N)
C
C Read experimental concentrations
         DO 15  J=1,LENX(N)
15          READ (2,*) EXTIME(J,N),EXTENT(J,N)
         READ(2,*) LENT(N)
C Read experimental temperatures
         DO 10  J=1,LENT(N)
            READ(2,*)ETTIME(J,N),ETEMP(J,N)
10          ETEMP(J,N)=ETEMP(J,N)+273.15
         WRITE(7,17)RUNID,LENX(N),LENT(N)
17       FORMAT ( A15,' HAS ',I3,' CONCS AND ',I4,' TEMPS')
18    CONTINUE
C
C Set initial guesses for parameters
      READ(3,*)(PARS(JJ),JJ=1,NPAR)
      PARS(2)=CO20(1)
      WRITE(7,*)(PARS(JJ),JJ=1,NPAR)
C
C Set initial old parameter values the same as initial guesses
      DO 20  J=1,NPAR
20       PARSOL(J)=PARS(J)
C
C Set IMSL messages on/off: 0 is all off, 4 is all on
      CALL UERSET (4,LVLOLD)
C
C Calculate step,move along careful  ill optimum is straddled,fit
C   quadratic and find minimum. Repe.  until convergence
```

```
      ERROR=1.0D-6
      EPSLON=1.0D-40
25    CALL OBJECT (NPAR,PARS,STEP,GRAD,HESIAN,SUM,SENS)
      WRITE(7,100) (PARS(N),N=1,NPAR),SUM
      WRITE(1,100) (PARS(N),N=1,NPAR),SUM
100   FORMAT(2(2X,F10.4),4X,F20.2)
      X=1.0D0
      FSTEP=1.0D-1
      BOUND=5.0D2
      XACC=1.00D-6
      MAXFN=90
C     Use IMSL routine ZXLSF to find minimum by quadratic interpolation
      CALL ZXLSF(QMIN,X,FSTEP,BOUND,XACC,MAXFN,IER)
      WRITE(7,*) 'X=',X
      DO 85  J=1,NPAR
         PARSOL(J)=PARS(J)
85       PARS(J)=PARS(J)+X*STEP(J,1)
      CHANGE=DABS((PARS(1)-PARSOL(1))/(PARS(1)+EPSLON))
      DO 90  K=2,NPAR
C     Calculate maximum relative error in the parameters
90    CHANGE=DMAX1(CHANGE,DMAX1(DABS((PARS(K-1)-PARSOL(K-1))/(PARS(K-1)
     # +EPSLON)),DABS((PARS(K)-PARSOL(K))/(PARS(K)+EPSLON))))
C     Check for convergence
      IF (CHANGE.GT.ERROR) GOTO 25
C
C Dump optimum parameters,gradient,hessian matrix to disk and screen
      CALL OBJECT (NPAR,PARS,STEP,GRAD,HESIAN,SUM,SENS)
      WRITE (7,*) RUNID
      WRITE (1,*) RUNID
      WRITE(7,105)SUM
      WRITE(1,105)SUM
105   FORMAT ('Sum of squared errors: ',F18.4)
      WRITE(7,110) (PARS(N),N=1,NPAR)
      WRITE(1,110) (PARS(N),N=1,NPAR)
      WRITE(3,108) (PARS(N),N=1,NPAR)
108   FORMAT( 3(1X,F16.10))
110   FORMAT('Optimum parameters',/,3(1X,F16.9))
       DO 112 J5=1,NPAR
112      GRAD(J5,1)=GRAD(J5,1)/SUM*PARS(J5)
      WRITE (7,115) (GRAD(I,1),I=1,NPAR)
      WRITE (1,115) (GRAD(I,1),I=1,NPAR)
115   FORMAT( 'Gradient at optimum',/,3(3X,F21.8))
       DO 116 J5=1,NPAR
          DO 116 J6=1,NPAR
116      HESIAN(J5,J6)=HESIAN(J5,J6)/SUM*PARS(J5)*PARS(J6)
      WRITE (7,*) 'Hessian matrix at optimum'
      WRITE (1,*) 'Hessian matrix at optimum'
      WRITE (7,120) ((HESIAN(L,I),I=1,NPAR),L=1,NPAR)
      WRITE (1,120) ((HESIAN(L,I),I=1,NPAR),L=1,NPAR)
120   FORMAT( 2(4X,F21.10))
      NXDATA=0
C     Calculate variance-covariance matrix
      DO 142 N3=1,NEXP
         DO 135 K1=1,LENT(N3)
135         PSI(K1+NXDATA,1)=TWAIT/2.D0
         DO 140 K2=1,LENX(N3)
140         PSI(LENT(N3)+K2+NXDATA,1)=GWAIT/2.D0
         NXDATA=NXDATA+LENT(N3)+LENX(N3)
142   CONTINUE
```

```
      NN(1)=NXDATA
      NN(2)=0
      NN(3)=0
      NN(4)=NPAR
      CALL VMULBF (PSI,2500,SENS,2500,NN,PSIX,2500)
      CALL VMULFM (SENS,PSIX,NXDATA,NPAR,NPAR,2500,2500,XTPSIX,5,IER)
      IDGT=4
      CALL LINV1F (XTPSIX,NPAR,5,COVAR,IDGT,WKAREA,IER)
      VAR=SUM/(NXDATA-NPAR)
      DO 141 J11=1,NPAR
         DO 141 J12=1,NPAR
141      COVAR(J11,J12)=COVAR(J11,J12)*VAR
      DO 145 J1=1,NPAR
         SERROR(J1)=DSQRT(COVAR(J1,J1))/PARS(J1)*100.D0
         DO 145 J2=1,NPAR
145      CORR(J1,J2)=COVAR(J1,J2)/DSQRT(COVAR(J1,J1)*COVAR(J2,J2))
      WRITE(7,147)(SERROR(JY),JY=1,NPAR)
      WRITE(1,147)(SERROR(JY),JY=1,NPAR)
147   FORMAT ('Standard errors',/2(3X,3F20.12))
      WRITE(7,*)'Variance-covariance matrix'
      WRITE(1,*)'Variance-covariance matrix'
      WRITE(7,150) ((COVAR(I,J),J=1,NPAR),I=1,NPAR)
      WRITE(1,150) ((COVAR(I,J),J=1,NPAR),I=1,NPAR)
150   FORMAT (2(4X,F25.15))
      WRITE(7,*) 'CORRELATION MATRIX'
      WRITE(1,*) 'CORRELATION MATRIX'
      WRITE(7,155) ((CORR(I,J),J=1,NPAR),I=1,NP
      WRITE(1,155) ((CORR(I,J),J=1,NPAR),I=1,NP
155   FORMAT ( 2(1X,F14.9))
C
      STOP
      END
C
C     Function used by IMSL routine ZXLSF to evaluate sum of squares
      REAL FUNCTION QMIN*8 (X)
      IMPLICIT REAL*8 (A-H),REAL*8 (O-Z)
      DIMENSION HESIAN(5,5),GRAD(5,1),SENS(2500,5),DPARS(5),DUMSTP(5,1)
      COMMON /STPCOM/ STEP(5,1),PARS(5),NPAR
      DO 400 J=1,NPAR
400   DPARS(J)=PARS(J)+X*STEP(J,1)
      CALL OBJECT (NPAR,DPARS,DUMSTP,GRAD,HESIAN,SUMSQS,SENS)
      QMIN=SUMSQS
      RETURN
      END
```

```
C Subroutine to calculate gradient,hessian and sum of squares
C ------------------------------------------------------------------
      SUBROUTINE OBJECT(NPAR,PARS,STEP,GRAD,HESIAN,SUMSQS,SENS)
      IMPLICIT REAL*8 (A-H),REAL*8 (O-Z)
      EXTERNAL DIFFEQ,FCNJ
      DIMENSION TGRAD(5),CGRAD(5),GRAD(5,1),STEP(5,1)
      DIMENSION IWK(8),WK(137),Y(8),WKAREA(5),PARS(5),SENS(2500,5)
      DIMENSION THESS(5,5),CHESS(5,5),HESIAN(5,5),DHESS(5,5)
      COMMON /EXDATA/ LENT(5),LENX(5),ETTIME(500,5),ETEMP(500,5)
      COMMON /EXDATA/ EXTIME(50,5),EXTENT(50,5),WT,WC,NEXP
      COMMON /PARMS/ DPAR(5),N1,NPARMS,NDEPV
C
      NPARMS=NPAR
      NDEPV=2
      NEQ=NDEPV+NDEPV*NPAR
C Initialize variables
      DO 200 K=1,NPAR
200   DPAR(K)=PARS(K)
      SUMSQS=0.D0
      DO 205 J1=1,NPAR
        GRAD(J1,1)=0.D0
        DO 205 J2=1,NPAR
          HESIAN(J1,J2)=0.D0
205   CONTINUE
C
      NDATA=0
      TOL=1.0D-6
      METH=1
      MITER=0
C  Loop through number of experiments
      DO 238 N1=1,NEXP
        DO 207 J7=1,NPAR
          SENS(1+NDATA,J7)=0.D0
          SENS(1+NDATA+LENT(N1),J7)=0.D0
          TGRAD(J7)=0.D0
          CGRAD(J7)=0.D0
          DO 207 J8=1,NPAR
            THESS(J7,J8)=0.D0
207         CHESS(J7,J8)=0.D0
        SSET=0.D0
        SSEC=0.D0
C Solve differential equations at temperature times
        H=1.0D-6
208     INDEX=1
C Set initial conditions
        Y(1)=EXTENT(1,N1)
        Y(2)=ETEMP(1,N1)
        DO 210 JJ=3,NEQ
210       Y(JJ)=0.D0
        BTIME=ETTIME(1,N1)
        DO 220 M=2,LENT(N1)
          CALL DGEAR(NEQ,DIFFEQ,FCNJ,BTIME,H,Y,ETTIME(M,N1),TOL,METH,
     #       MITER,INDEX,IWK,WK,IER)
          SSET=SSET+(Y(2)-ETEMP(M,N1))**2
          DO 215 J1=1,NPAR
            SENS(M+NDATA,J1)=Y(2+J1*2)
            TGRAD(J1)=TGRAD(J1)+(Y(2)-ETEMP(M,N1))*Y(2+J1*2)
            DO 215 J2=1,NPAR
              THESS(J1,J2)=THESS(J1,J2)+Y(2+J1*2)*Y(2+J2*2)
215         CONTINUE
```

```
220      CONTINUE
C
C Solve differential equations at concentration times
         H=1.0D-6
223      INDEX=1
C Set initial condititons
         Y(1)=EXTENT(1,N1)
         Y(2)=ETEMP(1,N1)
         DO 225 JJ=3,NEQ
225         Y(JJ)=0.D0
         BTIME=EXTIME(1,N1)
         DO 235 M=2,LENX(N1)
            CALL DGEAR(NEQ,DIFFEQ,FCNJ,BTIME,H,Y,EXTIME(M,N1),TOL,METH,
     #           MITER,INDEX,IWK,WK,IER)
            SSEC=SSEC+(Y(1)-EXTENT(M,N1))**2
            DO 230 J1=1,NPAR
               SENS(LENT(N1)+M+NDATA,J1)=Y(1+J1*2)
               CGRAD(J1)=CGRAD(J1)+(Y(1)-EXTENT(M,N1))*Y(1+J1*2)
               DO 230 J2=1,NPAR
                  CHESS(J1,J2)=CHESS(J1,J2)+Y(1+J1*2)*Y(1+J2*2)
230            CONTINUE
235      CONTINUE
C End of loop through number of experiments
         NDATA=NDATA+LENX(N1)+LENT(N1)
C
C Calculate weighted sum of squares,gradient,hessian matrix
      SUMSQS=SUMSQS+SSET*WT/2.D0+SSEC*WC/2.D0
      DO 240 J1=1,NPAR
         GRAD(J1,1)=GRAD(J1,1)+WT*TGRAD(J1)+WC*CGRAD(J1)
         DO 240 J2=1,NPAR
240         HESIAN(J1,J2)=HESIAN(J1,J2)+WT*THESS(J1,J2)+WC*CHESS(J1,J2)
238   CONTINUE
C
C Solve matrices to get step
      IDGT=3
      NRGHT=1
C Create dummy variables
      DO 245 J=1,NPAR
        STEP(J,1)=-GRAD(J,1)
        DO 245 K=1,NPAR
245     DHESS(J,K)=HESIAN(J,K)
      CALL LEQT1F(DHESS,NRGHT,NPAR,5,STEP,IDGT,WKAREA,IER)
C
      RETURN
      END
C
C Subroutine containing model differential equations
C ____________________________________________________
      SUBROUTINE DIFFEQ (N,T,Y,YPRIME)
      IMPLICIT REAL*8 (A-H),REAL*8 (O-Z)
      DIMENSION YPRIME(N),Y(N),DER(5,5),PDER(5,5),SCALE(5)
      COMMON /INITL/ TS(5),VOL,CO20(5),RHEAT(5),UCP(5),WCOAL(5),AREA(5)
      COMMON /PARMS/ PARS(5),NO,NPAR,NDEPV
C
C Calculate actual parameter values for COMMON block INITL
      SCALE(1)=1.0D-3
      SCALE(2)=1.0D0
      D=PARS(1)*SCALE(1)
      CO=PARS(2)*SCALE(2)
C     CO=CO20(NO)
```

```
      C=Y(1)

C Y(1) is concentration,Y(2) is temperature
      YPRIME(1)=-D*C/(C0-C)
      YPRIME(2)=-RHEAT(N0)*YPRIME(1)-UCP(N0)*(Y(2)-TS(N0))

C DER(ndepv1,ndepv2) contains the derivatives of the dependent variables
C     wrt to the dependent variables
C   i.e. DER(ndepv1,ndepv2) is derivative of YPRIME(ndepv1) wrt ndepv2

      DER(1,1)=-D*C0/((C0-C)*(C0-C))
      DER(1,2)=0.D0
      DER(2,1)=-RHEAT(N0)*DER(1,1)
      DER(2.2)=-RHEAT(N0)*DER(1,2)-UCP(N0)

C PDER(ndepv,npar) contains the partial derivatives of the
C     independent variables wrt to the parameters
C     i.e. PDER(j,k) is partial derivative of variable k wrt parameter j
      PDER(1,1)=-C/(C0-C)
      PDER(1,2)=D*C/((C0-C)*(C0-C))

      PDER(2,1)=-RHEAT(N0)*PDER(1,1)
      PDER(2,2)=-RHEAT(N0)*PDER(1,2)

      DO 300 L0=1,NPAR
         NUM=NDEPV*L0
         DO 300 L1=1,NDEPV
         SUMDER=0.D0
         DO 310 L2=1,NDEPV
310         SUMDER=SUMDER+DER(L1,L2)*Y(NUM+L2)
300      YPRIME(NUM+L1)=SCALE(L0)*(SUMDER+PDER(L1,L0))

      RETURN
      END
C
C Dummy subroutine used by DGEAR
C ------------------------------
      SUBROUTINE FCNJ (N,X,Y,PD)
      IMPLICIT REAL*8 (A-H),REAL*8 (O-Z)
      DIMENSION Y(N),PD(N,N)
      RETURN
      END
```

B.5 Calculation of fitted curves

This program was used to calculate temperature-time and concentration-time curves by solving the appropriate differential equations. The output was stored on disk for plotting by a graphics package (*SAS/GRAPH*). The subroutine *DIFFEQ* of the previous section is used for the calculation of the derivatives.

```
C PROGRAM TO CALCULATE TEMP-TIME AND CONC-TIME CURVES FOR PLOTTING
C ================================================================
      IMPLICIT REAL*8 (A-H),REAL*8 (O-Z)
      EXTERNAL DIFFEQ,PLOT
      DIMENSION IWK(8),WK(137),Y(8)
      CHARACTER*15 RUNID
      DIMENSION LENT(5),LENX(5),ETTIME(500,5),ETEMP(500,5)
      DIMENSION EXTIME(50,5),EXTENT(50,5)
      COMMON /INITL/ TS(5),VOL,CO2O(5),RHEAT(5),UCP(5),WCOAL(5),AREA(5)
      COMMON /PARMS/ PARS(5),NRUN,NPAR,NDEPV
C
C Set constants used in COMMON block INITL
      VOL=1.8700D-3
      TWAIT=2.D0/2.6329D-4
      CWAIT=2.D0/0.01389
      NDEPV=2
      NPAR=1
C
      READ(2,*) NEXP
      WRITE(7,3)NEXP
3     FORMAT ( 'NUMBER OF EXPERIMENTS:',I2)
      DO 18 N=1,NEXP
         READ(2,4) RUNID
4        FORMAT ( A15)
         READ (2,*)  TS(N),RHEAT(N),UCP(N),WCOAL(N),AREA(N),CO2O(N)
C        WRITE (7,*) TS(N),RHEAT(N),UCP(N),WCOAL(N),AREA(N),CO2O(N)
         TS(N)=TS(N)+273.15
         READ( 2,*) LENX(N)
C
C Read experimental concentrations
         DO 15  J=1,LENX(N)
15         READ (2,*) EXTIME(J,N),EXTENT(J,N)
         READ(2,*) LENT(N)
C Read experimental temperatures
         DO 10  J=1,LENT(N)
            READ(2,*)ETTIME(J,N),ETEMP(J,N)
10          ETEMP(J,N)=ETEMP(J,N)+273.15
         WRITE(7,17)N,RUNID,LENX(N),LENT(N)
17       FORMAT (I4.3X,A8,' HAS ',I3,' CONCS AND ',I4,' TEMPS')
18    CONTINUE
C
      READ(3,*)(PARS(JJ),JJ=1,NPAR)
      WRITE(7,6)(PARS(JJ),JJ=1,NPAR)
6     FORMAT( 'PARS ARE ',3(1X,F18.9))
      NRUN=1
C     GO TO 199
C     WRITE(7,*)' ENTER NUMBER OF RUN FOR WHICH CURVES ARE REQUIRED'
C     READ(7,*) NRUN
C
C Dump data to disk for plotting purposes
199   DO 210 J1=1,LENT(NRUN)
         RTEMP=ETEMP(J1,NRUN)-273.15
210   WRITE (4,*) ETTIME(J1,NRUN),RTEMP
      DO 220 J1=1,LENX(NRUN)
220   WRITE (5,*) EXTIME(J1,NRUN),EXTENT(J1,NRUN)
C Set number of points to be calculated
      NPT=49

      NEQ=NDEPV+NDEPV+NPAR
```

```
      TOL=1.0D-6
      METH=1
      MITER=0
      INDEX=1
      H=1.0D-8
C Set initial conditions
      Y(1)=EXTENT(1,NRUN)
      Y(2)=ETEMP(1,NRUN)
      DO 215 JJ=NDEPV+1,NEQ
215   Y(JJ)=0.D0
      BTIME=ETTIME(1,NRUN)
      RTEMP=ETEMP(1,NRUN)-273.15
      WRITE(9,151)ETTIME(1,NRUN),RTEMP
      WRITE(7,*)'TEMPERATURE POINTS BEING CALCULATED'
      DO 50 M=2,NPT+1
         CTIME=ETTIME(1,NRUN)+(M-1)*(ETTIME(LENT(NRUN),NRUN)
     #        -ETTIME(1,NRUN))/NPT
         CALL DGEAR(NEQ,DIFFEQ,FCNJ,BTIME,H,Y,CTIME,TOL,
     #      METH,MITER,INDEX,IWK,WK,IER)

C Dump temp-time values to disk for plotting
         RXTEMP=Y(2)-273.15
         WRITE (9,141)CTIME,RXTEMP
C        WRITE (7,141)CTIME,RXTEMP,Y(1),H
141      FORMAT (F8.3,1X,F13.5,1X,F14.6,1X,F15.10)
         SENS1=Y(4)
         SENS2=Y(6)
C        WRITE (10,81)CTIME,SENS1,SENS2
81       FORMAT (F7.3,3(1X,F20.6))
50    CONTINUE

      INDEX=1
      H=1.0D-8
C Set initial conditions
      Y(1)=EXTENT(1,NRUN)
      Y(2)=ETEMP(1,NRUN)
      DO 225 JJ=NDEPV+1,NEQ
225   Y(JJ)=0.D0
      BTIME=EXTIME(1,NRUN)
      WRITE(8,151)EXTIME(1,NRUN),EXTENT(1,NRUN)

      WRITE(7,*)'CONCENTRATION POINTS BEING CALCULATED'
      DO 60 M=2,NPT+1
         CTIME=EXTIME(1,NRUN)+(M-1)*(EXTIME(LENX(NRUN),NRUN)
     #        -EXTIME(1,NRUN))/NPT
         CALL DGEAR(NEQ,DIFFEQ,FCNJ,BTIME,H,Y,CTIME,TOL,
     #      METH,MITER,INDEX,IWK,WK,IER)
C Dump conc-time values to disk for plotting
         WRITE (8,151)CTIME,Y(1)
C        WRITE (7,151)CTIME,Y(1)
151      FORMAT (F8.3,1X,F13.5)
         SENS1=Y(3)
         SENS2=Y(5)
C        WRITE (11,81)CTIME,SENS1,SENS.
60    CONTINUE

      STOP
      END
```

APPENDIX C: EXPERIMENTAL DATA

C.1 Surface Areas

The isotherm data for the coal particle size ranges reported in table 4.1 is given here, as well as plots of the isotherms and the straight-line form of the BET equation used to obtain the monolayer capacity.

Particle size range: -45μm

p/p_o	0.0175	0.0281	0.0420	0.0578	0.0691	0.0899	0.106
$n/mmol.g^{-1}$	0.763	0.841	0.915	0.917	0.958	0.983	1.018

BET constants: c=263 n_m=0.940 $mmol.g^{-1}$ Area=96.2 $m^2.g^{-1}$

Particle size range: -63+45μm

p/p_o	0.0086	0.0197	0.0304	0.0457	0.0648	0.0769	0.0979
$n/mmol.g^{-1}$	0.659	0.685	0.722	0.768	0.895	0.868	0.928

BET constants: c=175 n_m=0.871 $mmol.g^{-1}$ Area=89.2 $m^2.g^{-1}$

Particle size range: -90+63μm

p/p_o	0.0126	0.0189	0.0251	0.0326	0.0364	0.0470	0.0520
$n/mmol.g^{-1}$	0.595	0.558	0.521	0.697	0.681	0.736	0.712

BET constants: c=133 n_m=0.779 $mmol.g^{-1}$ Area=79.7 $m^2.g^{-1}$

Particle size range: -125+90μm

p/p_o	0.0381	0.0596	0.0956	0.143	0.177	0.214
$n/mmol.g^{-1}$	0.546	0.642	0.625	0.675	0.717	0.777

BET constants: c=166 n_m=0.613 $mmol.g^{-1}$ Area=62.8 $m^2.g^{-1}$

Particle size range: -180+125μm

p/p_o	0.0111	0.0184	0.0295	0.0339	0.0472	0.0571
$n/mmol.g^{-1}$	0.399	0.390	0.473	0.461	0.438	0.520

BET constants: c=243 n_m=0.496 $mmol.g^{-1}$ Area=50.8 $m^2.g^{-1}$

Particle size range: -180+125μm

p/p_o	0.0162	0.0274	0.0472	0.0631	0.0853	0.115
$n/mmol.g^{-1}$	0.407	0.481	0.479	0.452	0.501	0.523

BET constants: c=453 n_m=0.467 $mmol.g^{-1}$ Area=47.8 $m^2.g^{-1}$

Particle size range: -180+125μm

p/p_o	0.0111	0.0133	0.0238	0.0358	0.0514	0.0748	0.0900
$n/mmol.g^{-1}$	0.362	0.458	0.381	0.443	0.454	0.499	0.523

BET constants: c=219 n_m=0.487 $mmol.g^{-1}$ Area=49.9 $m^2.g^{-1}$

Particle size range: -355+250μm

p/p_o	0.0134	0.0189	0.0260	0.0320	0.0407	0.0539
$n/mmol.g^{-1}$	0.402	0.319	0.370	0.512	0.455	0.424

BET constants: c=292 n_m=0.446 $mmol.g^{-1}$ Area=45.7 $m^2.g^{-1}$

Particle size range: -500+355μm

p/p_o	0.0197	0.0295	0.0445	0.0561	0.0814
$n/mmol.g^{-1}$	0.354	0.296	0.387	0.339	0.374

BET constants: c=439 n_m=0.350 $mmol.g^{-1}$ Area=35.8 $m^2.g^{-1}$

Particle size range: -710+500μm

p/p_o	0.0145	0.0199	0.0204	0.0284	0.0387	0.0544	0.0625
$n/mmol.g^{-1}$	0.347	0.415	0.307	0.269	0.286	0.356	0.339

BET constants: c=1327 n_m=0.318 $mmol.g^{-1}$ Area=32.5 $m^2.g^{-1}$

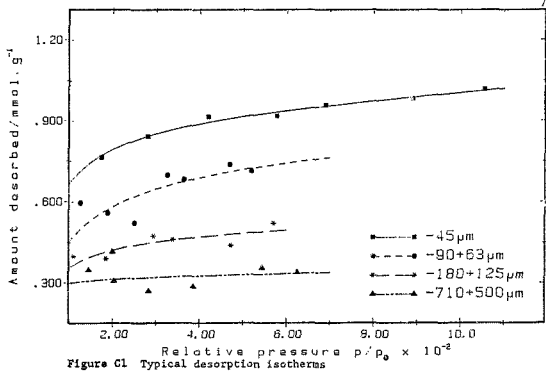

Figure C1 Typical desorption isotherms

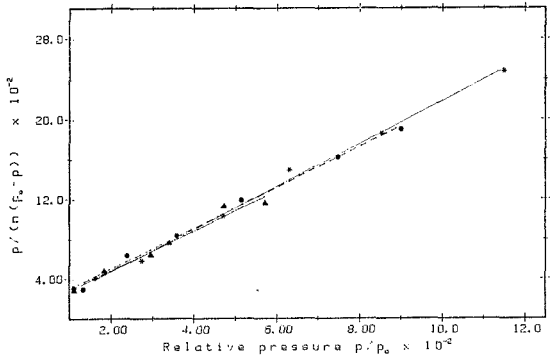

Figure C2 Replicate BET straight-line plots for -180+125μm coal

C.2 Blank Runs

Blank runs were performed in order to measure the heat capacity of the reactor. The results are summarised in table C1 below.

Table C1 Reactor heat transfer characteristics

Steady-state temperature	Heat transfer coefficient U	Heat transfer time constant U/C_p	Reactor heat capacity C_p
^oC	$W.K^{-1}$	min^{-1}	$J.K^{-1}$
60.37	0.101	0.0329	183
60.59	0.109	0.0329	199
67.08	0.137	0.0435	189
79.8	0.187	0.0503	224

The first two blank runs in the table above were performed under identical conditions. The same heat-transfer time constants were obtained, but the heat-transfer coefficient showed a variation of about 10%, which is carried through in the reactor heat capacity. The technique used for determining U is not as accurate as that for U/C_p, which is to be expected as the heat-transfer coefficient is determined from a single point, while the time constant is calculated from a whole group of points.

C.3 Runs 1-1 to 1-7

Run 1-1
Coal particle size: -180+125μm
Drying conditions: Both O_2 and N_2 bubbled through saturated zinc chloride solutions.
Steady-state temperature T_s: 80.39°C
Heat transfer coefficient U: 0.189 WK^{-1}
Heat transfer time constant U/C_p: 0.02194 min^{-1}
Calculated heat of reaction $V\Delta H/C_p$: 0.974 m^3 K mol^{-3}

The concentration and temperature data are given in tables C2 and C3 on the following pages. The temperature data are tabulated as deviations from the steady-state temperature T_s in °C, and the times are given in minutes.

Table C2 Concentration data for run 1-1

Time/min	Concentration/mol.m^{-3}				
	CO_2	H_2O	O_2	N_2	CO
13.9	0.0084	0.1582	26.96	22.231	0.0761
37.2	0.0271	0.1380	25.52	22.736	0
62.3	0.0442	0.5841	24.34	22.494	0.1018
85.8	0.0600	0.5050	23.66	22.569	0.0980
109.7	0.0744	0.6312	22.92	22.475	0.1104
133.7	0.0890	0.5316	22.56	22.687	0
157.4	0.1008	0.6548	21.82	22.479	0.1333
182.1	0.1153	0.2757	21.49	22.648	0.1524
205.7	0.1246	0.7604	20.84	22.454	0.1574
232.0	0.1369	0.6873	20.51	22.671	0.1599
256.8	0.1515	0.3445	20.26	22.733	0.1720
313.4	0.1738	0.6563	19.22	22.567	0.1914
337.1	0.1855	0.6597	18.98	22.612	0.2014
393.0	0.2115	0.7683	18.28	22.493	0.2136
470.2	0.2422	0.7462	17.40	22.483	0.2417
623.9	0.2950	0.7024	15.93	22.547	0.2787
648.7	0.3052	0.7062	15.76	22.569	0.2407
678.5	0.3141	0.7725	15.46	22.582	0.2846
710.6	0.3239	0.7131	15.15	22.594	0.2911

Table C3 Temperature deviation data of run 1-1

t	ΔT	t	ΔT	t	ΔT	t	ΔT	t	ΔT
20.6	.48	21.7	.55	22.8	.59	24.4	.67	25.9	.72
27.6	.80	29.2	.84	30.8	.90	32.5	.97	34.3	1.02
35.9	1.06	37.5	1.11	39.1	1.16	40.8	1.18	42.4	1.23
44.0	1.24	45.7	1.27	47.3	1.32	49.0	1.34	50.6	1.32
52.2	1.37	53.9	1.40	55.5	1.41	57.1	1.42	58.8	1.41
60.[illegible]	1.43	62.0	1.41	63.6	1.45	65.1	1.44	66.8	1.45
68.4	1.46	70.0	1.47	71.6	1.45	73.3	1.44	74.9	1.48
76.6	1.48	78.2	1.47	79.9	1.46	81.5	1.47	83.1	1.43
84.8	1.44	86.3	1.44	87.9	1.44	89.6	1.42	91.2	1.43
92.9	1.43	94.5	1.44	96.2	1.40	97.8	1.42	99.4	1.43
101.1	1.43	102.7	1.41	104.3	1.42	106.0	1.39	107.6	1.41
109.2	1.41	110.9	1.39	112.6	1.39	114.2	1.38	115.8	1.39
117.5	1.38	119.1	1.38	120.7	1.35	122.4	1.33	124.0	1.33
125.7	1.32	127.4	1.30	129.0	1.31	130.7	1.31	132.3	1.27
133.9	1.26	135.6	1.28	137.2	1.27	138.8	1.30	140.5	1.29
142.1	1.22	143.7	1.26	145.4	1.28	147.0	1.24	148.7	1.24
150.3	1.21	152.0	1.19	153.6	1.20	155.2	1.16	156.9	1.20
158.5	1.15	160.1	1.15	161.7	1.16	163.4	1.14	165.0	1.14
166.7	1.11	168.3	1.12	170.0	1.11	171.6	1.11	173.2	1.08
174.9	1.09	176.5	1.07	178.1	1.05	179.8	1.08	181.5	1.05
183.1	1.07	184.8	1.03	186.4	1.00	188.0	1.00	189.7	.98
191.3	.96	192.9	.96	194.6	.94	196.2	.97	197.9	.97
199.5	.97	201.2	.96	202.8	.94	204.4	.93	206.0	.93
207.6	.92	209.2	.92	210.9	.93	212.5	.93	214.1	.92
215.8	.92	217.5	.93	219.1	.91	220.7	.91	222.4	.88
224.0	.89	225.6	.89	227.3	.89	228.9	.88	230.5	.87
232.2	.84	233.9	.88	235.5	.86	237.2	.84	238.8	.84
240.4	.84	242.1	.83	243.7	.80	245.3	.81	247.0	.78
248.6	.79	250.3	.79	251.9	.78	253.6	.78	255.2	.77
256.9	.75	258.4	.74	260.0	.74	261.7	.74	263.3	.73
264.9	.73	266.6	.71	268.3	.71	269.9	.72	271.5	.72
273.2	.73	274.6	.73	276.4	.72	278.1	.74	279.7	.73

t	ΔT	t	ΔT	t	ΔT	t	ΔT	t	ΔT
281.3	.72	283.0	.71	284.6	.68	286.2	.67	287.9	.66
289.5	.65	291.2	.66	292.8	.68	294.4	.70	296.1	.69
297.7	.67	299.3	.70	301.0	.69	302.6	.68	304.3	.70
305.9	.70	307.5	.66	309.2	.64	310.8	.65	312.5	.65
314.0	.64	315.7	.62	317.3	.62	318.9	.61	320.5	.60
322.1	.62	323.7	.59	325.3	.58	326.9	.59	328.6	.60
330.2	.61	331.8	.62	333.5	.64	335.1	.63	336.7	.59
338.3	.58	340.0	.59	341.6	.60	343.2	.61	344.9	.61
346.5	.62	348.1	.61	349.8	.59	351.4	.59	353.0	.58
354.7	.59	356.4	.60	358.0	.57	359.6	.57	361.3	.57
362.9	.58	364.5	.56	366.2	.55	367.8	.54	369.4	.54
371.1	.52	372.8	.50	374.4	.50	376.1	.49	377.7	.48
379.3	.48	381.0	.45	382.6	.44	384.2	.48	385.8	.45
387.5	.46	389.1	.46	390.8	.46	392.4	.46	394.0	.47
395.7	.47	397.3	.47	398.9	.45	400.6	.50	402.2	.50
403.9	.48	405.5	.49	407.2	.48	408.8	.46	410.4	.49
412.1	.48	413.7	.45	415.3	.46	417.0	.47	418.6	.46
420.3	.49	421.9	.49	423.6	.48	425.2	.48	426.9	.45
428.5	.45	430.1	.44	431.8	.43	433.4	.42	435.0	.42
436.7	.43	438.3	.44	439.9	.44	441.6	.43	443.3	.43
444.9	.44	446.5	.44	448.2	.39	449.8	.43	451.4	.38
453.1	.37	454.6	.40	456.7	.40	456.8	.41	460.9	.45
462.9	.44	464.9	.44	466.9	.42	468.9	.40	471.0	.40
473.0	.41	475.0	.43	477.1	.41	479.1	.44	481.1	.43
483.1	.43	485.1	.42	487.2	.43	489.2	.42	491.2	.42
493.4	.40	495.6	.42	497.6	.42	499.6	.44	501.6	.40
503.6	.41	505.7	.38	507.7	.40	509.7	.39	511.7	.41
513.7	.42	515.7	.41	517.7	.40	519.7	.40	521.7	.39
523.7	.36	525.8	.35	527.8	.35	529.8	.36	531.8	.37
533.8	.39	535.9	.39	537.9	.38	539.9	.40	541.9	.39
543.9	.38	545.9	.38	548.0	.39	550.0	.38	552.0	.39
554.0	.39	556.0	.37	558.0	.39	560.0	.35	562.0	.36

Table C3 (continued)

t	ΔT	t	ΔT	t	ΔT	t	ΔT	t	ΔT
564.1	.35	566.1	.36	568.1	.39	570.1	.39	572.1	.38
574.2	.37	576.2	.38	578.2	.38	580.2	.36	582.2	.37
584.2	.39	586.2	.38	588.2	.38	590.3	.37	592.3	.37
594.3	.39	596.3	.41	598.3	.37	60.4	.37	602.4	37
604.5	.39	606.5	.36	608.5	.34	610.5	.37	612.6	.36
614.6	.38	616.6	.38	618.6	.37	620.6	.40	622.6	40
624.8	.38	626.8	.37	628.8	.36	630.8	.38	632.8	.40
634.8	.39	636.9	.40	638.9	.42	640.9	.40	642.9	.44
644.9	.40	646.9	.38	649.0	.38	651.0	.37	653.0	.36
655.0	.35	657.0	.36	659.0	.38	661.0	.36	663.1	.36
665.1	.39	667.1	.39	669.1	.39	671.1	.40	673.1	.38
675.1	.35	677.2	.37	679.3	.32	681.3	.32	683.3	.33
685.3	.32	687.3	.34	689.3	.34	691.3	.34	693.4	.34
695.4	.32	697.4	.30	699.4	.31	701.4	.29	703.4	.31
703.4	.31	703.4	.31	703.4	.31				

Run 1-2

Coal particle size: -180+125μm

Drying conditions: Both O_2 and N_2 bubbled through saturated zinc chloride solutions.

Steady-state temperature T_s: 80.65°C

Heat transfer coefficient U: 0.184 WK^{-1}

Heat transfer time constant U/C_p: 0.02194 min^{-1}

Calculated heat of reaction $V\Delta H/C_p$: 1.24 m^3 K mol^{-3}

Table C4 Concentration data for run 1-2

Time/min	Concentration/mol.m^{-3}				
	CO_2	H_2O	O_2	N_2	CO
40.1	0.0302	0.5020	50.40	1.984	0.1491
65.6	0.0580	0.4944	48.44	2.689	0.1467
92.6	0.0805	0.5899	46.97	3.134	0.1640
120.7	0.1163	0.6397	46.75	2.007	0.1928
146.5	0.1416	0.6605	46.01	1.964	0.2156
174.1	0.1559	0.5725	44.34	2.827	0.2208
204.1	0.1915	0.5965	44.54	2.178	0.2536
262.6	0.2221	0.6015	41.82	3.080	0.2677
287.7	0.2414	0.5410	41.69	3.056	0.2868
316.5	0.2747	0.6175	41.56	2.339	0.3117
347.2	0.2986	0.5670	41.05	2.333	0.3258
370.8	0.3166	0.4820	40.85	2.227	0.3436
452.2	0.3634	0.5646	39.19	2.301	0.3818
628.0	0.4687	0.6180	36.56	2.578	0.4622
695.9	0.5109	0.7044	35.94	2.332	0.4841
735.8	0.5250	0.6328	35.4	2.575	0.4873
764.2	0.5525	0.6723	35.25	2.296	0.5003

The temperature data are tabulated overleaf.

Table C5 Temperature deviation data of run 1-2

t	ΔT	t	ΔT	t	ΔT	t	ΔT	t	ΔT
20.5	.28	21.5	.34	22.6	.41	23.7	.47	24.8	.53
25.9	.59	26.9	.65	28.0	.70	29.1	.76	30.2	.81
31.2	.85	32.3	.88	33.4	.92	34.5	.99	35.6	1.01
36.6	1.07	37.7	1.10	38.8	1.14	39.9	1.18	41.1	1.22
42.1	1.27	43.2	1.27	44.3	1.30	45.4	1.35	46.5	1.40
47.5	1.44	48.6	1.46	49.7	1.51	50.8	1.54	51.8	1.57
52.9	1.60	54.0	1.63	55.1	1.65	56.1	1.65	57.2	1.70
58.3	1.70	59.4	1.72	60.5	1.75	61.5	1.77	62.6	1.77
63.7	1.81	64.8	1.81	65.8	1.82	66.9	1.82	68.0	1.87
69.1	1.87	70.2	1.87	71.2	1.89	72.3	1.90	73.4	1.94
74.5	1.94	75.5	1.93	76.6	1.95	77.7	1.95	78.7	1.99
79.8	1.99	80.9	1.99	82.0	2.00	83.1	2.01	84.2	2.03
85.2	2.03	86.3	2.04	87.4	2.04	88.5	2.04	89.5	2.04
90.6	2.04	91.7	2.05	92.8	2.06	93.9	2.04	95.0	2.03
96.0	2.03	97.1	2.03	98.2	2.03	99.3	2.06	100.3	2.07
101.4	2.05	102.5	2.05	103.6	2.05	104.7	2.08	105.7	2.09
106.8	2.07	107.9	2.07	109.0	2.08	110.0	2.07	111.1	2.05
112.2	2.04	113.3	2.03	114.3	2.03	115.5	2.03	116.5	2.03
117.6	2.02	118.7	2.00	119.7	1.99	120.9	1.99	122.2	2.00
123.6	2.03	124.8	2.04	126.1	2.05	127.3	2.06	128.6	2.10
129.9	2.13	131.2	2.10	132.4	2.10	133.7	2.12	134.9	2.16
136.2	2.14	137.5	2.13	138.7	2.13	140.0	2.13	141.3	2.11
142.5	2.11	143.8	2.07	145.1	2.07	146.3	2.06	147.7	2.08
149.0	2.09	150.2	2.04	151.5	2.05	152.8	2.05	154.0	2.06
155.3	2.06	156.6	2.01	157.8	1.99	159.1	2.01	160.4	2.00
161.6	1.97	162.9	1.98	164.1	1.95	165.4	1.97	166.7	1.96
167.9	1.93	169.2	1.92	170.5	1.93	171.8	1.94	173.0	1.92
174.4	1.90	175.6	1.89	176.9	1.88	178.1	1.87	179.4	1.85
180.6	1.82	181.9	1.85	183.2	1.85	184.5	1.84	185.7	1.82
187.0	1.78	188.2	1.80	189.5	1.81	190.8	1.81	192.0	1.77
193.3	1.74	194.5	1.77	195.9	1.76	197.1	1.75	198.4	1.72
199.6	1.72	200.9	1.73	202.2	1.73	203.4	1.72	204.7	1.69
206.0	1.70	207.2	1.69	208.5	1.68	209.8	1.67	211.1	1.65

t	ΔT	t	ΔT	t	ΔT	t	ΔT	t	ΔT
212.3	1.66	213.6	1.68	214.8	1.66	216.1	1.64	217.4	1.62
218.6	1.64	219.9	1.65	221.1	1.63	222.4	1.59	223.7	1.60
225.0	1.59	226.2	1.63	227.5	1.60	228.7	1.56	230.2	1.58
231.6	1.59	233.1	1.58	234.5	1.54	236.0	1.53	237.5	1.56
238.9	1.55	240.3	1.52	241.8	1.51	243.2	1.51	244.7	1.50
246.1	1.48	247.6	1.47	249.0	1.49	250.5	1.49	251.9	1.47
253.4	1.46	254.9	1.46	256.3	1.47	257.8	1.45	259.2	1.44
260.7	1.47	262.1	1.45	263.6	1.45	265.0	1.41	266.5	1.41
267.9	1.45	269.4	1.40	270.8	1.39	272.3	1.39	273.7	1.41
275.2	1.40	276.6	1.35	278.1	1.36	279.5	1.39	281.0	1.40
282.4	1.35	283.7	1.33	285.2	1.33	286.6	1.34	287.9	1.32
289.4	1.30	290.8	1.34	292.3	1.34	293.7	1.32	295.2	1.29
296.6	1.28	298.1	1.30	299.6	1.28	301.0	1.26	302.5	1.28
303.9	1.28	305.4	1.29	306.8	1.27	308.3	1.24	309.7	1.27
311.2	1.26	312.6	1.25	314.1	1.23	315.6	1.21	317.0	1.21
318.4	1.20	319.9	1.19	321.3	1.21	322.8	1.20	324.2	1.21
325.7	1.18	327.1	1.16	328.6	1.21	329.9	1.20	331.3	1.19
332.8	1.18	334.2	1.19	335.7	1.19	337.1	1.21	338.6	1.16
340.0	1.16	341.5	1.19	342.9	1.19	344.4	1.19	345.9	1.16
347.3	1.18	348.7	1.19	350.2	1.17	351.6	1.16	353.0	1.17
354.5	1.18	355.9	1.18	357.4	1.16	358.8	1.15	360.3	1.18
361.8	1.16	363.2	1.14	364.7	1.18	366.1	1.17	367.6	1.17
369.0	1.14	370.5	1.14	371.8	1.16	373.3	1.15	374.7	1.12
376.2	1.11	377.7	1.15	379.1	1.14	380.6	1.12	382.0	1.11
383.5	1.13	384.9	1.15	386.4	1.12	387.8	1.11	389.2	1.13
390.7	1.11	392.1	1.07	394.3	1.09	396.3	1.12	398.3	1.12
400.3	1.09	402.3	1.07	404.3	1.05	406.3	1.05	408.3	1.07
410.3	1.04	412.4	1.04	414.4	1.04	416.4	1.03	418.4	1.00
420.4	1.05	422.5	1.00	424.5	1.01	426.5	1.02	428.5	1.02
430.6	1.01	432.6	.99	434.6	1.00	436.6	1.01	438.6	1.02
440.6	1.00	442.7	.99	444.7	1.01	446.7	1.01	448.7	.98
450.7	.97	452.8	.97	454.9	.96	456.9	.99	458.9	.99
460.9	.98	462.9	.97	464.9	.94	467.0	.96	469.0	.98

Table C5 (continued)

t	ΔT	t	ΔT	t	ΔT	t	ΔT	t	ΔT
471.0	.98	473.0	.99	475.0	.99	477.1	.96	479.1	.93
481.1	.99	483.1	.98	485.1	.96	487.1	.96	489.1	.94
491.3	.96	493.4	.95	495.4	.94	497.4	.94	499.5	.94
501.5	.93	503.5	.95	505.5	.95	507.5	.93	509.5	.93
511.5	.95	513.5	.89	515.5	.93	517.5	.92	519.5	.88
521.6	.90	523.6	.93	525.6	.91	527.7	.91	529.7	.94
531.7	.91	533.7	.92	535.7	.93	537.7	.91	539.7	.91
541.8	.92	543.8	.89	545.8	.90	547.8	.92	550.0	.89
552.0	.94	554.0	.91	556.0	.92	558.0	.90	560.0	.94
562.0	.89	564.1	.90	566.1	.89	568.1	.88	570.1	.89
572.1	.89	574.1	.88	576.1	.89	578.1	.89	580.1	.87
582.1	.88	584.2	.88	586.2	.86	588.2	.87	590.2	.89
592.2	.85	594.2	.85	596.3	.86	598.3	.84	600.3	.85
602.3	.86	604.3	.86	606.3	.85	608.4	.85	610.4	.85
612.4	.82	614.4	.87	616.4	.84	618.4	.83	620.4	.86
622.4	.86	624.4	.84	626.4	.86	628.5	.83	630.5	.87
632.5	.85	634.5	.83	636.5	.84	638.5	.84	640.5	.81
642.5	.83	644.6	.82	646.6	.81	648.6	.85	650.6	83
652.6	.82	654.6	.84	656.8	.81	658.8	.81	660.8	.82
662.8	.82	664.8	.81	666.8	.86	668.8	.84	670.9	.79
672.9	.82	674.9	.81	676.9	.78	678.9	.82	680.9	.81
682.9	.79	685.0	.81	687.0	.80	689.0	.78	691.0	.79
693.0	.80	695.0	.78	697.1	.81	699.1	.81	701.1	.80
703.1	.81	705.1	.81	707.1	.86	709.1	.81	711.1	.80
713.1	.79	715.2	.80	717.2	.80	719.2	.78	721.2	.79
723.2	.79	725.2	.79	727.2	.81	729.2	.78	731.3	.77
733.3	.78	735.3	.78	737.3	.76	739.5	.80	741.5	.80
743.5	.75	745.5	.78	747.5	.77	749.6	.78	751.6	.79
753.6	.77	755.6	.78	757.6	.80	759.6	.77	761.7	.77
763.7	.79	765.8	.76	767.8	.77	769.8	.76	771.8	.75
773.8	.74	775.8	.76	777.8	.72	779.9	.75	781.9	.77
783.9	.73	785.9	.77	787.9	.77	789.9	.73	791.9	.78
791.9	.78	791.9	.76	791.9	.78				

Run 1-3
Coal particle size: -180+125μm
Drying conditions: Both O_2 and N_2 bubbled through saturated zinc chloride solutions.
Steady-state temperature T_s: 79.72°C
Heat transfer coefficient U: not measured
Heat transfer time constant U/C_p: not measured

Table C6 Concentration data for run 1-3

Time/min	Concentration/mol.m^{-3}				
	CO_2	H_2O	O_2	N_2	CO
13.0	0	0.2303	11.27	43.314	0.0175
37.6	0.0103	0.2338	10.71	43.167	0
85.0	0.0272	0.3691	10.14	42.83	0.0529
108.9	0.0329	0.4033	9.59	42.993	0.0440
143.0	0.0427	0.5598	9.19	42.865	0.0569

The temperature data is given on the following page.

Table C7 Temperature deviation data of run 1-3

t	ΔT	t	ΔT	t	ΔT	t	ΔT	t	ΔT
21.8	.31	22.4	.32	23.2	.35	23.8	.37	24.5	.37
24.8	.39	25.3	.42	25.8	.41	26.3	.43	26.9	.47
27.4	.46	27.9	.46	28.4	.47	28.9	.47	29.5	.48
30.0	.49	30.5	.49	31.4	.47	31.5	.48	32.2	.47
32.7	.48	33.2	.49	33.8	.50	34.3	.52	34.8	.52
35.3	.52	35.9	.54	36.4	.55	36.9	.54	37.4	.55
38.0	.55	38.5	.58	39.0	.59	39.5	.59	40.1	.62
40.6	.60	41.1	.60	41.6	.61	42.2	.59	42.7	.60
43.2	.58	43.7	.60	44.3	.60	44.9	.61	45.4	.61
45.9	.62	46.5	.61	47.0	.61	47.5	.63	48.0	.65
48.5	.68	49.0	.68	49.5	.68	50.1	.68	50.6	.68
51.2	.68	51.7	.69	52.2	.69	52.8	.67	53.3	.68
53.8	.67	54.3	.68	54.9	.66	55.4	.67	55.9	.68
56.4	.68	56.9	.68	57.4	.71	58.0	.71	58.5	.72
59.0	.72	59.5	.72	60.0	.72	60.5	.73	61.0	.72
61.7	.73	62.2	.74	62.7	.74	63.2	.74	63.7	.74
64.3	.73	64.8	.74	65.3	.72	65.8	.70	66.3	.71
66.8	.73	67.3	.70	67.8	.71	68.3	.72	68.9	.72
69.4	.72	69.9	.72	70.4	.71	71.0	.74	71.5	.74
72.0	.74	72.5	.74	73.0	.74	73.5	.74	74.1	.75
74.6	.76	75.1	.73	75.6	.74	76.1	.74	76.6	.7
77.1	.71	77.6	.74	78.2	.72	78.7	.70	79.2	.73
79.7	.72	80.2	.71	80.8	.73	81.3	.74	81.8	.74
82.3	.73	82.8	76	83.3	.77	83.8	.75	84.3	.75
84.8	.75	85.9	.76	87.0	.74	88.1	.73	89.2	.72
90.2	.72	91.3	.69	92.4	.72	93.5	.72	94.5	.71
95.6	.73	96.7	.73	97.8	.72	98.9	.74	99.9	.72
101.0	.72	102.1	.70	103.2	.70	104.2	.71	105.3	.70
106.4	.74	107.5	.74	108.6	.73	109.8	.76	110.8	.73
111.9	.74	113.0	.73	114.0	.71	115.1	.71	116.2	.69
117.3	.69	118.3	.71	119.4	.72	120.5	.74	121.6	.73
122.7	.72	123.8	.69	124.8	.70	125.9	.69	127.0	.68
128.0	.67	129.1	.67	130.2	.67	131.3	.69	132.4	.67

Run 1-4
Coal particle size: -63+45μm
Drying conditions: Both O_2 and N_2 bubbled through saturated zinc chloride solutions.
Steady-state temperature T_s: 80.09°C
Heat transfer coefficient U: 0.188 WK^{-1}
Heat transfer time constant U/C_p: 0.02353 min^{-1}
Calculated heat of reaction $V\Delta H/C_p$: 1.36 m^3 K mol^{-3}

Table C8 Concentration data for run 1-4

Time/min	Concentration/mol.m^{-3}				
	CO_2	H_2O	O_2	N_2	CO
11.2	0.1530	0.5476	41.10	4.230	0.1798
157.2	0.1990	0.5813	38.92	4.581	0.2239
180.4	0.2455	0.6522	39.20	3.466	0.2687
203.1	0.2678	0.6843	38.30	3.450	0.2802
227.4	0.2790	0.7509	37.14	4.014	0.2846
251.0	0.3126	0.8216	36.84	3.513	0.3068
273.8	0.3187	0.7555	36.03	3.854	0.3199
309.6	0.3368	0.7270	35.06	4.308	0.3376
337.6	0.3845	0.7554	34.97	3.611	0.3741
370.6	0.3555	0.6397	33.21	4.871	0.3386
448.9	0.4385	0.7475	32.73	4.067	0.4062
474.0	0.4792	0.8035	32.67	3.497	0.4300
509.37	0.5027	0.7411	32.25	3.628	0.4198

Table C9 containing the temperature data is given overleaf.

Table C9 Temperature deviation data of run 1-4

t	ΔT	t	ΔT	t	ΔT	t	ΔT	t	ΔT
20.3	1.73	20.8	1.76	21.4	1.82	21.9	1.83	22.4	1.85
22.9	1.91	23.5	1.95	24.0	1.98	24.5	1.99	25.0	2.01
25.6	2.07	26.1	2.08	26.6	2.12	27.2	2.13	27.7	2.15
28.2	2.18	28.7	2.22	29.2	2.24	29.7	2.27	30.2	2.31
30.6	2.31	31.2	2.32	31.7	2.35	32.2	2.39	32.7	2.42
33.2	2.43	33.8	2.43	34.3	2.46	34.8	2.50	35.3	2.51
35.8	2.53	36.3	2.58	36.8	2.59	37.3	2.60	37.8	2.63
38.4	2.65	38.9	2.66	39.4	2.66	39.8	2.70	40.4	2.71
40.9	2.72	41.4	2.75	41.9	2.75	42.4	2.79	42.9	2.80
43.5	2.83	44.0	2.83	44.5	2.86	45.0	2.87	45.5	2.88
46.0	2.92	46.5	2.95	47.1	2.95	47.6	2.96	48.1	2.96
48.6	3.00	49.2	3.03	49.7	3.02	50.3	3.04	50.9	3.05
51.4	3.05	51.9	3.06	52.4	3.08	52.9	3.09	53.4	3.10
53.9	3.10	54.5	3.13	55.0	3.16	55.5	3.16	56.0	3.15
56.5	3.16	57.0	3.16	57.5	3.17	58.0	3.16	58.5	3.17
59.0	3.19	59.5	3.18	60.1	3.20	60.6	3.21	61.1	3.21
61.6	3.21	62.1	3.21	62.6	3.22	63.1	3.25	63.6	3.26
64.1	3.26	64.6	3.26	65.2	3.26	65.7	3.26	66.2	3.27
66.7	3.27	67.2	3.27	67.7	3.31	68.2	3.29	6.7	3.30
69.2	3.30	69.8	3.31	70.3	3.34	70.8	3.35	71.3	3.36
71.8	3.33	72.4	3.37	72.9	3.37	73.4	3.37	73.9	3.35
74.4	3.38	74.9	3.39	75.4	3.36	75.9	3.37	76.5	3.38
77.0	3.39	77.5	3.39	78.1	3.37	78.6	3.40	79.1	3.39
79.6	3.39	80.1	3.40	80.6	3.38	81.1	3.41	81.7	3.38
82.2	3.38	82.7	3.39	83.2	3.40	83.7	3.40	84.2	3.41
84.7	3.41	85.2	3.41	85.7	3.39	86.2	3.39	86.7	3.39
87.3	3.38	87.8	3.38	88.3	3.38	88.8	3.37	89.3	3.36
89.9	3.36	90.4	3.37	90.9	3.37	91.4	3.37	91.9	3.35
92.4	3.37	93 0	3.36	93.5	3.36	94.0	3.37	94.5	3.37
95.0	3.38	95.5	3.36	96.0	3.39	96.5	3.37	97.1	3.38
97.6	3.38	98.1	3.39	98.6	3.39	99.1	3.35	99.6	3.38

t	ΔT	t	ΔT	t	ΔT	t	ΔT	t	ΔT
100.2	3.38	100.7	3.36	101.2	3.36	101.7	3.37	102.2	3.34
102.7	3.34	103.2	3.34	103.8	3.35	104.3	3.35	104.8	3.35
105.3	3.35	105.8	3.32	106.3	3.32	106.9	3.33	107.4	3.32
107.9	3.32	108.4	3.33	108.9	3.33	109.5	3.31	110.0	3.31
110.5	3.31	111.0	3.29	111.5	3.32	112.0	3.29	112.5	3.29
113.0	3.28	113.5	3.27	114.1	3.27	114.6	3.27	115.1	3.24
115.6	3.24	116.1	3.22	116.7	3.25	117.2	3.23	117.7	3.23
118.2	3.21	118.7	3.21	119.2	3.21	119.7	3.22	120.3	3.22
120.8	3.20	121.3	3.20	121.9	3.20	122.4	3.20	122.9	3.19
123.4	3.17	123.9	3.17	124.5	3.16	125.0	3.16	125.5	3.17
126.3	3.15	127.2	3.15	128.1	3.14	129.0	3.14	129.8	3.11
130.7	3.12	131.6	3.11	132.5	3.12	133.4	3.10	134.3	3.11
135.2	3.09	136.1	3.10	137.0	3.07	137.9	3.05	138.8	3.05
139.7	3.05	140.5	3.05	141.4	3.03	142.3	3.01	143.2	3.01
144.1	3.02	145.0	2.99	145.9	2.95	146.8	2.96	147.7	2.94
148.6	2.94	149.5	2.92	150.3	2.92	151.2	2.91	152 1	2.89
153.0	2.89	153.9	2.90	154.8	2.87	155.6	2.86	156.5	2.86
157.3	2.87	158.2	2.84	159.1	2.84	159.9	2.80	160.8	2.79
161.7	2.77	162.6	2.77	163.5	2.78	164.4	2.75	165.3	2.75
166.2	2.75	167.1	2.74	168.0	2.74	168.8	2.71	169.7	2.71
170.6	2.69	171.5	2.69	172.4	2.68	173.3	2.68	174.2	2.66
175.1	2.66	176.0	2.65	176.9	2.66	177.7	2.65	178.6	2.63
179.5	2.63	180.5	2.63	181.3	2.60	182.2	2.61	183.3	2.58
184.1	2.58	185.0	2.57	185.9	2.57	186.8	2.58	187.7	2.56
188.6	2.55	189.5	2.54	190.3	2.51	191.2	2.52	192.2	2.50
193.0	2.52	193.9	2.51	194 8	2.49	195.7	2.49	196.6	2.48
197.5	2.48	198.4	2.44	199.2	2.44	200.1	2.44	201.0	2.45
202.0	2.42	202.8	2.42	203.6	2.42	204.5	2.44	205.4	2.40
206.3	2.40	207.1	2.38	208.0	2.39	208.9	2.37	209.8	2.37
210.	2.37	211.6	2.35	212.5	2.33	213.4	2.32	214.3	2.33
215.2	2.32	216.0	2.32	216.9	2.29	217.8	2.27	218.7	2.27
219.6	2.24	220.5	2.23	221.4	2.21	222.3	2.19	223.2	2.20
224.1	2.16	225.0	2.16	225.8	2.13	226.7	2.11	227.6	2.12

Table C9 (continued)

ε	ΔT	ε	ΔT	ε	ΔT	ε	ΔT	ε	ΔT
228.7	2.09	229.4	2.09	230.2	2.09	231.2	2.09	232.1	2.07
233.0	2.08	233.9	2.06	234.8	2.06	235.7	2.02	236.5	2.02
237.4	2.01	238.3	1.99	239.2	1.98	240.1	2.00	241.0	2.00
241.9	1.98	242.8	1.98	243.7	1.96	244.6	1.97	245.4	1.93
246.3	1.94	247.2	1.92	248.1	1.93	249.0	1.90	249.9	1.88
250.8	1.86	251.7	1.87	252.6	1.83	253.5	1.84	254.4	1.83
255.2	1.81	256.1	1.80	257.0	1.80	257.9	1.80	258.8	1.78
259.7	1.77	260.6	1.77	261.5	1.77	262.4	1.76	263.3	1.76
264.1	1.75	265.1	1.72	266.5	1.73	267.7	1.71	269.0	1.70
270.3	1.70	271.6	1.68	272.8	1.68	274.1	1.68	275.3	1.65
276.6	1.66	277.8	1.67	279.1	1.65	280.4	1.65	281.6	1.65
282.9	1.63	284.2	1.63	285.4	1.63	286.7	1.61	288.0	1.58
289.2	1.58	290.5	1.54	291.8	1.55	293.0	1.54	294.3	1.56
295.5	1.53	296.8	1.53	298.1	1.52	299.4	1.50	300.6	1.48
301.9	1.48	303.1	1.48	304.4	1.44	305.7	1.49	306.9	1.45
308.2	1.43	309.4	1.44	310.8	1.40	312.9	1.39	314.9	1.42
316.9	1.40	318.0	1.38	321.0	1.36	323.0	1.33	325.0	1.33
327.0	1.32	329.0	1.33	331.1	1.32	333.1	1.30	335.1	1.29
337.1	1.29	339.1	1.30	341.2	1.25	343.2	1.25	345.2	1.24
347.2	1.22	349.2	1.24	351.2	1.24	353.3	1.22	355.3	1.22
357.3	1.23	359.3	1.23	361.3	1.23	363.3	1.22	365.3	1.24
367.3	1.24	369.3	1.21	371.4	1.19	373.9	1.21	376.8	1.18
379.2	1.21	381.7	1.16	384.3	1.15	386.9	1.14	389.5	1.15
392.0	1.12	394.6	1.14	397.2	1.14	399.7	1.15	402.4	1.11
404.9	1.11	407.5	1.08	410.1	1.08	412.6	1.07	415.2	1.07
417.8	1.05	420.4	1.06	422.9	1.05	425.5	1.05	428.1	1.05
430.7	1.03	433.3	1.04	435.8	1.04	438.4	1.02	441.0	1.02
443.6	1.02	446.1	1.01	448.7	.98	451.3	1.00	453.9	.98
456.5	.98	459.1	.98	461.7	.97	464.2	.98	466.8	.97
469.4	.94	471.9	.96	474.5	.95	477.1	.95	479.6	.95
482.2	.92	484.8	.92	487.4	.95	490.0	.93	492.5	.90
495.1	.90	497.7	.91	500.3	.92	502.8	.91	505.4	.90

Run 1-5

Coal particle size: -500+355μm

Drying conditions: Both O_2 and N_2 bubbled through saturated zinc chloride solutions.

Steady-state temperature T_s: 79.94°C

Heat transfer coefficient U: 0.188 WK^{-1}

Heat transfer time constant U/C_p: 0.02258 min^{-1}

Calculated heat of reaction $V\Delta H/C_p$: 1.47 m^3 K mol^{-3}

Table C10 Concentration data for run 1-5

Time/min	Concentration/mol.m^{-3}				
	CO_2	H_2O	O_2	N_2	CO
12.1	0	0.3312	50.65	2.664	0.1226
36.1	0.0340	0.3791	48.91	2.911	0.1230
82.7	0.0831	0.6593	46.25	2.907	0.1542
133.8	0.1370	0.7169	44.04	3.019	0.1934
158.0	0.1608	0.7456	43.44	3.027	0.2084
210.3	0.2050	0.6736	41.85	3.198	0.2428
266.6	0.2435	0.7826	40.53	3.104	0.2655
326.1	0.2610	0.6532	38.59	4.072	0.2860
397.4	0.3108	0.6305	37.69	3.844	0.3379
454.2	0.3647	0.9084	37.12	3.168	0.3616
496.5	0.3919	0.9463	36.41	3.079	0.3837
566.6	0.4231	0.9495	35.56	3.329	0.4198
650.2	0.4654	0.7569	34.26	3.554	0.4090
686.0	0.4691	0.8010	33.79	3.581	0.4472
710.3	0.4946	0.9487	33.81	3.206	0.4549

The temperature points are tabulated on the following page.

Table C11 Temperature deviation data of run 1-5

t	ΔT	t	ΔT	t	ΔT	t	ΔT	t	ΔT
21.3	1.34	22.3	1.42	23.4	1.46	24.5	1.54	25.6	1.62
26.7	1.72	27.7	1.77	28.8	1.82	29.9	1.88	31.0	1.95
32.0	2.00	33.1	2.03	34.2	2.11	35.3	2.15	36.3	2.19
37.4	2.25	38.5	2.30	39.6	2.33	40.6	2.38	41.7	2.41
42.8	2.44	43.8	2.49	44.9	2.53	46.0	2.56	47.1	2.61
48.2	2.61	49.3	2.66	50.3	2.68	51.5	2.66	52.5	2.72
53.6	2.73	54.7	2.73	55.7	2.77	56.8	2.79	57.9	2.78
59.0	2.81	60.1	2.81	61.2	2.83	62.2	2.86	63.3	2.86
64.4	2.87	65.4	2.88	66.5	2.89	67.6	2.90	68.7	2.91
69.8	2.91	70.9	2.93	71.9	2.93	73.0	2.93	74.1	2.93
75.1	2.93	76.2	2.97	77.3	2.96	78.4	2.97	79.4	2.97
80.5	2.96	81.6	2.96	82.8	2.96	83.8	2.98	84.9	2.96
86.0	2.96	87.0	2.97	88.1	2.96	89.2	2.99	90.3	2.98
91.3	3.01	92.4	2.97	93.5	2.99	94.6	3.00	95.7	2.99
96.7	2.96	97.8	2.96	98.9	2.96	100.0	2.96	101.0	2.94
102.1	2.93	103.2	2.94	104.3	2.95	105.4	2.93	106.4	2.93
107.6	2.93	108.6	2.90	109.8	2.91	110.9	2.90	111.9	2.88
113.0	2.88	114.1	2.88	115.1	2.88	116.3	2.88	117.3	2.88
118.4	2.86	119.5	2.84	120.6	2.84	121.6	2.84	122.7	2.82
123.8	2.84	124.8	2.82	125.9	2.82	127.0	2.79	128.1	2.79
129.2	2.78	130.2	2.75	131.3	2.72	132.4	2.75	133.5	2.72
134.6	2.72	135.7	2.72	136.7	2.69	137.8	2.69	138.9	2.69
140.0	2.68	141.1	2.66	142.1	2.66	143.2	2.65	144.3	2.64
145.4	2.61	146.4	2.61	147.5	2.60	148.6	2.59	149.7	2.59
150.8	2.58	151.8	2.58	152.9	2.56	154.0	2.56	155.1	2.50
156.2	2.53	157.3	2.52	158.3	2.53	159.3	2.53	160.4	2.51
161.5	2.51	162.6	2.48	163.7	2.48	164.7	2.42	165.8	2.46
166.9	2.46	167.9	2.43	169.0	2.42	170.1	2.42	171.1	2.39
172.2	2.41	173.3	2.38	174.4	2.38	175.5	2.37	176.6	2.35
177.6	2.35	178.7	2.35	179.8	2.33	180.8	2.33	181.9	2.33
182.9	2.31	184.0	2.35	185.1	2.33	186.3	2.33	187.4	2.30

t	ΔT	t	ΔT	t	ΔT	t	ΔT	t	ΔT
188.5	2.30	189.6	2.29	190.6	2.30	191.7	2.30	192.8	2.28
193.9	2.28	194.9	2.28	196.0	2.28	197.1	2.25	198.2	2.25
199.3	2.25	200.3	2.24	201.4	2.24	202.5	2.24	203.6	2.22
204.6	2.22	205.7	2.22	206.8	2.19	207.9	2.19	209.0	2.18
210.1	2.19	211.1	2.15	212.2	2.17	213.3	2.15	214.4	2.15
215.4	2.13	216.5	2.16	217.6	2.14	218.6	2.14	219.8	2.10
220.8	2.11	221.9	2.11	223.0	2.09	224.1	2.12	225.1	2.12
226.2	2.11	227.3	2.09	228.3	2.12	229.4	2.08	230.5	2.08
231.6	2.05	232.7	2.08	233.8	2.05	234.8	2.04	235.9	2.06
237.0	2.02	238.1	2.02	239.1	2.02	240.2	2.00	241.3	2.03
242.4	1.98	243.5	2.02	244.5	2.00	245.6	1.98	246.7	1.98
247.8	1.96	248.8	1.95	249.9	1.97	251.0	1.95	252.1	1.95
253.1	1.93	254.2	1.93	255.3	1.93	256.4	1.94	257.5	1.94
258.5	1.94	259.6	1.92	260.7	1.92	261.8	1.93	262.8	1.90
263.9	1.93	265.0	1.95	266.1	1.89	267.2	1.89	268.3	1.89
269.4	1.88	270.4	1.90	271.5	1.89	272.6	1.87	273.7	1.89
274.7	1.90	275.8	1.90	276.9	1.89	278.0	1.89	279.1	1.86
280.1	1.86	281.2	1.87	282.3	1.83	283.4	1.84	284.4	1.84
285.5	1.83	286.7	1.85	287.8	1.82	288.9	1.85	290.0	1.81
291.1	1.82	292.1	1.82	293.2	1.81	294.3	1.80	295.4	1.76
296.5	1.79	297.5	1.79	298.6	1.80	299.7	1.78	300.8	1.78
301.9	1.78	303.0	1.79	304.0	1.76	305.1	1.76	306.2	1.76
307.3	1.75	308.3	1.75	309.4	1.74	310.5	1.77	311.6	1.74
312.7	1.76	313.7	1.75	314.8	1.71	315.9	1.72	317.0	1.72
318.0	1.7[illegible]	319.1	1.72	320.2	1.71	321.2	1.71	322.3	1.72
323.4	1.7[illegible]	324.5	1.69	325.6	1.69	326.8	1.70	327.8	1.70
328.9	1.7[illegible]	330.0	1.71	331.1	1.67	332.2	1.65	333.3	1.69
334.3	1.69	335.4	1.68	336.5	1.68	337.6	1.68	338.7	1.69
339.7	1.68	340.8	1.68	341.9	1.67	343.0	1.69	344.0	1.67
345.1	1.70	346.2	1.69	347.3	1.68	348.4	1.68	349.4	1.69
350.5	1.66	351.6	1.67	352.7	1.67	353.7	1.65	354.8	1.65
355.9	1.65	357.0	1.66	358.1	1.67	359.1	1.67	360.2	1.67
361.3	1.65	362.4	1.68	363.4	1.67	364.5	1.69	365.6	1.66
365.6	1.66								

Run 1-6

Coal particle size: -710+500μm

Drying conditions: Both O_2 and N_2 bubbled through saturated zinc chloride solutions.

Steady-state temperature T_s: 80.39°C

Heat transfer coefficient U: 0.191 WK^{-1}

Heat transfer time constant U/C_p: 0.02337 min^{-1}

Calculated heat of reaction $V\Delta H/C_p$: 1.15 m^3 K mol^{-3}

Table C12 Concentration data for run 1-6

Time/min	Concentration/mol.m^{-3}				
	CO_2	H_2O	O_2	N_2	CO
16.9	0	0.2406	53.32	1.542	0.0855
41.4	0.0274	0.4329	51.43	1.776	0.1038
64.1	0.0506	0.4754	50.24	1.940	0
92.1	0.0739	0.5201	48.95	2.962	0.1462
115.6	0.0942	0.6077	48.08	2.004	0.1554
143.0	0.1107	0.6888	46.70	2.210	0.1751
194.0	0.1415	0.6139	44.62	3.075	0.1951
240.8	0.1843	0.5702	44.49	2.293	0.2254
300.1	0.2257	0.5552	43.16	2.153	0.2535
327.5	0.2419	0.7105	42.40	2.357	0.2764
406.6	0.2866	0.7368	41.02	2.221	0.3125
484.5	0.3277	0.6779	39.73	2.437	0.3355
604.8	0.3602	0.6525	37.07	3.307	0.3565
722.2	0.4451	0.8157	36.43	2.572	0.4186
758.3	0.4569	0.8328	35.71	2.722	0.4336
780.9	0.4681	0.6576	35.85	2.568	0.4349

Table C13 Temperature deviation data of run 1-6

t	ΔT	t	ΔT	t	ΔT	t	ΔT	t	ΔT
22.8	.96	24.0	.98	25.0	1.00	26.1	1.05	27.2	1.09
28.3	1.15	29.3	1.20	30.4	1.22	31.5	1.27	32.5	1.30
33.6	1.34	34.7	1.39	35.8	1.41	36.9	1.45	38.6	1.48
40.2	1.52	41.8	1.58	43.5	1.60	45.1	1.61	46.7	1.66
48.4	1.69	50.0	1.72	51.6	1.74	53.1	1.76	54.7	1.78
56.4	1.79	58.0	1.80	59.6	1.85	61.3	1.85	62.9	1.88
64.6	1.89	66.2	1.90	67.8	1.93	69.5	1.92	71.1	1.92
72.7	1.93	74.4	1.93	76.0	1.91	77.6	1.94	79.3	1.92
80.9	1.91	82.5	1.93	84.2	1.93	85.9	1.94	87.5	1.95
89.1	1.95	90.8	1.95	92.3	1.94	93.9	1.96	95.6	1.95
97.2	1.97	98.8	1.96	100.5	1.97	102.1	1.95	103.8	1.96
105.4	1.98	107.1	1.99	108.7	1.99	110.3	1.99	112.0	2.00
113.6	1.96	115.2	1.99	116.8	1.99	118.5	2.00	120.1	2.00
121.8	1.96	123.4	1.97	125.0	1.98	126.7	1.95	128.3	1.95
129.9	1.94	131.6	1.92	133.2	1.91	134.8	1.91	136.5	1.91
138.2	1.89	139.8	1.87	141.4	1.85	143.1	1.85	144.7	1.86
146.3	1.84	147.9	1.83	149.5	1.81	151.2	1.81	152.8	1.81
154.4	1.81	156.1	1.80	157.7	1.79	159.4	1.76	160.9	1.78
162.6	1.79	164.3	1.77	165.9	1.75	167.5	1.73	169.1	1.74
170.8	1.75	172.4	1.72	174.1	1.71	175.7	1.71	177.3	1.70
179.0	1.65	180.6	1.66	182.2	1.66	183.9	1.62	185.5	1.66
187.1	1.64	188.8	1.63	190.5	1.60	192.1	1.61	193.7	1.59
195.4	1.60	197.0	1.57	198.7	1.60	200.3	1.59	201.9	1.57
203.6	1.57	205.2	1.57	206.8	1.55	208.5	1.54	210.2	1.55
211.8	1.55	213.4	1.55	215.1	1.55	216.7	1.53	218.3	1.53
220.0	1.52	221.6	1.50	223.3	1.49	224.9	1.48	226.6	1.46
228.2	1.49	229.7	1.43	231.4	1.46	233.0	1.45	234.6	1.48
236.3	1.45	237.9	1.44	239.5	1.44	241.2	1.45	242.9	1.43
244.5	1.41	246.1	1.40	247.8	1.41	249.4	1.38	251.0	1.40
252.7	1.39	254.3	1.38	256.0	1.37	257.6	1.36	259.2	1.39
260.9	1.35	262.5	1.31	264.0	1.33	265.5	1.36	267.2	1.33

t	ΔT	t	ΔT	t	ΔT	t	ΔT	t	ΔT
268.8	1.32	270.4	1.34	272.1	1.34	273.7	1.36	275.3	1.30
277.0	1.30	278.7	1.27	280.3	1.26	281.9	1.27	283.6	1.27
285.2	1.25	286.8	1.25	288.5	1.25	290.1	1.26	291.7	1.24
293.4	1.25	295.0	1.24	296.7	1.25	298.3	1.25	299.9	1.24
301.5	1.25	303.2	1.22	304.8	1.24	306.4	1.21	308.1	1.24
309.7	1.23	311.3	1.22	313.0	1.21	314.6	1.23	316.3	1.22
317.9	1.20	319.5	1.21	321.2	1.22	322.8	1.20	324.4	1.19
326.1	1.19	327.7	1.21	329.4	1.18	331.1	1.15	332.7	1.14
334.3	1.12	336.0	1.11	337.6	1.12	339.2	1.14	340.9	1.12
342.5	1.12	344.2	1.11	345.8	1.12	347.5	1.07	349.1	1.11
350.7	1.10	352.4	1.08	354.0	1.07	355.7	1.07	357.3	1.06
358.8	1.05	360.5	1.07	362.1	1.07	363.7	1.10	365.4	1.06
367.1	1.05	368.7	1.05	370.3	1.05	372.0	1.04	373.6	1.05
375.2	1.09	376.9	1.05	378.5	1.05	380.2	1.05	381.8	1.05
383.5	1.04	385.1	1.04	386.7	1.05	388.4	1.03	390.0	1.01
391.7	1.00	393.3	1.02	394.9	1.00	396.6	1.01	398.2	1.00
399.9	1.02	401.5	1.00	403.2	1.01	404.8	1.03	406.4	1.00
408.0	1.03	409.6	1.02	411.2	1.00	412.9	1.01	414.5	1.01
416.1	1.01	417.8	1.01	419.3	1.00	421.1	.99	422.7	1.01
424.4	.98	426.0	.99	427.6	1.01	429.3	1.00	430.9	.98
432.5	.96	434.1	1.01	435.8	.99	437.5	.98	439.1	1.00
440.7	1.00	442.4	.97	444.0	.98	445.6	.98	447.3	.98
448.9	.95	450.5	.96	452.2	.95	453.9	.93	455.5	.95
457.1	.97	458.8	.95	460.4	.95	462.0	.95	463.6	.96
465.2	.91	466.9	.91	468.5	.89	470.1	.91	471.8	.91
473.4	.93	475.1	.92	476.7	.92	478.3	.89	480.2	.91
482.1	.91	483.9	.87	485.8	.91	487.7	.89	489.5	.86
491.4	.86	493.2	.85	495.0	.84	496.8	.83	498.7	.85
500.5	.86	502.3	.83	504.1	.84	505.9	.85	507.8	.81
509.6	.82	511.5	.84	513.3	.82	515.1	.82	516.9	.83
518.7	.82	520.6	.84	522.4	.82	524.2	.82	526.0	.83
527.9	.82	529.7	.82	531.5	.80	533.4	.79	535.2	.83

Run 1-7
Coal particle size: -125+90μm
Drying conditions: Both O_2 and N_2 bubbled through saturated zinc chloride solutions.
Steady-state temperature T_s: 79.44°C
Heat transfer coefficient U: 0.191 WK^{-1}
Heat transfer time constant U/C_p: 0.02273 min^{-1}
Calculated heat of reaction VAH/C_p: 1.28 m^3 K mol^{-3}

Table C14 Concentration data for run 1-7

Time/min	Concentration/mol.m^{-3}				
	CO_2	H_2O	O_2	N_2	CO
23.1	0	0.7099	35.25	15.217	0.1175
47.7	0.0210	0.6407	34.36	14.932	0.1061
71.0	0.0381	0.8093	33.54	15.030	0.1060
118.9	0.0731	0.8323	32.19	14.881	0.1309
147.9	0.0863	0.8386	31.16	15.184	0.1375

The temperature data is given in table C15 overleaf.

Table C15 Temperature deviation data of run 1-7

t	ΔT	t	ΔT	t	ΔT	t	ΔT	t	ΔT
31.1	.76	31.4	.77	32.1	.79	32.7	.80	33.2	.81
33.7	.82	34.2	.83	34.7	.84	35.2	.85	35.7	.87
36.3	.88	37.0	.90	37.5	.90	38.1	.91	38.6	.94
39.2	.95	39.8	.97	40.1	.99	40.6	1.01	41.1	1.03
41.7	1.04	42.2	1.04	42.7	1.07	43.3	1.06	43.8	1.06
44.3	1.09	44.8	1.10	45.3	1.10	45.8	1.11	46.3	1.12
46.9	1.13	47.4	1.12	48.0	1.16	48.5	1.15	49.0	1.18
49.5	1.18	50.0	1.19	50.6	1.21	51.1	1.19	51.6	1.20
52.1	1.22	52.6	1.22	53.2	1.23	53.7	1.26	54.2	1.27
54.7	1.27	55.2	1.27	55.7	1.30	56.3	1.29	56.8	1.30
57.3	1.31	57.8	1.32	58.4	1.33	58.9	1.34	59.4	1.35
59.9	1.34	60.4	1.36	60.9	1.35	61.4	1.36	62.0	1.38
62.5	1.39	63.0	1.38	63.5	1.41	64.1	1.41	64.6	1.39
65.1	1.43	65.6	1.40	66.1	1.44	66.6	1.45	67.1	1.45
67.6	1.44	68.2	1.45	68.7	1.44	69.2	1.48	69.7	1.48
70.3	1.49	70.8	1.48	71.3	1.49	71.8	1.49	72.3	1.48
72.8	1.52	73.3	1.51	73.9	1.53	74.4	1.56	74.9	1.57
75.4	1.55	76.0	1.57	76.5	1.57	77.0	1.57	77.5	1.57
78.0	1.58	78.5	1.59	79.0	1.59	79.6	1.59	80.1	1.61
80.6	1.59	81.1	1.59	81.7	1.60	82.2	1.59	82.7	1.61
83.2	1.60	83.7	1.60	84.2	1.59	84.7	1.62	85.3	1.62
85.8	1.63	86.3	1.65	86.8	1.64	87.4	1.63	87.9	1.66
88.4	1.67	88.9	1.65	89.5	1.67	90.0	1.67	90.5	1.65
91.0	1.68	91.6	1.67	92.1	1.68	92.6	1.65	93.1	1.64
93.6	1.65	94.2	1.66	94.7	1.64	95.3	1.64	95.8	1.65
96.3	1.67	96.8	1.67	97.4	1.66	97.9	1.68	98.4	1.69
98.9	1.68	99.4	1.67	99.9	1.67	100.4	1.68	100.9	1.68
101.5	1.69	102.0	1.69	102.5	1.67	103.0	1.68	103.6	1.68
104.1	1.68	104.6	1.69	105.1	1.66	105.6	1.67	106.1	1.66
106.6	1.69	107.2	1.69	107.7	1.69	108.2	1.69	108.7	1.68
109.3	1.71	109.8	1.68	110.3	1.71	110.8	1.71	111.3	1.67
111.8	1.68	112.3	1.69	112.9	1.67	113.4	1.68	113.9	1.65

t	ΔT	t	ΔT	t	ΔT	t	ΔT	t	ΔT
114.4	1.65	115.0	1.66	115.5	1.66	116.0	1.66	116.5	1.66
117.0	1.65	117.5	1.67	118.0	1.66	118.6	1.65	119.1	1.68
119.7	1.67	120.2	1.67	120.7	1.66	121.2	1.67	121.7	1.66
122.2	1.66	122.6	1.66	123.3	1.65	123.8	1.63	124.3	1.64
124.9	1.63	125.4	1.64	125.9	1.61	126.4	1.60	126.9	1.63
127.4	1.61	127.9	1.63	128.5	1.62	129.0	1.60	129.5	1.62
130.0	1.59	130.6	1.60	131.1	1.60	131.6	1.60	132.1	1.59
132.6	1.59	133.1	1.5.	133.6	1.58	134.2	1.59	134.7	1.57
135.2	1.58	135.7	1.59	136.3	1.56	136.8	1.56	137.3	1.59
137.8	1.57	138.3	1.57	138.8	1.59	139.3	1.58	139.9	1.60
140.4	1.60	140.9	1.60	141.4	1.57	142.0	1.60	142.5	1.58
143.0	1.61	143.5	1.59	144.0	1.59	144.5	1.57	145.0	1.59
145.6	1.59	146.1	1.57	146.6	1.56	147.1	1.57	147.7	1.55
148.2	1.55	148.7	1.55	149.2	1.54	149.7	1.55	150.2	1.54
150.8	1.57	151.4	1.57	152.0	1.58	152.5	1.57	153.0	1.56
153.6	1.54	154.1	1.56	154.6	1.55	155.1	1.54	155.6	1.55
156.1	1.52	156.6	1.53	157.2	1.52	157.7	1.52	158.2	1.50
158.7	1.50	159.3	1.50	159.8	1.49	160.3	1.48	160.8	1.50
161.3	1.50	161.8	1.50	162.3	1.49	162.9	1.49	163.4	1.49
163.4	1.49								

Appendix C

C.4 Runs 2-1 to 2-6

Run 2-1
Coal particle size: -45μm
Drying conditions: O_2 and N_2 dry, purged overnight
Steady-state temperature T_s: 60.73°C
Heat transfer coefficient U: 0.0975 WK^{-1}
Heat transfer time constant U/C_p: 0.01404 min^{-1}

Table C16 Concentration data for run 2-1

Time/min	Concentration/mol.m^{-3}				
	CO_2	H_2O	O_2	N_2	CO
1.5	0	0.2003	32.34	16.297	0.1381
27.7	0	0.3774	31.50	16.234	0.1409
53.5	0.0128	0.4036	31.00	15 979	0.1455
83.7	0.0217	0.4647	30.24	16.300	0.1481
107.8	0.0281	0.4199	29.96	16.406	0
133.0	0.0311	0.4399	29.55	16.307	0.1347
157.7	0.0373	0.4416	29.12	16.345	0.1480
181.5	0.0433	0.4578	28.65	16.382	0.1426
221.4	0.0515	0.4727	28.22	16.299	0.1564
263.0	0.0603	0.4550	27.73	16.253	0.1514
286.7	0.0645	0.4794	27.55	16.226	0.1548
312.4	0.0679	0.4297	27.25	16.224	0.1425
337.0	0.0718	0.4257	26.99	16.108	0.1558
367.5	0.0776	0.4153	26.73	16.187	0.1625
392.0	0.0803	0.4418	26.59	16.124	0.1627
416.6	0.0847	0.4494	26.34	16.182	0.1621
441.1	0.0891	0.4820	26.30	16.996	0.1670
472.4	0.0934	0.4504	25.89	16.247	0.1770

The temperature data are given in Table C17 overleaf.

Table C17 Temperature deviation data of run 2-1

t	ΔT	t	ΔT	t	ΔT	t	ΔT	t	ΔT
16.7	.01	7.8	.04	8.9	.08	10.0	.13	11.0	.14
12.4	.18	13.9	.20	15.3	.25	16.7	.30	18.2	.34
19.6	.38	21.1	.41	22.5	.47	24.0	.53	25.4	.56
26.9	.60	28.2	.62	29.6	.66	31.1	.68	32.5	.75
34.0	.75	35.4	.77	36.9	.82	38.3	.85	39.8	.90
41.2	.94	42.7	.94	44.2	.96	45.6	1.02	47.1	1.04
48.5	1.07	50.0	1.11	51.4	1.13	52.9	1.14	54.3	1.15
55.8	1.16	57.2	1.20	58.7	1.18	60.2	1.19	61.6	1.24
63.1	1.26	64.5	1.26	66.0	1.27	67.4	1.29	68.9	1.29
70.3	1.33	71.8	1.36	73.2	1.33	74.7	1.34	76.2	1.32
77.6	1.36	79.1	1.37	80.5	1.37	81.9	1.39	83.4	1.38
84.9	1.41	86.2	1.41	87.6	1.44	89.1	1.43	90.6	1.43
92.0	1.45	93.5	1.46	94.9	1.48	96.4	1.46	97.8	1.46
99.3	1.49	100.8	1.48	102.2	1.50	103.7	1.48	105.2	1.48
106.6	1.48	108.0	1.51	109.5	1.50	110.9	1.48	112.4	1.46
113.8	1.47	115.3	1.50	116.7	1.49	118.2	1.47	119.6	1.46
121.1	1.49	122.6	1.49	124.0	1.53	125.5	1.50	126.9	1.49
128.4	1.51	129.8	1.51	131.3	1.51	132.7	1.49	134.1	1.47
135.6	1.48	137.0	1.49	138.5	1.50	139.9	1.49	141.4	1.50
142.8	1.47	144.3	1.48	145.7	1.48	147.2	1.49	148.6	1.47
150.1	1.44	151.6	1.46	153.0	1.47	154.5	1.47	155.9	1.47
157.4	1.43	158.7	1.44	160.2	1.43	161.6	1.45	163.1	1.45
164.5	1.42	166.0	1.42	167.3	1.44	168.7	1.47	170.2	1.45
171.6	1.43	173.1	1.44	174.5	1.41	176.0	1.44	177.4	1.41
178.9	1.41	180.3	1.38	181.8	1.37	183.2	1.39	184.5	1.37
186.0	1.38	187.4	1.35	188.9	1.36	190.3	1.38	191.8	1.36
193.2	1.35	194.7	1.35	196.1	1.35	197.4	1.33	198.9	1.33
200.3	1.32	201.8	1.31	203.2	1.31	204.7	1.31	206.1	1.32
207.6	1.31	209.0	1.27	210.5	1.29	211.9	1.31	213.4	1.31
214.9	1.31	216.3	1.27	217.8	1.28	219.2	1.28	220.7	1.30
222.2	1.27	223.6	1.26	225.1	1.26	226.5	1.26	228.0	1.27
229.5	1.26	230.9	1.24	232.4	1.22	233.8	1.24	235.3	1.24

Run 2-2
Coal particle size: -45μm
Drying conditions: Both O_2 and N_2 bubbled through pure water
Steady-state temperature T_s: 60.78°C
Heat transfer coefficient U: 0.107 WK^{-1}
Heat transfer time constant U/C_p: 0.01315 min^{-1}

Table C18 Concentration data for run 2-2

Time/min	Concentration/mol.m^{-3}				
	CO_2	H_2O	O_2	N_2	CO
20.7	0	1.1265	35.52	10.131	0.2223
44.8	0.0140	1.0745	34.61	10.741	0.1959
71.6	0.0227	0.9435	34.31	10.815	0.1828
102.9	0.0331	1.0005	33.77	10.957	0.1566
129.5	0.0439	1.9312	33.57	11.027	0.3620
202.0	0.0457	1.4827	32.84	10.323	0.1426
238.6	0.0565	1.2657	32.12	10.919	0.1552
269.1	0.0598	1.1096	32.10	10.878	0.1435
303.4	0.0636	1.2985	31.58	10.483	0.1455
328.4	0.0684	1.1761	31.38	10.793	0.1525
352.9	0.0720	1.1439	31.28	10.757	0.1419
381.6	0.0765	1.1547	31.00	10.842	0.1413
405.5	0.0804	1.1119	31.06	10.809	0.1491
431.5	0.0835	1.1051	30.95	10.747	0.1476
458.8	0.0887	1.0988	30.63	10.890	0.1478

Table C19 on the following page contains the temperature data.

Table C19 Temperature deviation data of run 2-2

t	ΔT	t	ΔT	t	ΔT	t	ΔT	t	ΔT
22.6	.03	25.7	.04	24.8	.05	25.9	.06	27.0	.07
28.0	.10	29.1	.13	31.0	.16	32.8	.20	34.7	.22
36.5	.25	38.3	.32	40.2	.34	42.0	.38	44.0	.41
45.8	.45	47.6	.48	49.4	.51	51.3	.56	53.1	.57
54.9	.60	56.7	.63	58.6	.66	60.4	.66	62.2	.69
64.1	.69	65.9	.75	67.7	.72	69.5	.76	71.3	.76
73.3	.82	75.2	.83	77.0	.84	78.9	.85	80.7	.86
82.5	.88	84.3	.93	86.2	.91	88.0	.93	89.8	.96
91.6	.98	93.5	1.00	95.3	.98	97.1	.98	99.0	.98
100.8	1.03	102.6	1.02	104.4	1.04	106.3	1.06	108.1	1.06
109.9	1.06	111.7	1.08	113.6	1.06	115.4	1.07	117.2	1.07
119.1	1.05	120.9	1.03	122.7	1.06	124.5	1.08	126.4	1.07
128.2	1.02	130.2	1.04	132.0	1.09	133.8	1.08	135.6	1.09
137.5	1.07	139.3	1.11	141.1	1.12	142.9	1.12	144.8	1.12
146.6	1.15	148.4	1.14	150.2	1.14	152.1	1.14	154.0	1.14
155.9	1.14	157.8	1.14	159.7	1.13	161.5	1.11	163.3	1.13
165.1	1.15	166.9	1.12	168.8	1.12	170.6	1.15	172.4	1.15
174.2	1.13	176.1	1.15	177.9	1.17	179.7	1.15	181.6	1.15
183.4	1.17	185.2	1.15	187.1	1.18	188.9	1.18	190.7	1.17
192.5	1.19	194.4	1.19	196.2	1.21	198.0	1.21	199.9	1.21
201.7	1.18	203.5	1.16	205.4	1.17	207.2	1.17	209.0	1.16
210.8	1.18	212.7	1.17	214.5	1.18	216.3	1.18	218.2	1.19
220.0	1.18	221.8	1.17	223.6	1.17	225.5	1.15	227.3	1.15
229.1	1.15	230.9	1.14	232.7	1.14	234.6	1.12	236.4	1.12
238.2	1.10	240.2	1.11	242.0	1.11	243.8	1.11	245.6	1.15
247.5	1.15	249.3	1.12	251.7	1.14	253.6	1.12	255.4	1.12
257.2	1.11	259.1	1.08	260.9	1.09	262.	1.09	264.5	1.10
266.4	1.10	268.2	1.10	270.1	1.12	271.9	1.08	273.8	1.09
275.6	1.0.	277.4	1.07	279.3	1.07	281.1	1.07	282.9	1.04
284.7	1.04	286.6	1.04	288.4	1.03	290.2	1.03	292.0	1.04
293.9	1.03	295.7	1.03	297.5	1.01	299.4	1.01	301.2	1.01
303.0	1.02	304.9	1.02	306.8	1.03	308.6	1.02	310.4	1.02
312.2	1.01	314.1	1.01	315.9	1.03	317.7	1.03	319.6	1.00
321.4	.99	323.2	.99	325.0	.97	326.9	.97	328.7	1.00
330.5	.97	332.4	1.00	334.2	1.00	336.0	1.02	337.8	1.00
339.7	1.01	341.5	1.00	343.3	1.00	345.1	1.00	347.0	1.00
348.8	.99	350.6	1.02	352.5	1.00	354.3	.98	356.1	.99
357.9	.98	359.8	.98	361.6	.95	363.4	.96	365.2	.96
367.0	.95	368.9	.94	370.7	.94	372.6	.94	374.4	.92
376.2	.92	378.0	.92	379.8	.89	381.7	.89	383.5	.89
385.4	.87	387.3	.90	389.1	.93	391.0	.92	392.8	.93
394.6	.93	396.4	.91	398.2	.91	400.1	.88	401.9	.89
403.7	.87	405.6	.88	407.4	.87	409.2	.87	411.1	.85
412.9	.85	414.7	.89	416.5	.89	418.4	.87	420.2	.87
422.0	.87	423.8	.85	425.7	.88	427.5	.85	429.3	.85
431.2	.85	433.1	.87	434.9	.87	436.7	.86	438.5	.84
440.4	.84	442.2	.87	444.0	.85	445.8	.85	447.7	.85
449.5	.86	451.3	.83	453.2	.85	455.0	.80	457.6	.76
460.1	.81	462.7	.82	465.3	.82	467.9	.83	470.4	.82
472.9	.82	475.6	.82	478.1	.82	480.7	.82	483.3	.79
485.8	.77	488.4	.80	491.0	.79	493.6	.77	496.2	.76
498.8	.79	501.4	.78	504.0	.76	506.6	.76	509.1	.76
509.1	.76								

Run 2-3
Coal particle size: -90+63μm
Drying conditions: Both O_2 and N_2 bubbled through water at 20°C.
Steady-state temperature T_s: 66.95°C
Heat transfer coefficient U: 0.1347 WK^{-1}
Heat transfer time constant U/C_p: 0.01757 min^{-1}

Table C20 Concentration data for run 2-3

Time/min	Concentration/mol.m^{-3}				
	CO_2	H_2O	O_2	N_2	O
55.9	0.0160	1.3295	37.33	8.007	0.2313
79.4	0.0259	1.1871	36.98	7.797	0.2149
105.3	0.0364	1.1167	37.22	7.525	0.1293
225.5	0.0723	0.5234	35.13	8.167	0.2024
249.2	0.0800	0.9.09	34.49	7.988	0.1946
275.6	0.0868	0.9310	34.18	7.980	0.2052
309.6	0.0934	1.0410	33.78	7.931	0.1911
323.7	0.0990	0.8950	33.47	8.026	0.1899
348.3	0.1083	0.8163	33.56	7.947	0.1965

The temperature-time curve points are given overleaf.

Table C21 Temperature deviation data of run 2-3

t	ΔT	t	ΔT	t	ΔT	t	ΔT	t	ΔT
38.2	1.15	39.7	1.20	41.4	1.23	42.9	1.23	44.5	1.21
46.2	1.34	47.8	1.36	49.4	1.38	51.1	1.39	52.7	1.41
54.3	1.45	56.0	1.47	57.6	1.49	59.2	1.52	60.9	1.56
62.6	1.58	64.2	1.56	65.8	1.59	67.5	1.63	69.3	1.64
70.8	1.65	72.4	1.66	74.2	1.63	75.7	1.67	77.5	1.68
79.0	1.69	80.6	1.71	82.4	1.75	83.9	1.73	85.4	1.76
87.0	1.76	88.7	1.79	90.3	1.79	92.0	1.79	93.6	1.83
95.3	1.83	96.9	1.82	98.5	1.82	100.2	1.82	101.8	1.81
103.5	1.83	105 1	1.81	106 7	1.80	108.3	1.79	109.9	1.80
111.6	1.79	113.2	1.80	114.9	1.79	116.5	1.80	118.2	1.77
119.8	1.77	121.3	1.77	122.8	1.76	124.5	1.77	126.1	1.76
127.7	1.75	129.4	1.73	131.0	1.75	132.7	1.75	134.3	1.76
135.9	1.75	137.6	1.76	139.2	1.72	140.8	1.70	142.5	1.71
144.1	1.71	145.8	1.70	147.4	1 67	149.0	1.71	150.6	1.66
152.3	1.65	153.9	1.65	155.6	1.63	157.2	1.64	158.8	1.61
160.5	1.60	162.0	1.60	163.6	1.58	165.3	1.59	167.0	1.57
168.6	1.57	170.2	1.56	171.9	1.54	173.5	1.53	175.1	1.53
176.8	1.52	178.4	1.50	180.0	1.52	181.7	1.50	183.3	1.51
185.0	1.50	186.6	1.46	188.3	1.48	189.9	1.47	191.5	1.47
193.2	1.45	194.8	1.44	196.4	1.42	198.1	1.43	199.7	1.40
201.3	1.41	202.9	1.39	204.6	1.38	206.2	1.35	207.8	1.35
209.5	1.33	211.1	1.35	212.7	1.35	214.4	1.33	216.0	1.32
217.7	1.32	219.3	1.32	221.0	1.31	222.6	1.30	224.2	1.30
225.8	1.27	227.4	1.28	229.1	1.28	230.7	1.26	232.3	1.27
234.0	1.25	235.7	1.21	237.3	1.22	238.9	1 19	240.5	1.21
242.2	1.20	243.8	1.19	245.5	1.19	247.1	1.16	248.8	1.17
250.4	1.19	252.1	1.19	253.8	1.21	255.4	1.23	257.0	1.23
258.7	1.15	260.3	1.25	261.9	1.26	263.6	1.26	265.2	1.27
266.8	1.27	268.5	1.25	270.1	1.25	271.8	1.27	273.4	1.17
275.1	1.26	276.6	1.25	278.2	1.26	279.7	1.23	281.4	1.25
283.0	1.23	284.6	1.22	286 9	1.22	287.8	1.19	289.4	1.17
291.1	1.17	292.7	1.18	294.4	1.17	296.0	1.18	297.6	1.17
299.3	1.18	300.9	1.20	302.6	1.21	304.3	1.21	305.9	1.20
307.5	1.23	309.2	1.22	310.8	1.22	312.4	1.22	314.1	1.22
315.7	1.23	317.4	1.19	319.0	1.19	320.6	1.22	322.3	1.19
324.0	1.18	325.6	1.18	327.2	1.18	328.9	1.19	330.5	1.20
332.1	1.17	333.8	1.19	335.4	1.18	337.0	1.18	338.7	1.16
340.4	1.16	342.0	1.15	343.6	1.18	345.3	1.15	346.9	1.15
348.5	1.15	350.1	1.13	351.7	1.12	353.4	1.12	355.0	1.12
356.7	1.12	358.3	1.11	360.0	1.11	361.6	1.12	363.3	1.12
364.9	1.12	366.5	1.11	368.2	1.09	369.8	1.11	371.5	1.09
373.1	.09	374.8	1.09	376.4	1.11	378.1	1.13	379.7	1.11
381.3	1.39	382.9	1.11	384 5	1.08	386.1	1.09	387.8	1.09
389.4	1.06	391.0	1.03	392.7	1.09	394.4	1.09	396.0	1.09
397.6	1.09	399.3	1.09	400.9	1.09	402.5	1.09	404.1	1.08
405.8	1.07	407 4	1.08	409.1	1.08	410.7	1.08	412.4	1.04
412.4	1.04	412.4	1.04	412.4	1.04				

Run 2-4
Coal particle size: -90+63μm
Drying conditions: N_2 purge for two hours while reactor heated up.
Steady-state temperature T_s: 67.45°C
Heat transfer coefficient U: 0.1372 WK^{-1}
Heat transfer time constant U/C_p: 0.01295 min^{-1}

Table C22 Concentration data for run 2-4

Time/min	Concentration/mol.m^{-3}				
	CO_2	H_2O	O_2	N_2	CO
78.2	0	3.0026	40.46	9.853	0.1042
128.5	0	3.7407	39.09	9.964	0.0936
158.4	0	3.7922	38.55	9.904	0.1089
186.3	0	5.8488	36.39	9.672	0.0967
218.8	0	5.1820	36.57	9.787	0.1116
247.0	0.0344	5.1803	36.11	9.860	0.1149
292.0	0.0658	5.3846	35.42	9.602	0.1209
316.9	0.0784	6.1587	34.45	9.432	0.1170
347.8	0.0873	4.4084	35.24	10.018	0.1282

The temperatire data points are on the following page.

Table C23 Temperature deviation data of run 2-4

t	ΔT	t	ΔT	t	ΔT	t	ΔT	t	ΔT
27.1	-.55	28.2	-.52	29.2	-.50	30.3	-.45	31.4	-.43
32.5	-.41	33.5	-.39	34.6	-.37	35.7	-.35	36.8	-.33
37.9	-.32	39.0	-.24	40.1	-.21	41.2	-.22	42.2	-.19
43.3	-.17	44.4	-.14	45.4	-.13	46.6	-.08	47.6	-.05
48.8	-.04	49.9	-.05	51.0	-.01	52.1	.01	53.2	.04
54.2	.06	55.3	.06	56.4	.08	57.5	.10	58.6	.11
59.6	.11	60.7	.15	61.8	.17	62.9	.18	63.9	.20
65.0	.24	66.1	.24	67.2	.27	68.2	.26	69.4	.28
70.4	.30	71.5	.30	72.6	.33	73.7	.35	74.7	.37
75.8	.39	76.9	.40	78.0	.40	79.0	.41	80.1	.44
81.2	.44	82.3	.47	83.4	.49	84.5	.49	85.5	.53
86.6	.52	87.7	.53	88.8	.58	89.8	.56	90.9	.60
92.0	.60	93.1	.59	94.2	.62	95.2	.62	96.3	.62
97.4	.63	98.5	.62	99.5	.64	100.6	.65	101.7	.67
102.8	.67	103.9	.68	105.0	.70	106.1	.72	107.2	.72
108.2	.73	109.3	.73	110.4	.73	111.5	.77	112.5	.78
113.6	.79	114.7	.78	115.8	.78	116.9	.78	117.9	.79
119.0	.80	120.1	.82	121.2	.83	122.2	.84	123.3	.86
124.4	.84	125.5	.85	126.5	.85	127.7	.84	128.7	.84
129.8	.87	130.8	.87	131.9	.88	133.0	.89	134.1	.89
135.1	.86	136.2	.90	137.3	.88	138.4	.92	139.5	.92
140.6	.92	141.6	.92	142.7	.91	143.8	.91	144.9	.90
145.9	.91	147.0	.93	148.1	.92	149.1	.92	150.3	.93
151.3	.91	152.4	.92	153.5	.90	154.6	.90	155.6	.93
156.7	.99	157.8	.98	158.8	.95	159.9	.96	161.0	.96
162.1	.97	163.2	.97	164.2	.99	165.3	.98	166.4	.96
167.4	.97	168.5	.97	169.6	.99	170.7	.99	171.8	.99
172.9	.99	174.0	.99	175.0	.99	176.1	.99	177.2	.98
178.2	.99	179.3	1.00	180.4	1.00	181.5	.99	182.5	.99
183.6	1.01	184.7	.98	185.8	.97	187.0	.97	188.0	.98
189.1	1.00	190.2	1.01	191.2	1.00	192.3	.99	193.4	.99
194.5	1.00	195.5	1.00	196.7	1.00	197.7	1.00	198.8	1.00
199.9	.99	201.0	.99	202.0	1.00	203.1	1.00	204.2	.98
205.3	.99	206.3	.98	207.5	.98	208.5	.96	209.6	.99
210.7	.96	211.7	.97	212.8	.96	213.9	.94	215.0	.95
216.0	.95	217.1	.97	218.2	.99	219.2	.99	220.3	.97
221.4	.95	222.4	.95	223.5	.95	224.6	.97	225	.98
226.7	.99	227.8	.99	228.9	.98	230.0	.98	231.	.98
232.2	.97	233.2	.97	234.3	.96	235.4	.94	236.5	.95
237.5	.96	238.6	.94	239.7	.92	240.8	.94	241.9	.94
242.9	.96	244.0	.95	245.1	.93	246.2	.93	247.2	.94
248.3	.94	249.4	.94	250.5	.94	251.5	.95	252.6	.94
253.7	.95	254.8	.95	255.9	.95	256.9	.95	258.0	.95
259.1	.94	260.2	.96	261.2	.96	262.3	.96	263.4	.96
264.5	.95	265.6	.95	266.7	.97	267.7	.96	268.8	.9.
269.9	.97	270.9	.95	272.0	.96	273.1	.95	274.2	.95
275.2	.93	276.4	.95	277.4	.96	278.5	.93	279.6	.93
280.7	.94	281.7	.94	282.8	.94	283.9	.92	284.9	.94
286.0	.91	287.1	.95	288.2	.91	289.3	.91	290.4	.93
291.4	.92	292.4	.92	293.5	.92	294.6	.91	295.7	.91
296.7	.89	297.8	.89	298.9	.90	300.0	.91	301.1	.89
302.2	.90	303.2	.90	304.3	.91	305.4	.92	306.5	.92
307.5	.89	308.6	.93	309.7	.92	310.8	.91	311.9	.91
313.0	.90	314.0	.89	315.1	.89	316.2	.90	317.3	.89
318.4	.89	319.5	.88	320.5	.89	321.6	.88	322.7	.90
323.8	.88	324.9	.91	326.0	.88	327.0	.88	328.1	.89
329.2	.88	330.3	.89	331.3	.89	332.4	.89	333.5	.88
334.6	.88	335.7	.89	336.7	.89	337.8	.89	338.9	.89
340.0	.88	341.0	.88	342.1	.87	343.2	.87	344.3	.85
345.4	.89	346.5	.85	347.5	.85	348.5	.84	349.6	.84
350.7	.86	351.8	.87	352.8	.88	353.9	.87	355.0	.86
356.1	.87	357.2	.85	358.3	.89	359.3	.87	360.4	.85
361.5	.83	362.6	.83	363.6	.84	364.7	.83	365.8	.85
365.8	.85								

Run 2-5

Coal particle size: -90+63μm

Drying conditions: Reactor purged for two days with dry N_2 at 80°C, then at 60°C overnight. O_2 dry.

Steady-state temperature T_s: 67.46°C

Heat transfer coefficient U: 0.1372 WK^{-1}

Heat transfer time constant U/C_p: 0.01295 min^{-1}

Table C24 Concentration data for run 2-5

Time/min	Concentration/mol.m^{-3}				
	CO_2	H_2O	O_2	N_2	CO
7.6	0	0.0954	49.42	2.119	0.2204
59.2	0	0.2521	47.77	2.723	0.1799
83.2	0	0.3808	47.02	2.845	0.1942
106.8	0	0.3566	46.25	2.942	0.1880
135.2	0	0.3955	46.05	2.907	0.2081
158.7	0	0.3951	45.75	2.848	0.2091
183.4	0	0.4191	45.13	2.930	0.2025
216.4	0.0662	0.4233	44.68	2.946	0.2121
256.1	0.0746	0.5085	43.90	3.097	0.2132
287.5	0.0881	0.4133	43.92	2.983	0.2190
312.2	0.1013	0.3884	43.72	2.473	0.2299
375.1	0.1127	0.4376	43.11	2.320	0.2296
390.7	0.1233	0.3458	42.85	2.430	0.2410
418.5	0.1291	0.3350	42.54	2.398	0.2332

Table G25 Temperature deviation data of run 2-5

t	ΔT	t	ΔT	t	ΔT	t	ΔT	t	ΔT
15.3	-.85	15.7	-.83	16.0	-.83	16.3	-.80	16.6	-.78
17.0	-.77	17.3	-.76	17.6	-.74	17.9	-.72	18.3	-.69
18.6	-.69	19.0	-.66	19.3	-.64	19.6	-.60	19.9	-.61
20.3	-.58	20.6	-.58	20.9	-.55	21.2	-.54	21.6	-.54
21.9	-.51	22.3	-.49	22.6	-.48	22.9	-.46	23.2	-.46
23.6	-.43	23.9	-.41	24.2	-.40	24.5	-.41	24.9	-.37
25.2	-.37	25.5	-.35	25.9	-.32	26.2	-.29	26.5	-.27
26.9	-.29	27.2	-.28	27.5	-.25	27.8	-.23	28.2	-.22
28.5	-.20	28.8	-.19	29.1	-.17	29.5	-.15	29.8	-.15
30.2	-.15	30.5	-.12	30.8	-.12	31.1	-.09	31.5	-.09
31.8	-.06	32.1	-.08	32.4	-.04	32.8	-.04	33.1	.01
33.5	.01	33.8	.01	34.0	.03	34.4	.03	34.7	.05
35.4	.08	36.1	.11	36.8	.13	37.5	.16	38.2	.19
38.9	.21	39.6	.23	40.3	.26	41.0	.31	41.7	.34
42.4	.36	43.1	.37	44.1	.39	44.8	.43	45.5	.45
46.3	.48	47.0	.51	47.7	.51	48.4	.52	49.1	.55
49.8	.55	50.5	.58	51.2	.60	51.9	.59	52.6	.63
53.4	.63	54.1	.66	54.8	.66	55.5	.71	56.2	.72
56.9	.73	57.6	.77	58.3	.79	59.0	.79	59.7	.84
60.4	.83	61.2	.85	61.9	.88	62.6	.90	63.3	.89
64.0	.89	64.7	.94	65.4	.94	66.1	.96	66.8	.98
67.5	.98	68.2	.98	68.9	1.01	69.6	1.01	70.3	1.03
71.0	1.03	71.7	1.05	72.4	1.05	73.1	1.07	73.8	1.08
74.5	1.08	75.2	1.11	75.9	1.11	76.6	1.12	77.3	1.14
78.0	1.14	78.7	1.17	79.4	1.20	80.1	1.20	80.8	1.22
81.5	1.25	82.2	1.25	82.9	1.25	83.7	1.27	84.4	1.27
85.1	1.29	85.8	1.30	86.5	1.29	87.2	1.29	87.9	1.31
88.6	1.31	89.3	1.32	90.0	1.31	90.7	1.31	91.4	1.33
92.1	1.33	92.8	1.34	93.5	1.37	94.2	1.37	94.9	1.36
95.6	1.39	96.3	1.36	97.0	1.39	97.7	1.40	98.5	1.41
99.2	1.42	99.9	1.42	100.6	1.42	101.3	1.45	102.0	1.44
102.7	1.44	103.4	1.44	104.1	1.46	104.8	1.44	105.4	1.46
106.2	1.46	106.9	1.45	107.6	1.48	108.3	1.48	109.0	1.50
109.7	1.48	110.4	1.49	111.1	1.49	111.8	1.49	112.5	1.52
113.2	1.52	113.9	1.51	114.6	1.54	115.3	1.54	116.1	1.54
116.8	1.54	117.5	1.55	118.2	1.55	118.9	1.56	119.6	1.56
120.3	1.56	121.0	1.56	121.7	1.55	122.4	1.58	123.1	1.60
123.8	1.59	124.5	1.59	125.2	1.59	125.9	1.62	126.6	1.58
127.3	1.57	128.0	1.60	128.8	1.59	129.5	1.59	130.1	1.61
130.8	1.62	131.5	1.62	132.2	1.62	132.9	1.62	133.6	1.61
134.3	1.64	135.0	1.64	135.7	1.66	136.4	1.64	137.1	1.66
137.8	1.65	138.5	1.66	139.6	1.62	140.6	1.65	141.7	1.64
142.8	1.64	143.9	1.64	144.9	1.64	146.1	1.62	147.1	1.64
148.2	1.63	149.3	1.63	150.4	1.63	151.4	1.64	152.5	1.64
153.6	1.63	154.7	1.66	155.7	1.66	156.8	1.64	157.9	1.64
159.1	1.67	160.2	1.67	161.3	1.66	162.3	1.67	163.4	1.67
164.5	1.67	165.6	1.64	166.7	1.66	167.7	1.64	168.8	1.63
169.9	1.63	171.0	1.65	172.1	1.63	173.1	1.63	174.2	1.61
175.3	1.61	176.4	1.61	177.4	1.58	178.5	1.59	179.6	1.59
180.7	1.60	181.8	1.60	182.9	1.58	183.9	1.58	184.9	1.58
186.0	1.56	187.1	1.57	188.2	1.60	189.2	1.59	190.3	1.58
191.4	1.58	192.5	1.58	193.6	1.59	194.7	1.58	195.7	1.58
196.8	1.59	197.9	1.57	199.0	1.57	200.0	1.58	201.1	1.57
202.2	1.58	203.3	1.57	204.4	1.58	205.4	1.58	206.5	1.55
207.6	1.55	208.7	1.58	209.7	1.55	210.8	1.54	211.9	1.54
213.0	1.54	214.0	1.54	215.2	1.53	216.2	1.51	217.5	1.51
218.8	1.53	220.0	1.53	221.3	1.51	222.5	1.51	223.8	1.52
225.1	1.53	226.3	1.50	227.6	1.52	228.9	1.50	230.2	1.52
231.4	1.50	232.7	1.50	233.9	1.50	235.2	1.50	236.5	1.50
237.7	1.50	239.0	1.49	240.2	1.51	241.5	1.49	242.8	1.49
244.1	1.49	245.3	1.49	246.6	1.46	247.9	1.45	249.1	1.47
250.4	1.43	251.7	1.42	252.9	1.46	254.2	1.42	255.5	1.45
256.8	1.45	258.0	1.45	259.3	1.45	260.6	1.45	261.8	1.42
263.1	1.41	264.3	1.41	265.6	1.41	266.9	1.41	268.1	1.40

Table C25 (continued)

269.4	1.38	270.7	1.38	272.0	1.38	273.2	1.36	274.5	1.36
275.8	1.36	277.0	1.37	278.3	1.37	279.5	1.38	280.8	1.39
282.1	1.38	283.4	1.38	284.6	1.35	285.9	1.35	287.2	1.35
288.5	1.34	289.8	1.37	291.1	1.33	292.3	1.32	293.6	1.31
330.3	1.22	332.5	1.23	334.6	1.27	336.6	1.22	338.6	1.22
340.6	1.23	342.6	1.23	344.7	1.24	346.7	1.22	348.7	1.23
350.7	1.25	352.7	1.25	354.8	1.22	356.8	1.22	358.8	1.22
360.8	1.22	362.8	1.23	364.8	1.23	366.9	1.21	368.9	1.23
370.9	1.20	372.9	1.16	374.9	1.18	376.9	1.16	379.0	1.16
381.0	1.15	383.0	1.15	385.0	1.18	387.0	1.17	389.0	1.14
391.2	1.14	393.2	1.14	395.4	1.13	397.6	1.13	399.6	1.11
401.6	1.11	403.6	1.09	405.6	1.09	407.6	1.07	409.6	1.06
411.6	1.07	413.6	1.03	415.7	1.03	417.7	1.01	419.8	1.01
421.8	.98	423.8	.98	425.8	.97	427.8	.95	429.9	.92
431.9	.93	433.9	91	435.9	.88	437.9	.88	439.9	.84
439.9	.86	439.9	.86						

Run 2-6

Coal particle size: -90+63μm

Drying conditions: Coal stored for six weeks in dessicator, purged with O_2-free N_2, containing concentrated sulphuric acid. Reactor purged with dry N_2 overnight prior to run.

Steady-state temperature T_s: 67.42°C

Table C26 Concentration data (on water-free basis) for run 2-6

Time/min	Concentration/mol.m^{-3}			
	[illegible]	O_2	N_2	CO
37.0		37.68	1.849	0.1270
63.5	[illegible]	36.92	1.877	0.1137
92.0	0.01227	36.10	1.984	0.1139
119.5	0.02011	36.05	1.963	0
144.7	0.02890	35.79	1.723	0.1313
168.4	0.07110	34.99	2.296	0.1427
192.7	0.06243	34.40	2.699	0.1606
217.1	0.07020	34.75	2.181	0.1478
244.0	0.07242	33.79	2.772	0.1547
276.7	0.09647	33.24	2.926	0.1777
303.2	0.09543	33.01	2.759	0.2160
330.2	0.1112	32.95	2.847	0.1752
356.7	0.1156	32.85	2.590	0.1784
430.5	0.1309	31.71	2.969	0.2121

Table C27 Temperature deviation data of run 2-6

t	ΔT	t	ΔT	t	ΔT	t	ΔT	t	ΔT
40.0	-.23	40.7	-.18	41.4	-.13	42.2	-.10	42.9	-.16
43.6	-.16	44.3	-.15	45.0	-.15	45.7	-.12	46.4	-.15
47.1	-.13	47.8	-.15	48.5	-.14	49.2	-.13	49.9	-.13
50.6	-.12	51.3	-.10	52.0	-.09	52.8	-.09	53.5	-.04
54.2	-.03	54.9	.02	55.6	.05	56.3	.05	57.0	.05
57.7	.06	58.4	.10	59.1	.07	59.8	.08	60.5	.09
61.2	.10	61.9	.11	62.6	.10	63.3	.11	63.9	.12
64.7	.12	65.4	.15	66.1	.15	66.8	.20	67.5	.19
68.2	.21	68.9	.22	69.6	.25	70.3	.25	71.0	.25
71.7	.26	72.5	.26	73.2	.27	73.9	.28	74.6	.26
75.3	.27	76.0	.28	76.7	.27	77.4	.27	78.1	.29
78.8	.32	79.5	.33	80.2	.36	80.9	.36	81.6	.36
82.3	.38	83.0	.39	83.7	.39	84.4	.40	85.2	.41
85.9	.39	86.6	.40	87.3	.39	88.0	.40	88.7	.41
89.4	.39	90.1	.40	90.8	.41	91.5	.41	92.0	.42
94.1	.47	95.2	.51	96.3	.49	97.4	.49	98.5	.49
99.5	.50	100.6	.48	101.7	.50	102.8	.54	103.8	.56
104.9	.55	106.0	.55	107.1	.56	108.2	.56	109.3	.55
110.3	.57	111.4	.52	112.5	.57	113.6	.58	114.6	.59
115.7	.62	116.8	.59	117.9	.63	119.0	.61	120.2	.60
121.3	.61	122.4	.61	123.5	.63	124.6	.65	125.6	.66
126.7	.64	127.8	.66	128.9	.64	129.9	.65	131.0	.63
132.1	.63	133.2	.64	134.3	.65	135.4	.66	136.5	.69
137.5	.70	138.6	.70	139.7	.70	140.8	.69	141.9	.70
143.0	.68	144.1	.73	145.3	.75	146.4	.74	147.5	.83
148.5	.80	149.6	.83	150.7	.86	151.8	.82	152.9	.89
154.0	.88	155.1	.90	156.2	.90	157.2	.92	158.3	.93
159.4	.95	160.5	.97	161.5	.97	162.6	.98	163.7	1.00
164.8	1.02	165.8	1.02	166.9	1.02	168.0	1.03	169.3	1.06
170.5	1.05	171.5	1.05	172.6	1.04	173.7	1.03	174.8	1.05
175.9	1.06	176.9	1.06	178.0	1.06	179.1	1.06	180.2	1.05

181.3	1.08	182.3	1.06	183.4	1.08	184.5	1.08	185.6	1.07
186.6	1.07	187.7	1.08	188.8	1.07	189.9	1.10	191.0	1.06
192.1	1.06	193.3	1.07	194.5	1.06	195.6	1.08	196.6	1.09
197.7	1.07	198.8	1.08	199.9	1.09	201.0	1.12	202.1	1.09
203.2	1.12	204.2	1.12	205.3	1.13	206.4	1.13	207.5	1.13
208.5	1.13	209.6	1.12	210.7	1.16	211.8	1.18	212.9	1.15
214.0	1.16	215.1	1.14	216.2	1.18	217.4	1.19	218.4	1.18
219.5	1.17	220.6	1.17	221.7	1.16	222.7	1.15	223.8	1.16
224.9	1.16	226.0	1.16	227.1	1.17	228.2	1.16	229.2	1.18
230.3	1.17	231.4	1.19	232.5	1.18	233.5	1.20	234.6	1.19
235.7	1.19	236.8	1.19	237.9	1.19	239.0	1.21	240.0	1.22
241.1	1.21	242.2	1.19	243.3	1.21	244.4	1.20	245.5	1.24
246.6	1.21	247.7	1.24	248.8	1.24	249.8	1.23	250.9	1.23
252.0	1.22	253.1	1.21	254.1	1.19	255.2	1.17	256.3	1.19
257.4	1.19	258.4	1.19	259.6	1.20	260.6	1.17	261.7	1.16
262.8	1.18	263.9	1.18	265.0	1.18	266.0	1.17	267.1	1.14
268.2	1.13	269.3	1.13	270.3	1.17	271.5	1.15	272.5	1.16
273.6	1.17	274.7	1.16	275.8	1.16	276.9	1.16	278.0	1.20
279.1	1.17	280.2	1.16	281.3	1.17	282.4	1.18	283.5	1.18
284.5	1.16	285.6	1.16	286.7	1.18	287.8	1.19	288.8	1.18
289.9	1.18	291.0	1.19	292.1	1.17	293.2	1.19	294.3	1.20
295.4	1.20	296.4	1.20	297.5	1.18	298.6	1.17	299.7	1.19
300.7	1.18	301.8	1.20	302.9	1.19	304.0	1.17	305.1	1.17
306.2	1.15	307.3	1.17	308.3	1.17	309.4	1.17	310.5	1.15
311.6	1.15	312.6	1.14	313.7	1.16	314.8	1.15	315.9	1.17
317.0	1.15	318.1	1.13	319.1	1.13	320.2	1.15	321.3	1.15
322.4	1.15	323.5	1.15	324.5	1.13	325.6	1.13	326.7	1.13
327.8	1.12	328.9	1.12	330.0	1.13	331.0	1.12	332.1	1.09
333.2	1.11	334.2	1.12	335.3	1.11	336.4	1.11	337.5	1.10
338.5	1.10	339.6	1.11	340.7	1.10	341.8	1.14	342.9	1.14
344.0	1.12	345.0	1.10	346.1	1.11	347.2	1.14	348.3	1.13
349.4	1.10	350.4	1.10	351.6	1.08	352.6	1.08	353.7	1.09
354.8	1.08	355.9	1.09	357.0	1.12	358.1	1.10	359.1	1.08

Table C27 (continued)

360.2	1.08	361.3	1.09	362.4	1.09	363.5	1.08	364.6	1.06
365.6	1.06	366.7	1.07	367.8	1.08	368.9	1.08	369.9	1.08
371.0	1.09	372.1	1.08	373.2	1.07	374.2	1.09	375.4	1.08
376.4	1.09	377.5	1.10	378.6	1.07	379.7	1.07	380.7	1.08
381.8	1.10	382.9	1.07	384.0	1.08	385.0	1.07	386.2	1.07
387.2	1.08	388.3	1.07	389.4	1.09	390.5	1.09	391.5	1.06
392.6	1.07	393.7	1.07	394.8	1.07	395.8	1.08	396.9	1.08
398.0	1.08	399.1	1.07	400.2	1.05	401.3	1.07	402.3	1.09
403.4	1.07	404.5	1.07	405.5	1.07	406.6	1.04	407.7	1.05
408.7	1.07	409.9	1.07	410.9	1.06	412.0	1.04	413.1	1.02
414.2	1.03	415.2	1.06	416.3	1.06	417.4	1.06	418.5	1.02
419.5	1.03	420.7	1.04	421.7	1.07	422.8	1.06	423.9	1.06
425.0	1.06	426.0	1.06	427.1	1.06	428.2	1.07	429.3	1.06
429.3	1.06								

APPENDIX D: MATHEMATICAL EXPRESSIONS

D.1 Derivation of Energy Balance

A system of R independent chemical reactions among S molecular species can be represented algebraically as (Abbott and Van Ness,1976)

$$\sum_{s=1}^{S} \alpha_{sr} A_s = 0 \qquad \ldots D\text{-}1$$

where, by convention, the stoichometric coefficients α_{sr} are negative for reactants and positive for products.

The extents e_r of the individual reactions in the reaction system above are defined by

$$N_s = N_s^0 + \sum_{r=1}^{R} \alpha_{sr} e_r \qquad \ldots D\text{-}2$$

where N_s is the number of moles of species s present at a point in time or space, and N_s^0 the amount at some arbitrary initial point where the extents are taken as zero.

In differential form the above equation becomes

$$dN_s = \sum_{r=1}^{R} \alpha_{sr} de_r \qquad \ldots D\text{-}3$$

In writing the energy balance, the reactor will be assumed homogeneous, thus the contents are uniform in temperature at any instant in time. The walls of the reactor are of thin glass, and will thus equilibrate in temperature with the coal quickly, and will not be affected by the surroundings because of the silvering and vacuum of the Dewar flask. The main objection to this assumption is that the coal particles could be hotter than the surroundings because of the reaction on the surface. This is not likely as the maximum rate of temperature rise measured is about 2°C in an hour, which allows sufficient time for the temperature to equilibrate.

In the course of the reaction, the temperature, pressure and concen-

tration change with time. The enthalpy can thus be considered as a function of these variables, giving, in differential form

$$dH = \left(\frac{\partial H}{\partial T}\right)_{TPN_j} dT + \left(\frac{\partial H}{\partial P}\right)_{TPN_j} dP + \sum_{s=1}^{S}\left(\frac{\partial H}{\partial N_s}\right)_{TPN_{j\neq s}} dN_s \qquad \ldots D\text{-}4$$

where there are S molecular species present, and $N_{j\neq s}$ implies summation over all N_j except N_s which is held constant. These differentials can be replaced by the following more familiar thermodynamic quantities (Abbott *et al*, 1976):

$$C_p = \left(\frac{\partial H}{\partial T}\right)_{TPN_j} \quad \text{, the heat capacity}$$

$$V(1-T\beta) = \left(\frac{\partial H}{\partial P}\right)_{TPN_j} \quad \text{, where } \beta \text{ is the volume expansivity}$$

$$\bar{H}_s = \left(\frac{\partial H}{\partial N_s}\right)_{TPN_j} \quad \text{, the partial molar enthalpy of } s$$

Substituting these differentials into D-4 above and dividing by the time differential dt results in

$$\frac{dH}{dt} = C_p \frac{dT}{dt} + V(1-T\beta)\frac{dP}{dt} + \sum_{s=1}^{S}\sum_{r=1}^{R} \alpha_{sr}\bar{H}_s \frac{da}{dt} \qquad \ldots D\text{-}5$$

If the reactor was perfectly adiabatic, then

$$\frac{dH}{dt} = 0 \qquad \ldots D\text{-}6$$

In this case, energy transfer between the reactor and surroundings occurs through the heat loss and by the rocking of the reactor, thus

$$\frac{dH}{dt} = f(T,T_o) + w_s \qquad \ldots D\text{-}7$$

where w_s is a shaft work term and f is some function of the reactor temperature T and the oven temperature T_o describing the heat loss. Over the small temperature changes of these experiments, it can be replaced simply by

$$L(T,T_o) = U(T-T_o) \qquad \ldots D\text{-}8$$

When no reaction occurs (or reaction is complete), the enthalpy change is again zero, thus from *D-7* and *D-8*

$$U(T_s-T_o) + w_s = 0$$

where T_s is the reactor temperature at steady state. The energy balance *D-7* above then simplifies to

$$\frac{dH}{dt} = U(T-T_o) + U(T_o-T_s) = U(T-T_s) \qquad \ldots D\text{-}9$$

Equating this with *D-5* above and rearranging gives

$$C_p \frac{dT}{dt} - V(1-T\beta) \frac{dP}{dt} + \sum_{s=1}^{S} \sum_{r=1}^{R} \alpha_{sr}\bar{H}_s \frac{de_r}{dt} = U(T-T_s) \qquad \ldots D\text{-}10$$

If there is no enthalpy of mixing (which is a good assumption in this case, as the gases can be considered ideal and the coal is a solid), then

$$\sum_{s=1}^{S} \alpha_{sr}\bar{H}_s = \Delta H_r \quad \text{, the heat of reaction for reaction r}$$

The term in dP/dt can be shown to be negligible as follows:

Assume typical reaction conditions for a reactive coal of V=2l, a temperature of 80°C, C_p=400 J/K , a pressure drop of 20kPa and a temperature rise of 5K in the first hour. The volume expansivity is of oxygen is β=3.674x10^{-3} s^{-1} (Liley & Gambill, 1973). For these values,

$$\frac{V}{C_p}(1-T\beta)\frac{dP}{dt} \approx 10^{-5} \text{ K/s}$$

The experimentally measured temperature rise is 5/3600 = 0.0014 K/s, thus the pressure term can be dropped from *D-10*.

The energy balance for the system is thus

$$\frac{dT}{dt} = -\sum_{r=1}^{R} \frac{\Delta H_r}{C_p} \frac{de_r}{dt} - \frac{U}{C_p}(T-T_s) \qquad \ldots 3.1$$

D.2 Rate Expression for Langmuir-Hinshelwood Kinetics with Ageing

D.2.1 Kinetic expression

The rate of reaction for Langmuir-Hinshelwood kinetics is

$$r = \frac{SkC_s}{1+KC_s} \qquad \ldots 4\text{-}2$$

where C_s is the oxygen concentration at the surface, S the total surface area and k and K are constants.

The rate of diffusion of the oxygen through a plane thickness Δx of the reacted coal is

$$r = \frac{sD}{\Delta x}(C-C_s) \qquad \ldots 4\text{-}1$$

with C the bulk O_2 concentration and *D the effective diffusivity.*

The capacity of the reacted layer is very much lower than that of the reacted material, thus the accumulation of O_2 in the oxycoal layer can be ignored (the pseudo steady-state approximation). The rate expressions *of 4-1 and 4-2* can thus be equated, leading to

$$\frac{SkC_s}{1+KC_s} = \frac{sD}{\Delta x}(C-C_s) \qquad \ldots D\text{-}11$$

The oxycoal layer thickness is not an easily measurable quantity, thus it must be eliminated from *D-11*. The amount of oxycoal formed is directly related to the drop in the oxygen concentration from

$$V(C_o-C) = S\rho_m \Delta x \qquad \ldots D\text{-}12$$

where C_o is the initial oxygen concentration when Δx is assumed zero, and ρ_m is the molar density of the reactive groups in the coal.

Substitution of *D-12* into *D-11* gives

$$\frac{SkC_s}{1+KC_s} = \frac{DS\rho_m}{V}\frac{C-C_s}{C_o-C} \qquad \ldots D\text{-}13$$

The surface concentration, which cannot be measured experimentally, is now eliminated by cross-multiplying *D-13* and rearranging.

Put $D\rho_m = D$, and $S/V = \alpha$

Then $kC_s\ (C_o-C) = \alpha D\ (C-C_s)\ (1+KC_s)$

$$= \alpha D\ (C + KC_sC - C_s - KC_s)$$

Grouping the powers of C_s together gives

$$K\alpha DC_s^2 + \beta C_s - \alpha DC = 0$$

where $\beta = \alpha D(1-KC) + k(C_o-C)$ $\qquad \ldots D\text{-}14$

The roots of this quadratic equation are

$$C_s = \frac{-\beta \pm \sqrt{\beta^2 + 4K\alpha^2D^2}}{2K\alpha D} \qquad \ldots D\text{-}15$$

The denominator and the second term inside the root sign are always positive, thus this expression has the form $-\gamma \pm \sqrt{(\gamma^2+\epsilon)}$, where $\epsilon>0$ *always. The surface concentration* C_s is positive for physical reasons therefore the positive root is required for all values of the parame[illegible]o ensure that *D-15* remains positive.

Substitution of *D-15* and *D-12* into the rate expression *4-1* leads to

$$r = \frac{\alpha SD}{C_o-C}\left[\, C - \frac{-\beta + \sqrt{\beta^2 + 4K\alpha^2D^2}}{2K\alpha D}\,\right]$$

The rate for a constant-volume batch reactor is defined as

$$r = -\frac{dC}{dt}$$

thus

$$\frac{dC}{dt} = \frac{-\alpha SD}{C_o - C}\left[C - \frac{-\beta + \sqrt{\beta^2 + 4K\alpha^2 D^2}}{2K\alpha D} \right] \qquad \ldots D\text{-}16$$

D.2.7 Partial derivatives required for optimisation

The optimisation method requires the following derivatives:

$$\frac{\partial}{\partial C}\left(\frac{dC}{dt}\right), \quad \frac{\partial}{\partial T}\left(\frac{dC}{dt}\right), \quad \frac{\partial}{\partial C}\left(\frac{dT}{dt}\right), \quad \frac{\partial}{\partial C}\left(\frac{dT}{dt}\right)$$

$$\frac{\partial}{\partial k}\left(\frac{dC}{dt}\right), \quad \frac{\partial}{\partial K}\left(\frac{dC}{dt}\right), \quad \frac{\partial}{\partial D}\left(\frac{dC}{dt}\right)$$

$$\frac{\partial}{\partial k}\left(\frac{dT}{dt}\right), \quad \frac{\partial}{\partial K}\left(\frac{dT}{dt}\right), \quad \frac{\partial}{\partial D}\left(\frac{dT}{dt}\right)$$

The expressions for these derivatives are given here. The structure has been simplified by the substitution of

$\gamma = \beta^2 + 4K\alpha^2 D^2$, with β defined as above.

$$\frac{\partial}{\partial C}\left(\frac{dC}{dt}\right) = \frac{1}{C_o - C}\frac{dC}{dt} - \frac{\alpha SD}{C_o - C}\left\{ 1 - \frac{1}{2K\alpha D}\left[-\frac{d\beta}{dC} + \frac{1}{2}\gamma^{-\frac{1}{2}}\left(2\beta\frac{d\beta}{dC} + 4K\alpha^2 D^2 \right) \right] \right\}$$

$$\frac{\partial}{\partial T}\left(\frac{dC}{dt}\right) = 0$$

$$\frac{\partial}{\partial C}\left(\frac{dT}{dt}\right) = \frac{V\Delta H}{C_p}\frac{\partial}{\partial C}\left(\frac{dC}{dt}\right)$$

$$\frac{\partial}{\partial T}\left(\frac{dT}{dt}\right) = -\frac{U}{C_p}$$

$$\frac{\partial}{\partial k}\left(\frac{dC}{dt}\right) = \frac{S}{2K(C_o - C)}\frac{d\beta}{dk}\left[\beta\gamma^{-\frac{1}{2}} - 1 \right]$$

$$\frac{\partial}{\partial K}\left(\frac{dC}{dt}\right) = \frac{-S}{2K(C_o-C)}\left[\frac{\gamma^{\frac{1}{2}}-\beta}{K} + \frac{d\beta}{dK} - \gamma^{-\frac{1}{2}}\left(\beta\frac{d\beta}{dk} + 2Ca^2D^2\right)\right]$$

$$\frac{\partial}{\partial D}\left(\frac{dC}{dt}\right) = \frac{1}{D}\left(\frac{dC}{dt}\right) - \frac{S}{2K(C_o-C)}\left[\frac{\gamma^{\frac{1}{2}}-\beta}{K} + \frac{d\beta}{dD} + \gamma^{-\frac{1}{2}}\left(\beta\frac{d\beta}{dD} + 4KCa^2D\right)\right]$$

The derivatives of the term β in the expressions above are

$$\frac{d\beta}{dC} = -KaD - k \qquad \frac{d\beta}{dk} = C_o - C$$

$$\frac{d\beta}{dK} = -aDC \qquad \frac{d\beta}{dD} = 0$$

D.3 Diffusion-limiting Model

D.3.1 Kinetic expression

Equation *D.15* for the surface concentration may be rewritten as

$$C_s = \frac{\beta}{2KaD}\left\{-1 + \left[1 + \frac{4KCa^2D^2}{\beta^2}\right]^{\frac{1}{2}}\right\} \qquad \ldots D.17$$

If

$$\frac{4KCa^2D^2}{\beta^2} \ll 1$$

then $C_s \approx 0$ from *D.17* above. In physical terms this means that the rate of diffusion of the O_2 through the oxycoal is limiting the reaction. The rate expression *simplifies to*

$$r = -\frac{dC}{dt} = \frac{SD}{\Delta x}C = \frac{SaD}{C_o - C}C \qquad \ldots D\text{-}18$$

Thus

$$\frac{dC}{dt} = -\frac{\alpha SDC}{C_o - C} \qquad \ldots 4\text{-}5$$

D.3.2 Partial derivatives required for optimisation

The derivatives with respect to the temperature are the same as in D.2.2. The other derivatives are

$$\frac{\partial}{\partial C}\left(\frac{dC}{dt}\right) = -\frac{\alpha SDC_o}{C_o - C}$$

$$\frac{\partial}{\partial D}\left(\frac{dC}{dt}\right) = -\frac{\alpha SC}{C_o - C}$$

D.4 Diffusion-limiting Model with Pre-ageing

D.4.1 Kinetic expression

If some oxycoal has been formed prior to the measurement of the kinetics, equation *D-12* changes to

$$V(C_o - C) = S\rho_m(\Delta x - \Delta x_o) \qquad \ldots D\text{-}19$$

where Δx_o is the thickness of the oxycoal formed by the pre-ageing. Rearranging:

$$\Delta x = \frac{V}{S\rho_m}(C - C_o) + \Delta x_o$$

Substitution of this into *D-18* results in

$$-\frac{dC}{dt} = \frac{\alpha SDC}{C_o + \Delta x_o \rho_m - C}$$

The term $\Delta x_o \rho_m$, with the units of concentration, accounts for the drop in reactivity due to pre-ageing. This may be incorporated into the initial concentration C_o to give a fictitious concentration C_o' which is larger than C_o. The increase in C_o is a measure of the amount of pre-ageing.

Thus

$$\frac{dC}{dt} = - \frac{\alpha SDC}{C'_o - C} \qquad \ldots 4\text{-}6$$

D.4.2 Partial derivatives required for optimisation

The temperature derivatives remain unchanged. The concentration derivatives are

$$\frac{\partial}{\partial C}\left(\frac{dC}{dT}\right) = - \frac{\alpha SDC'_o}{(C'_o - C)^2}$$

$$\frac{\partial}{\partial C'_o}\left(\frac{dC}{dt}\right) = \frac{\alpha SDC}{(C'_o - C)^2}$$

$$\frac{\partial}{\partial t}\left(\frac{dC}{dt}\right) = - \frac{\alpha^2 C}{C'_o - C}$$

APPENDIX E: BEST-FIT PARAMETERS AND PLOTS FOR RUNS 1-1 TO 1-7

In this appendix the output from the parameter estimation program is given, along with the plots of the fitted temperature-time and concentration-time curves. The line types used are consistent for all the plots: the short dashes represent the diffusion-limiting (one parameter) model fits, while the longer dashes are used for the pre-ageing model (two parameter) fits. The temperature data are represented as a solid line, and the concentration data as diamonds.

The weighting factors used in the optimisation were 10^{-3} for αSD, and unity for the fictitous initial concentration. These values were chosen so that the scaled parameters would be of the same order of magnitude. The gradients and Hessian matrixes reported below must thus be multiplied by the weighting factors to obtain the actual values. The first element of the vectors and matrices relates to αSD, and the second (which is only required for the two parameter fits) to C_0'.

Run 1-1: Diffusion-limiting model best-fit details

Optimum parameters αSD = 2.67022E-3

Sum of squared errors: 25322.3300

Gradient at optimum -29.308

Hessian matrix at optimum 8157.8610

Standard errors 0.07723

Variance-covariance matrix 0.0000042531

Run 1-1: Pre-ageing model best-fit details

Optimum parameters αSD = 3.582E-3
C_o^l = 27.967

Sum of squared errors: 7414.1807

Gradient at optimum 84.178 1.1240

Hessian matrix at optimum 29482.78 -2609.88
-2609.88 6199.48

Standard errors 0.0414 0.0904

Variance-covariance matrix 0.0000022055 0.0000072487
0.0000072487 0.0006392831

Correlation matrix 1.000 0.1930
1.0000

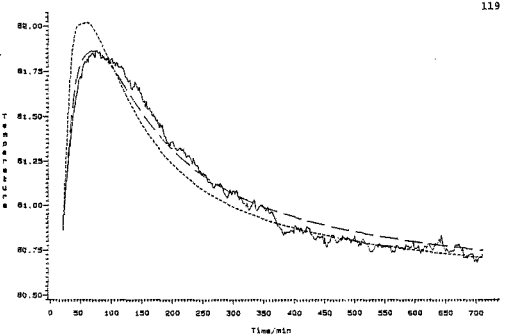

Figure E1 Model fits to temperature data of run 1-1

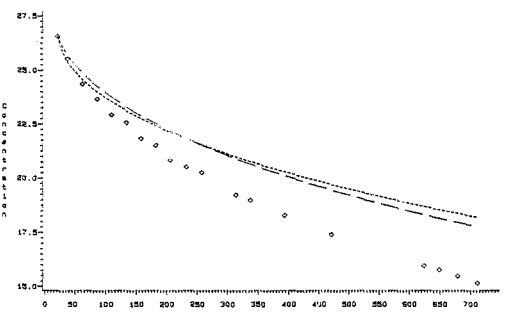

Figure E2 Model fits to concentration data of run 1-1

Run 1-2: Diffusion-limiting model best-fit details

Optimum parameters	αSD = 3.267E-3
Sum of squared errors:	396369.14
Gradient at optimum	-34.821
Hessian matrix at optimum	1736.466
Standard errors	0.15027
Variance-covariance matrix	0.000024147

Run 1-2: Pre-ageing model best-fit details

Optimum parameters	αSD = 8.747E-3 C_o^1 = 59.41
Sum of squared errors:	7507.8060
Gradient at optimum	5.910 0.0844
Hessian matrix at optimum	117604.766 -12752.005 -12752.005 13022.239
Standard errors	0.0158 0.0581
Variance-covariance matrix	0.000002860432293 0.000019025217265 0.000019025217265 0.001191730799135
Correlation matrix	1.000 0.325 0.325 1.000

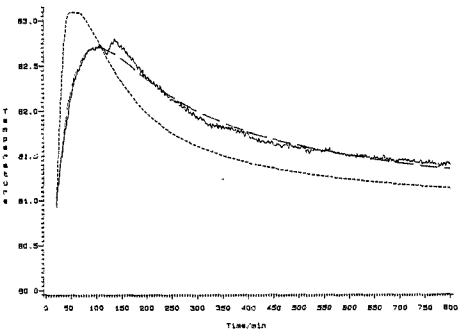

Figure E3 Model fits to temperature data of run 1-2

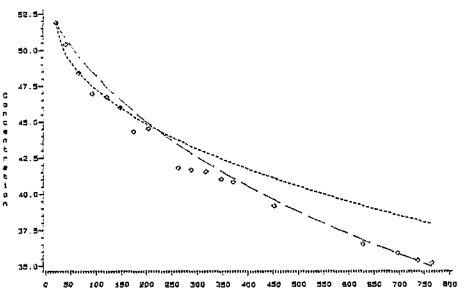

Figure E4 Model fits to concentration data of run 1-2

Run 1-3: Diffusion-limiting model best-fit details

Optimum parameters αSD = 1.189E-3

Sum of squared errors: 8271.75

Gradient at optimum -8.458

Hessian matrix at optimum 263.094

Standard errors 0.666746

Variance-covariance matrix 0.0000629020

Run 1-3: Pre-ageing model best-fit details

Optimum parameters αSD = 2.879E-3
C_o' = 12.33

Sum of squared errors: 581.1957

Gradient at optimum -37.708 17.127

Hessian matrix at optimum 3707.895 -7488.959
-7488.959 20486.353

Standard errors 0.348 0.148

Variance-covariance matrix 0.00010053 0.00015743
0.00015743 0.00033390

Correlation matrix 1.000 0.859
0.859 1.000

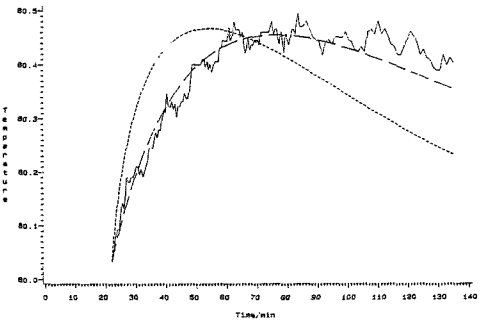

Figure E5 Model fits to temperature data of run 1-3

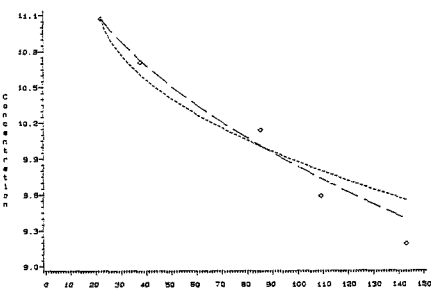

Figure E6 Model fits to concentration data of run 1-3

Run 1-4: Diffusion-limiting model best-fit details

Optimum parameters αSD = 6.742E-3

Sum of squared errors: 691701.84

Gradient at optimum -17.826

Hessian matrix at optimum 844.11

Standard errors 0.2185

Variance-covariance matrix 0.0002171

Run 1-4: Pre-ageing model best-fit details

Optimum parameters αSD = 18.116E-3
C'_o = 36.770

Sum of squared errors: 74268.54

Gradient at optimum 86.337 -2.950

Hessian matrix at optimum 9671.941 -2411.668
-2411.668 2819.265

Standard errors 0.0128 0.1349

Variance-covariance matrix 0.00017428 0.00046717
0.00046717 0.00587115

Correlation matrix 1.000 0.461
0.461 1.000

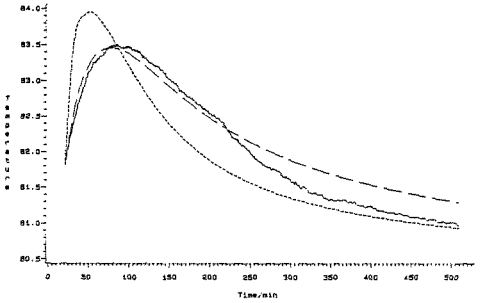

Figure E7 Model fits to temperature data of run 1-4

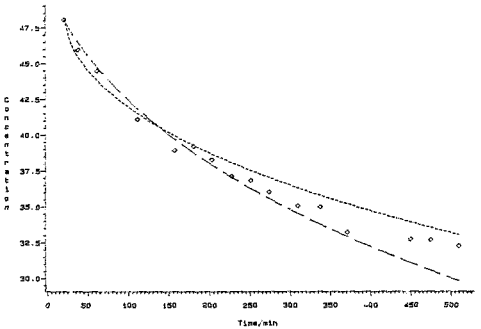

Figure E8 Model fits to concentration data of run 1-4

Run 1-5: Diffusion-limiting model best-fit details

Optimum parameters αSD = 6.124

Sum of squared errors: 508108.85

Gradient at optimum -24.421

Hessian matrix at optimum 785.075

Standard errors 0.275763

Variance-covariance matrix 0.00028521

Run 1-5: Pre-ageing model best-fit details

Optimum parameters αSD = 26.689E-3
C_o' = 68.94

Sum of squared errors: 38658.8194

Gradient at optimum 83.039 -2.248

Hessian matrix at optimum 11246.662 -2761.275
-2761.275 1538.665

Standard errors 0.0975 0.263

Variance-covariance matrix 0.00067792 0.003142830
0.00314283 0.033068528

Correlation matrix 1.000 0.663
0.663 1.000

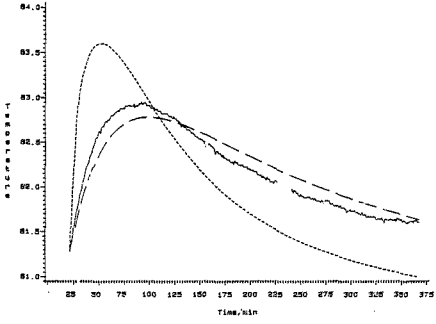

Figure E9 Model fits to temperature data of run 1-5

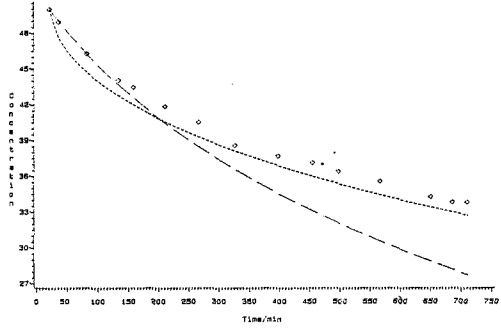

Figure E10 Model fits to concentration data of run 1-5

Run 1-6: Diffusion-limiting model best-fit details

Optimum parameters αSD = 2.917E-3

Sum of squared errors: 258153.76

Gradient at optimum -42.147

Hessian matrix at optimum 2457.38

Standard errors 0.13173

Variance-covariance matrix 0.000014775

Run 1-6: Pre-ageing model best-fit details

Optimum parameters αSD = 7.065E-3
C_o' = 59.74

Sum of squared errors: 3110.7636

Gradient at optimum 8.734 -0.313

Hessian matrix at optimum 245343.863 -24455.397
-24455.397 22736.383

Standard errors 0.0139 0.0458

Variance-covariance matrix 0.00000097383 0.00000885718
0.00000885718 0.00075137258

Correlation matrix 1.000 0.327
0.327 1.000

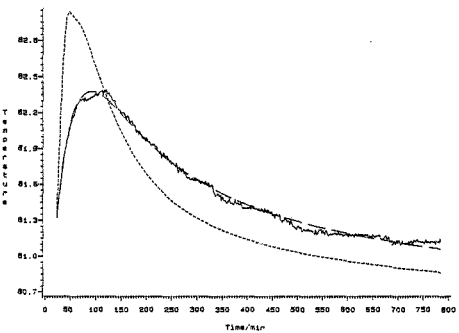

Figure E11 Model fits to temperature data of run 1-6

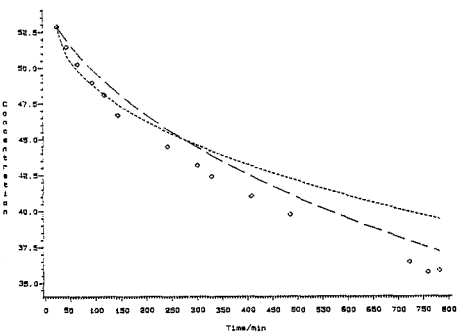

Figure E12 Model fits to concentration data of run 1-6

Run 1-7: Diffusion-limiting model best-fit details

Optimum parameters αSD = 1.8547E-3

Sum of squared errors:	161204.8
Gradient at optimum	-7.171
Hessian matrix at optimum	165.25
Standard errors	0.6835823
Variance-covariance matrix	0.000160746

Run 1-7: Pre-ageing model best-fit details

Optimum parameters αSD = 3.314E-3
C_O' = 36.92

Sum of squared errors:	43955.72	
Gradient at optimum	-22.998	13.340
Hessian matrix at optimum	537.8517	-1207.7613
	-1207.7613	4335.2560
Standard errors	0.6204	0.2185
Variance-covariance matrix	0.00042300	0.001312626
	0.00131262	0.006511047
Correlation matrix	1.000	0.790
	0.790	1.000

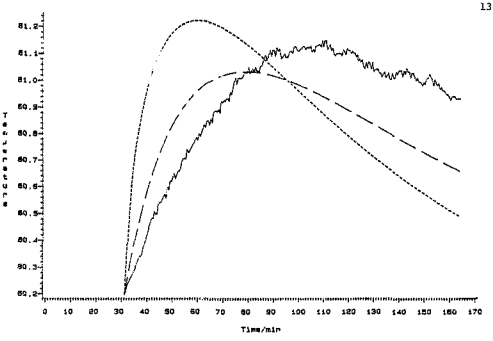

Figure E13 Model fits to temperature data of run 1-7

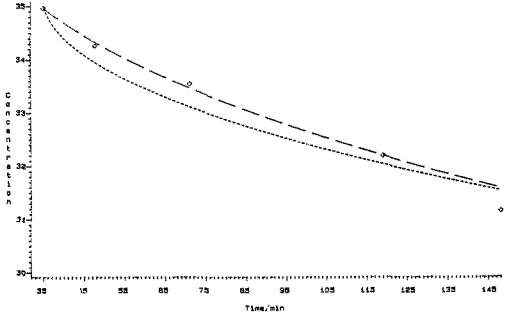

Figure E14 Model fits to concentration data of run 1-7